The Thesis Committee for **Christian Philip Armstrong**
Certifies that this is the approved version of the following thesis:

Effect of Fabric on the Swelling of Highly Plastic Clays

APPROVED BY
SUPERVISING COMMITTEE:

Supervisor:

Jorge G. Zornberg

Robert Gilbert

Effect of Fabric on the Swelling of Highly Plastic Clays

by

Christian Philip Armstrong, B.S.C.E.

Thesis

Presented to the Faculty of the Graduate School of

The University of Texas at Austin

in Partial Fulfillment

of the Requirements

for the Degree of

Master of Science in Engineering

The University of Texas at Austin

May 2014

Dedication

For Veronica Calderon-Stucky and Dwight Reel:

> *He will wipe every tear from their eyes, and there shall be no more death or mourning, wailing or pain, for the former things have passed away.*
>
> *The Book of Revelations 21:4*

Acknowledgements

I would like to first thank Dr. Jorge Zornberg for his support and help with this project along with general guidance and help throughout my time at the University of Texas. I would also like to thank the Texas Department of Transportation for their financial funding of my project along with the help from Mike Arellano and Clay Brown in terms of procuring soil for testing and valuable insight into practical applications. Dr. Zornberg's research group, especially Michael Plaisted, is very much appreciated for their help with advice and feedback during research seminars. I'd also like to thank Dwight Romanovicz and the Microscopy and Imaging Facility of the Institute for Cellular and Molecular Biology at The University of Texas at Austin for the tremendous amount of help using the SEM and with general advise into the examination of soils at the micro-level. I would like to thank Dr. Gilbert and Dr. Lawler for helping steer me into graduate school as this has been an incredible opportunity to learn and grow as a person. Finally, my family and friends that have helped support me throughout this entire process with their countless numbers of hours and help of reducing stress in my life and reminding me that I would indeed graduate are very much appreciated. My grandparents especially deserve gratitude for instilling in me how important education is and a strong work ethic. I am very much blessed by the amount of people who have helped with my research, and to each of you, I want to share a sincere thank you.

Abstract

Effect of Fabric on the Swelling of Highly Plastic Clays

Christian Armstrong, M.S.E.

The University of Texas at Austin, 2014

Supervisor: Jorge G. Zornberg

Expansive soils are extremely problematic in transportation projects, and significant research has been done into examining the effect of moisture content changes and index properties on the swelling of soils. However, little has been reported on the effect of soil structure, or fabric, on swelling. The purpose of this study is to examine the effect of the soil fabric on swelling while, at the same time, validating a new set-up for a centrifuge testing program developed over the course of the project to allow for testing of undisturbed specimens.

Testing to examine fabric was performed using two methods at the same effective stress, the conventional swelling test, ASTM D4546, and a new double infiltration approach in a centrifuge, on specimens of the Cook Mountain clay which were either compacted in the testing set-up or trimmed into cutting rings from soil compacted via ASTM D698, the Standard Proctor test. Specimens were compacted either dry of optimum to create a flocculated soil structure or wet of optimum to create a dispersed soil structure. Specimens were tested at their as-compacted moisture content or at a moisture conditioned moisture content to remove the effect of the initial moisture content.

The results show that soils with a dispersed structure tended to swell more, over a longer time frame, and with a higher amount of secondary swelling in relation to soils with a flocculated structure when tested using the same initial moisture content. The strong influence of the initial moisture content on swelling was also verified. Further, soil specimens prepared at a comparatively high dry density for a given fabric and initial moisture content were found to swell more than soils prepared at a comparatively low dry density. The new centrifuge set-up, involving submerged specimens, was validated and was found to produce similar swelling results as those obtained from the ASTM D4546 tests. In addition, the new centrifuge approach was found to be more expeditious and results in less secondary swelling than the conventional ASTM approach.

Table of Contents

List of Tables

List of Figures

CHAPTER 1: Introduction

1.1 Motivation

Expansive soils are characterized by undergoing significant volumetric changes during fluctuations of moisture. These volumetric changes can have a significant impact on human infrastructure, namely paved roadways and low rise buildings, with damages in the billions of dollars (Nelson and Miller 1992). Expansive soils exist throughout the United States, with approximately 20% of the US being covered with highly expansive soils (Krohn and Slosson 1980). The problem is particularly severe in Texas with central and east Texas having large areas with highly expansive soils as shown in Figure 1.1. These areas in Texas are especially vulnerable to damages in the transportation infrastructure due to the semi-arid climate of the region with drought-like conditions throughout most of the year and intermittent, heavy and short duration rainfall events.

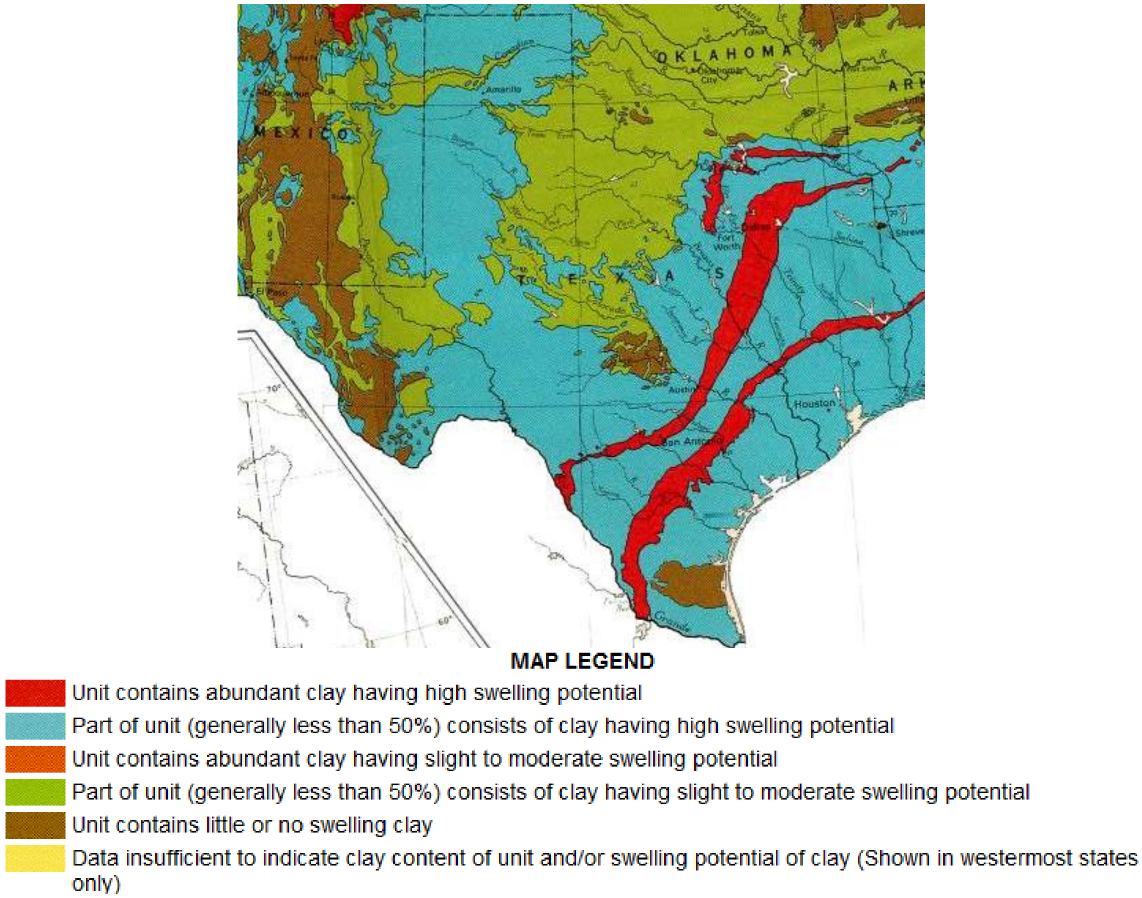

Figure 1.1: Expansive Soils in Texas (Olive et al., 1998)

Methods have been developed to determine a soil's potential to swell using either indirect or direct approaches. Indirect approaches rely on correlating standard geotechnical indices, such as the plasticity index or the liquid limit, to a soil's potential to swell, whereas direct approaches involve the experimental testing of soils to directly measure the potential of a soil to swell at a given moisture content, fabric, and density. However, issues with both approaches limit their application and effectiveness. The indirect approaches fail to account for fissures and voids within the soil mass and the clay composition of the soils, thereby leading to uncertainty whether swelling in the field will be comparable to the correlations. Direct methods are typically very time consuming and expensive, thereby leading to many transportation entities not utilizing them in practice. A centrifuge based approach using a data acquisition system (DAS) was developed at the University of Texas at Austin and tested reconstituted soil specimens to rapidly characterize sites (Plaisted 2009). Results from this approach indicated that the most important variable in the swelling of a highly plastic soil was the initial moisture content (Walker 2012). However, these studies did not assess the swelling potential of undisturbed specimens as the set-up did not allow for them to be tested. Thus, the effect that a soil's structure, namely the arrangement of clay particles and voids such as fissures or vugs within the soil mass, has on the swelling potential is yet to be determined. Therefore, further testing is necessary to determine whether a soil's initial structure affects the swelling potential of a deposit and, if so, whether undisturbed specimens are a necessity when designing roadways on expansive soils.

The current centrifuge test set-up at the University of Texas at Austin was modified in order to test specimens taken from in-situ conditions. By changing the design to allow for a cutting ring to be inserted into the current permeameter cups, the swelling potential of undisturbed specimens can be measured to determine the effect of fabric. Further, by incorporating infiltration through both the top and bottom of the specimen in a centrifuge environment, the time for the soil to swell will be decreased, leading to an even more rapid characterization of a site. By implementing the results from these tests into design considerations for transportation projects, a significant amount of money spent on maintenance and repair of cracking of roadways can be saved.

1.2 OBJECTIVES AND SCOPE OF RESEARCH

This study's main objective is to isolate the effect on swelling characteristics of the following variables: the initial fabric, the initial moisture content, and the initial dry density. The secondary objective was to validate the newly developed double infiltration centrifuge method. To achieve these objectives, the research program used a highly plastic clay obtained from Bastrop, Texas in order to use various tests to isolate each of these variables. Testing included the use of three direct approaches to characterize the swelling potential of a soil, the original single infiltration centrifuge set-up, the ASTM D4546 test, and the new double infiltration centrifuge set-up. Tests of reconstituted specimens were performed using both the original centrifuge set-up and ASTM D4546 tests to determine a baseline conditions to compare against results from trimmed specimens. Tests of trimmed samples were performed using both the ASTM D4546 tests and the new double infiltration centrifuge set-up to examine the effect that fabric has on the swelling of soil on specimens at either the compaction moisture content or at a moisture conditioned moisture content. The swelling of the soil was characterized via the vertical strain at the end of primary swelling, the time to reach the end of primary swelling, and the slope of the primary and secondary swelling portion of the swelling curves. These results were then compared to determine how a flocculated or dispersed structure affected the swelling characteristics of a soil and whether this effect was significant in comparison to the effects from the initial moisture content and density. The effects of the initial moisture content and dry density were determined by comparing results between tests that had similar fabric.

1.3 TERMINOLOGY

For this study, several terms that have loose definitions are defined for clarity through the rest of the report. The single infiltration centrifuge method is the original centrifuge based method developed by Plaisted (2009) in which water is ponded at the top of the soil sample with a freely draining boundary at the bottom of the soil sample. The double infiltration centrifuge method is the newly designed centrifuge based method in which water can infiltration at either the top or bottom of the soil sample due to submersion of the cutting ring in the permeameter cup. Reconstituted specimens are soil samples that are compacted within either the single infiltration centrifuge permeameter cup or the cutting ring used in ASTM D4546. Trimmed specimens are soil samples that are compacted within a proctor mold using standard effort and are then trimmed into cutting rings for use in ASTM D4546 or the double infiltration centrifuge method. The initial moisture content, ω_i, is the moisture content at the beginning of the swelling test. The as-compacted moisture content, ω_c, is the moisture content at the time of compaction.

1.4 Overview of Thesis

The thesis has been divided into seven chapters. Chapter one presented the motivation, objectives, and scope of the research. Chapter two focuses on previous research and background information on expansive soils, the indirect and direct methods to determine the swelling potential of a soil including centrifuge testing, the effect of cyclic wetting and drying of soils either from in-situ specimens or laboratory testing, and the properties of clays that are compacted via various methods. Chapter three presents the soil characterization obtained using results from standard geotechnical tests along with sampling and geological information. Chapter four reviews the equipment and procedures used in this testing program. Chapter five shows the suite of tests and results obtained from the testing program. Chapter six examines and analyzes the results from the testing program. Finally, chapter seven presents the main conclusions from the testing program and recommendations for future testing.

Chapter 2: Background Information

2.1 Expansive Clays and Environmental Conditions

2.1.1 Overview of Expansive Clays

The explanation for why certain clays are expansive while others are not lies in the physicochemical structure and mineralogy of clay particles as well as the genesis of these soils. Clays' typical structure includes sheets that are covalently or ionically bonded together to form basal layered units, which classify into different clay mineral groups. The three main structural groups for clays include kaolinites, which are generally non-expansive, micas, which include illites and vermiculites and can be expansive though typically are not an issue, and smectities, which include montmorillonites and are typically very problematic, expansive soils (Chen 1988). Clays typically have very large specific surface areas which lead to a high cation exchange capacity (CEC). Furthermore, the clay particles typically have a net negative charge due to isomorphous substitution, leading to a strong attraction for cations from the adsorbed water in the clay's crystal lattice. When an expansive clay is wetted, the repulsive forces between the negatively charged clay sheets is lessened as the clay will absorb enough water in order to counter act the negative charge on the clay particles from free cations in the water due to their high CEC. This influx of water leads to an increased distance between the clay sheets, leading to the soil's expansion. For the smectite group, the large specific surface area of the clay particles and the weak van der Waal forces between sheets lead to a high amount of water being drawn into the clay's structure, leading to the soil expanding significantly.

Further reasons for the smectite group, specifically montmorillonite, being highly expansive come from the genesis of the clay particles and the weathering of parent material. Typical parent material for this group of clays often include ferramagnesium minerals, calcic feldspars, and volcanic gas, and the depositional environment typically includes very high disintegration, hydration and a limited amount of leaching (Chen 1988).

In a typical expansive clay, three distinct areas exist in the volume of the soil: (1) the clay platelets, (2) the macro-pores, which are typically filled with air below the optimum moisture content, and (3) the micro-pores between clay platelets, in which the water will dominate due to the diffuse double layer (Ferber et al. 2009). During compaction of expansive soils, the macro-pores in the soil are controlled by the compaction technique whereas the micro-pores are typically dominated by the moisture content at the time of compaction. Further, as the macro-pores are typically decreased during swelling via the filling of water, micro-pores are typically the main driver of swelling. As shown in Figure 2.1, Ferber et al. (2009) were able to show that the void ratio of the macro-pores decreases when the swelling of a soil occurs whereas the void ratio of the micro-pores increases during the testing process. Note that void ratio of the micro-pores for Figure 2.1(a) is shown as e_m, and the initial void ratio of the soil mass is shown as e_i. For Figure 2.1(b), the void ratio of the macro-pores is shown as e_M, and the initial void ratio of the soil mass is shown as e_i.

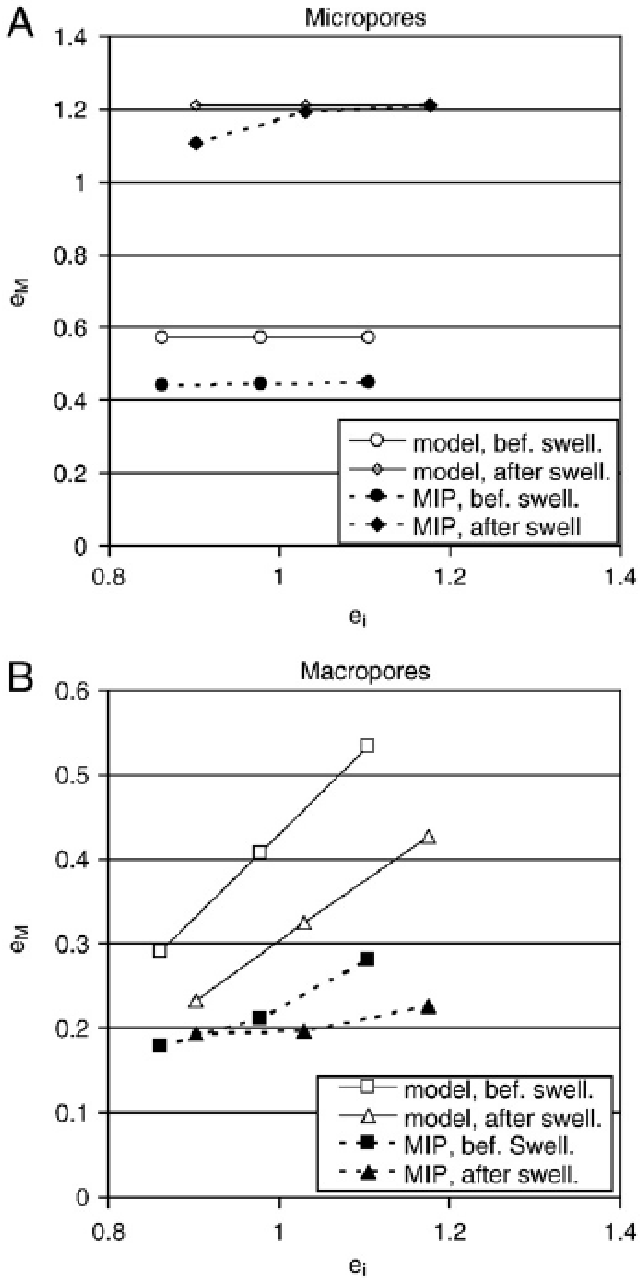

Figure 2.1: Micro-pores (A) and Macro-pores (B) void ratios at compaction and final swelling based on experimental data (MIP) and a theoretical model (Ferber et al. 2009)

Micro-pores also have a significant impact on the soil water retention curves and the air entry pressure of soils. With these micro-pores, significant matric suction can occur over a very wide range of moisture contents, thereby leading to an expansive soil remaining near or at saturation. This phenomena of "perpetual saturation" happens as the digenesis of the smectite clays lead to very small maximum pore sizes that do not allow for air to enter but is able to absorb water due to the hydration of the ions on its surface (Fityus and Buzzi 2009). A typical expansive soil's soil water retention curve is shown in Figure 2.2. Therefore, these expansive soils have significant impact on geotechnical engineering properties due to their potential to expand and unusual moisture retention characteristics and pore distributions.

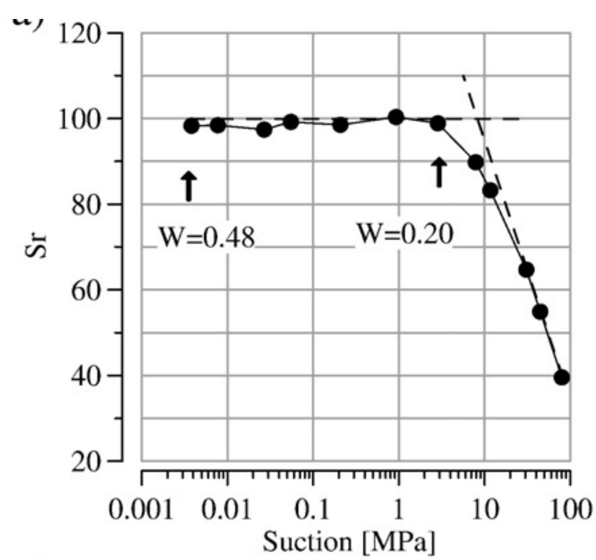

Figure 2.2: Soil Water Retention Curve for a Natural Expansive Soil Deposit (Fityus and Buzzi 2007)

2.1.2 Environmental Conditions and Expansive Soils

Significant moisture fluctuation must occur in order for soils to be expansive. In a typical soil profile, there exist two distinct zones: (1) the vadose, or unsaturated, zone where the soil is unsaturated due to evapotranspiration and (2) the saturated zone at which the soil lies below the groundwater table. In the vadose zone, another zone, the active zone, exists where the moisture content varies significantly due to seasonal moisture variation. Typically, in order for the soil to have a high potential to swell, these seasonal moisture variations must include a distinct dry, drought-like season in which the soil is desiccated closer towards the surface followed by a season characterized by quick, high intensity rainfalls that can rapidly saturate a soil. The active zone has typically been assumed to be only up to a depth of around 8 to 10 feet (Nelson and Miller 1992).

2.2 PREDICTIVE METHODS FOR THE SWELLING OF HIGHLY PLASTIC CLAYS

Many methods are currently in use to predict and/or measure the swelling of highly plastic soils. The methods can be grouped into indirect methods, in which the swelling of a clay is predicted based on geotechnical characteristics and properties of the soil strata, and direct methods, in which the swelling of a soil is directly measured experimentally either on reconstituted or undisturbed soil samples.

2.2.1 Potential Vertical Rise (PVR) Method (Tex-124-E)

TxDOT currently uses the Potential Vertical Rise method (PVR), which was originally developed by Chester McDowell in 1956 and then further modified by TxDOT in 1999 for use. The PVR is commonly used as an index property for projects in areas with known expansive soils as it requires solely the plasticity index (PI) to give an idea as to what the volumetric change would be for a project. The method divides the subgrade into two feet strata, taking into account the depth of subgrade that quantifies as the active zone, with a known or assumed moisture content (ω), unit weight (γ) in pcf, liquid limit (LL), plasticity index (PI), and percent soil binder (i.e. the percent of the stratum that passes through the No. 40 sieve). The moisture condition of each layer is divided into three conditions, dry (ω_d), wet (ω_w), and average (ω_a), as determined by which condition the moisture content of the soil strata is closest to. The dry condition is representative of a condition in which little shrinkage but maximum swell occurs, and the wet condition is considered to be where the maximum capillary absorption occurs. Equations 2.1, 2.2, and 2.3 show how each moisture condition is calculated:

$$\omega_d = .2 * LL + 2\% \quad (2.1)$$

$$\omega_w = .47 * LL + 2\% \quad (2.2)$$

$$\omega_a = \frac{\omega_d + \omega_w}{2} \quad (2.3)$$

Once the moisture condition is known or assumed, the percent volumetric strain (% Vol. Swell) of a soil under a one psi (6.9 kPa) surcharge is determined from Figure 2.3 via the PI and moisture condition of the strata.

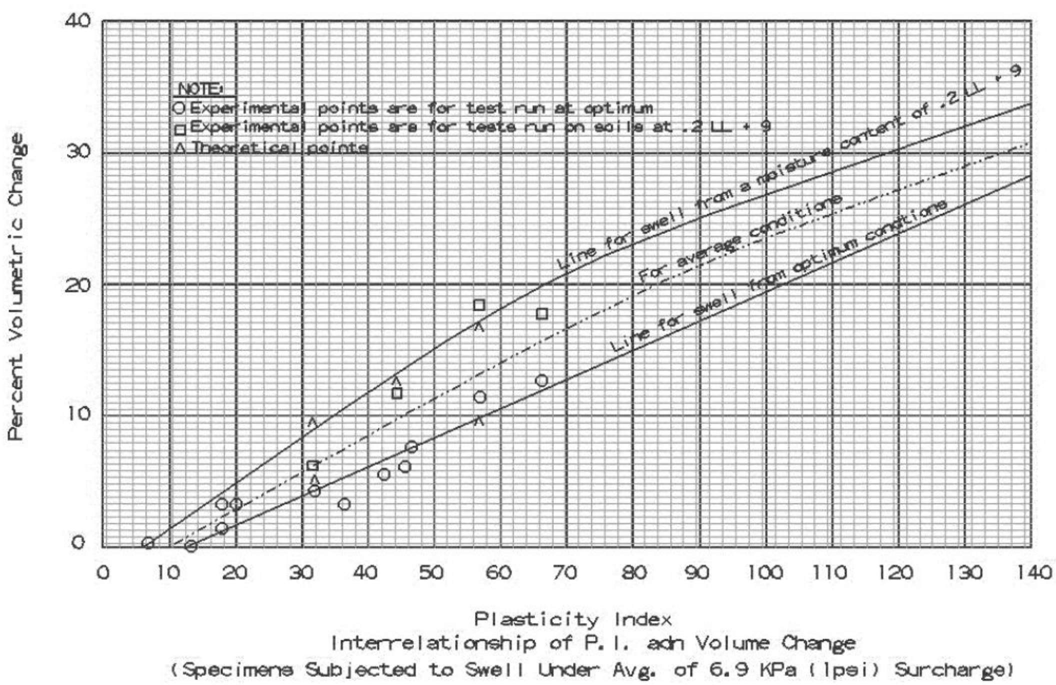

Figure 2.3: Percent Volumetric Change vs. Plasticity Index (TxDOT 1999).

In order to determine the PVR of a stratum, the percent volumetric strain must be converted to the percent volumetric change under no loading (% Free Swell) as follows:

$$\%\,Free\ Swell = (\%\,Vol\ Swell) * 1.07 + 2.6\% \qquad (2.4)$$

After the percent free swell is determined, the load at the top and bottom of each strata should be determined from the projects plans and/or boring logs. The PVR of the layer is then calculated by using Figure 2.4 to determine the PVR of the top and bottom of the strata under the load at each location and the percent free swell for the strata. The difference between the PVR at the top and bottom of the strata is considered the PVR of the entire strata. However, some corrections are necessary for the PVR as the method assumes that the unit weight of the soil is 125 pcf and that the entire soil strata passes the No. 40 sieve. These corrections are taken as the ratio of the actual unit weight and the percentage of the soil that passes the No. 40 sieve. After these corrections are added, the final PVR is then recorded.

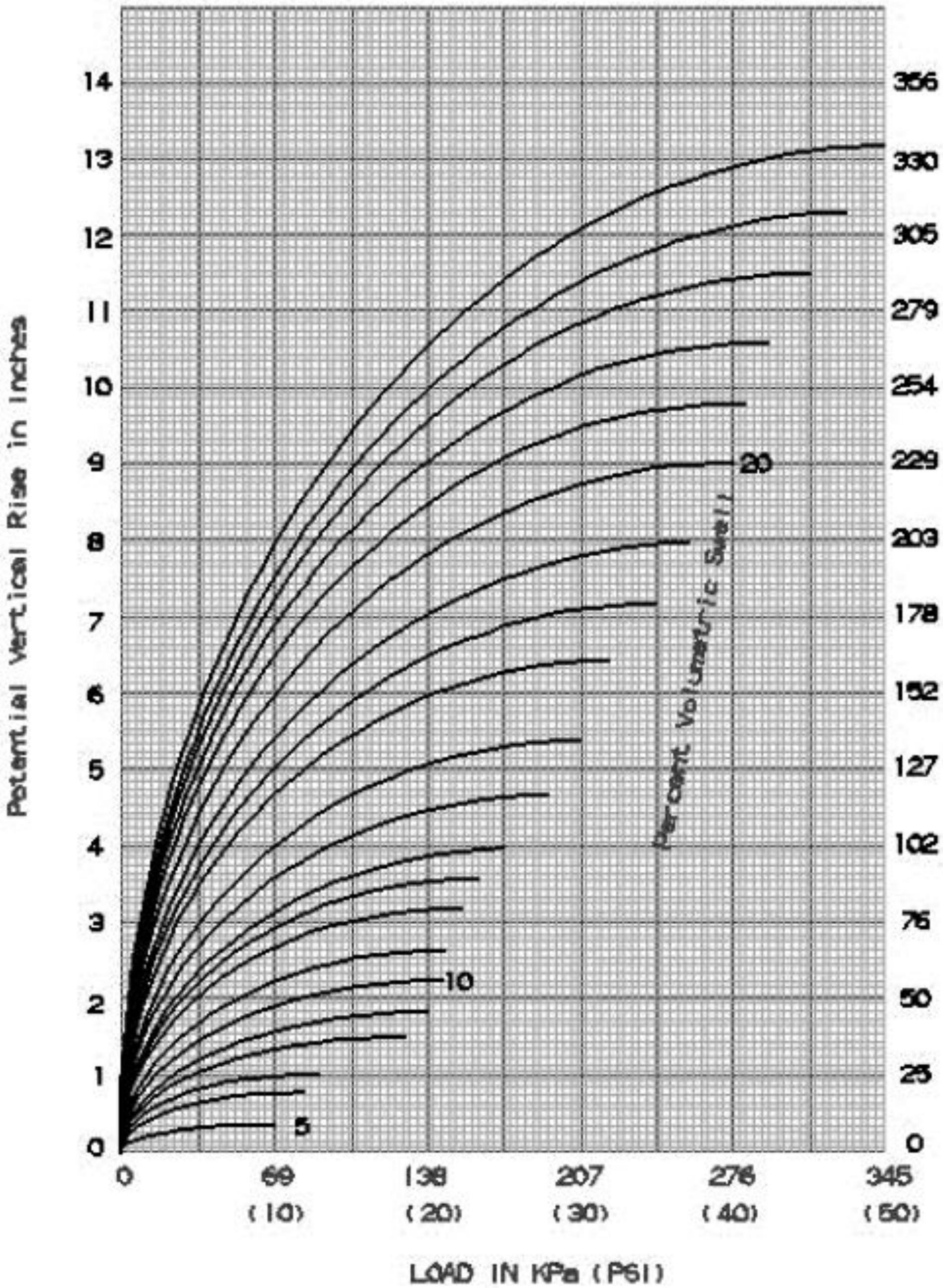

Figure 2.4: Potential Vertical Rise vs. Load (TxDOT 1999).

Overall, the methodology is used frequently by certain districts within TxDOT but has two significant limitations. The first limitation is that while the plasticity index is a good measure as to whether the soil has a high potential to swell, the soils in-situ can behave drastically different due to clay mineralogy. This limitation is seen as McDowell developed his relationships using a limited amount of soils from Guadalupe County, Texas. Examining Figure 2.3 in more detail, a limited amount of data points were used that are clustered towards the lower end of PI, and the curve fitting of the data points is questionable. The second limitation is the relative lack of influence of the initial moisture content. The moisture condition has a much more significant role in the swelling of a soil than dividing into three separate cases of “dry”, “wet”, and “average” as the difference between an initial condition of ± 3% can lead to major differences in the swelling potential (Walker 2012).

2.2.2 Potential Vertical Rise Revisited [Lytton et al. (2006)]

The original PVR method was re-examined by the Texas Transportation Institute. They reported that the PVR method typically overestimated the swelling of a sublayer and that many engineers used the method as an index property for sites rather than a design parameter. Thus, Lytton developed a method to estimate the heave at a site using a finite difference model of the soil profile that examined the moisture movement through a soil from the suction within the soil profile.

The methodology involves measuring the suction values throughout the soil profile via an evaporation test that measures the suction over time by thermocouple psychrometers. The values of the suctions are then plotted to determine the diffusion coefficient of a soil, α, via a best fit from a MatLAB program. The volumetric change is then determined via an equation that incorporates the matric suction and mean principal stress of a soil in order to determine the vertical rise.

Some major issues do exist in this predictive method. The only direct measurement from the soil is the diffusion coefficient, which comes from the desiccation, or drying, of the soil as opposed to the swelling, or wetting, of the soil. The suction of the soil may not match the wetting cycle of the soil due to hysteresis, and, therefore, the model is simplified via using a single diffusion coefficient for both wetting and drying. Further, the model uses numerous empirical relationships that do not indicate how much scatter and/or data was used to develop these models. Thus, the relationship leads to an indirect, convoluted method that does not directly measure the swelling potential of a soil.

2.2.3 Other Indirect Methods to Predict Soil Heave

Numerous other attempts have been made to quantify a soil's ability to swell using index properties of a soil. Table 2.1 describe a few correlations and has been modified from Rao (2004).

Table 2.1: Indirect Methods to Quantify Soil Heave

Source	Properties	Correlation
McDowell (1959)	Plasticity Index, PI (%) % Soil Binder (%) Water Content, ω (%) Bulk Density, γ (pcf)	Graphical Solution See section on PVR Methodology
Vijayvergiya & Ghazzaly (1973)	Liquid Limit, ω_L (%) Dry Unit Weight, γ_d (pcf)	$\log S = \frac{1}{19.5} * (\gamma_d + .65 * \omega_L - 130.5)$
Nayak & Christensen (1974)	Plasticity Index, I_P (%) Initial water content, ω_i (%) Clay Content, C (%)	$S = 2.3 * 10^{-2} * (I_P)^{1.45} * \frac{C}{\omega_i} + 6.4$
Covar & Lytton (2001)	Matric suction compression index, γ_h Initial and final water potentials, h_i and h_f Mean principal compression index, γ_σ Initial and final normal stress, σ_i and σ_f See Section 2.2.2	$S = -\gamma_h * \log_{10}\left(\frac{h_f}{h_i}\right) - \gamma_\sigma * \log_{10}\left(\frac{\sigma_f}{\sigma_i}\right)$
Rao et al. (2004)	Dry unit weight, γ (pcf) Initial water content, ω_0 (%) Overburden pressure, q (kPa) Free swell index, FSI	$S = 4.24 * \gamma_d - 0.47 * \omega_0 - 0.14 * q + 0.06 * FSI - 55$

The indirect methods tend to focus on geotechnical properties that are commonly measured, such as the moisture content, Atterberg Limits, and density of the soil. Other methods, such as Rao's 2004 predictive equation, define new parameters to determine the swelling such as the Free Swell Index. The Free Swell Index (FSI) is defined in Equation 2.5 where V_w is the volume of a soil mass passing a #40 sieve in water and V_k is the volume of a soil mass passing through a #40 sieve in kerosene. Note that the FSI typically performs fairly poorly in comparison to other methods, and the testing procedure has not become a standard index test due to issues stemming from the relationship between FSI and the swell potential.

$$FSI = \frac{(V_w - V_k) * 100}{V_k} \tag{2.5}$$

While these methods attempt to quantify the soil's heave more cost effectively, the author's opinion is that these methods should only be used as rough indices as inherent soil properties that dictate swelling, i.e. the mineralogy, soil structure, and composition of particles greater than the #40 sieve, are not taken into account.

2.3 Direct Methods for Measuring the Swelling Potential of Soils

In response to issues stemming from indirect methods, direct methods to quantify the swelling potential of a soil have been developed. Methods to measure the swell of a soil can be grouped into those using an oedometer and those using a centrifuge.

2.3.1 ASTM D4546 – One-Dimensional Swell of Cohesive Soils

The standard for a direct method of measuring the swelling potential or swelling pressure of a soil using an oedometer is contained in ASTM D4546. This method is also commonly known as the "Free Swell Test." The test set-up involves using a frame typically used for consolidation and a soil sample in a consolidation cell consisting of cutting ring that is between two porous disks held in place via three clamping nuts and confined via a load placed on the top porous stone. The consolidation cell is shown in Figure 2.5.

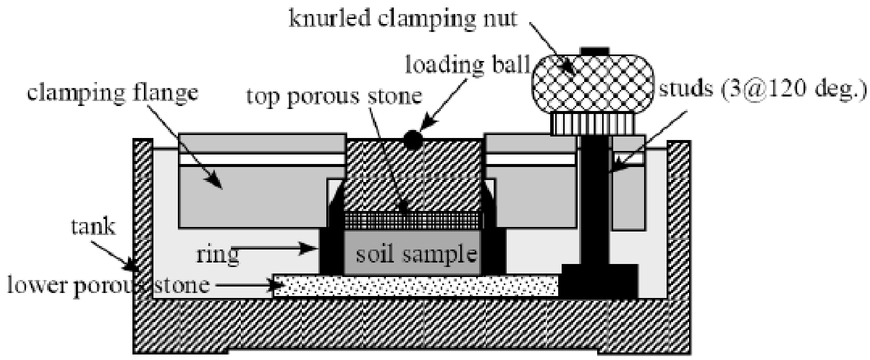

Figure 2.5: Fixed-Ring Consolidation Cell for ASTM D4546 (Olson 2007)

The testing procedures consist of three methods. Method A is known as the "wetting-after-loading tests on multiple specimens" and consists of measuring the swelling of identical soil samples, either remolded or taken from in-situ deposits, over a minimum of four different overburden pressures. The prepared or trimmed soil samples have a minimum initial height of 20 mm (0.8 in) and a minimum diameter of 50 mm (2.0 in) and have their initial water content and dry density measured within ±0.01 g/cm^3. Remolded specimens use only soils that pass the number 10 sieve. The soil samples are first compressed under a given overburden load, and then water is added to allow the sample to swell with free access to water. The sample height is measured at time intervals of 0.5, 1, 2, 4, 8, 15, 30, 60 minutes, etc. up until a time between 24 to 72 hours or whenever primary swelling finishes. A typical swelling curve versus time is shown in Figure 2.6.

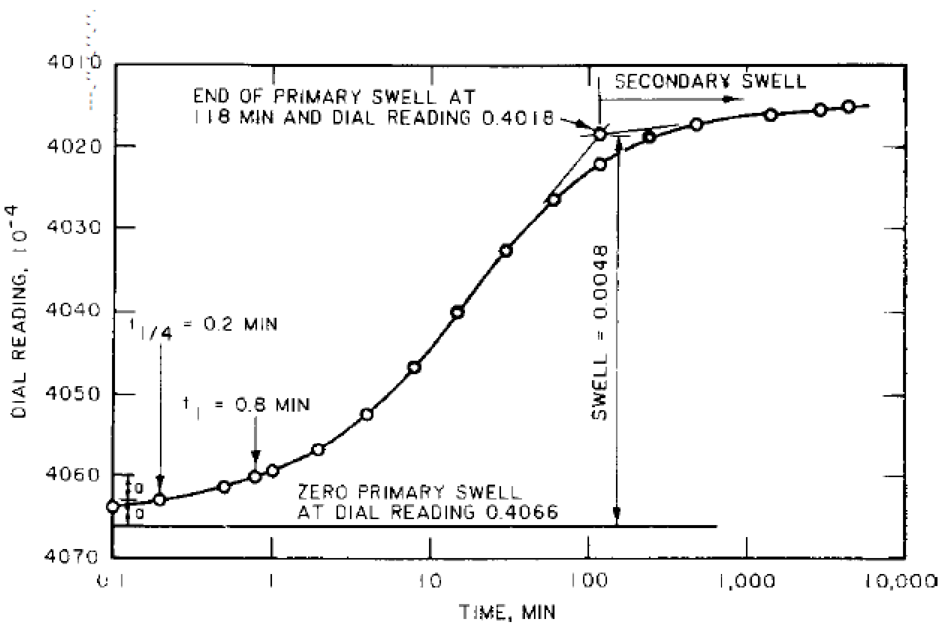

Figure 2.6: Swelling versus Time Curve for ASTM D4546 Method A

Combining the maximum primary swelling at each of the four overburden pressures, a swelling versus stress curve can be generated from the given data. The swell pressure, or the minimum pressure at which no swelling occurs, can then be determined via interpolation of the data. A typical swell versus stress curve is shown in Figure 2.7.

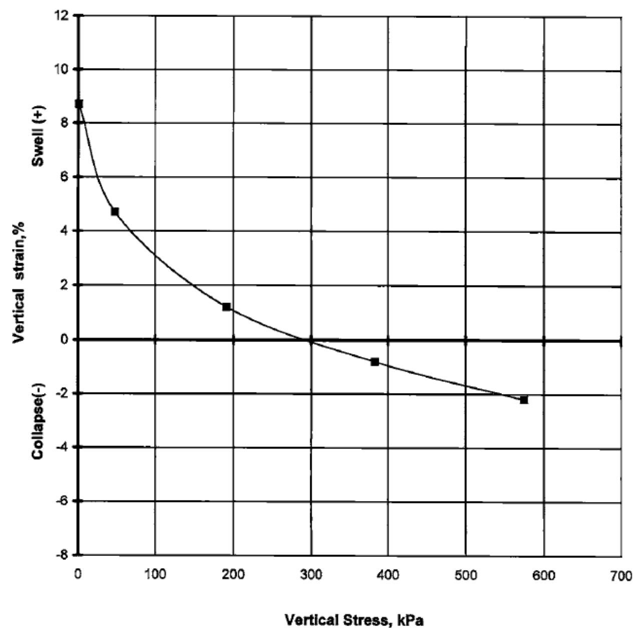

Figure 2.7: Deformation of Soil Samples versus Stress (ASTM D4546 Method A)

Method B consists of measuring the swell of a soil sample of a single in-situ sample at an overburden pressure similar to one encountered in the field. The method is comparable to Method A and is commonly known as the "single point wetting-after-loading test on a single specimen." Method C measures what is the deformation from loading a soil sample that has freely swelled. The soil sample is first swelled with no overburden load applied, and then a load is applied to determine the change in volume. This method is commonly used to match situations in which the soil has already swollen for the addition of more fill and/or structures and is similar to a consolidation test.

Issues with this test are that the specimens are typically the worst case scenario as the soil samples are inundated as compared to the infiltration typically seen in the field. Therefore, the final saturation of the soil (around 90-95%) is typically higher than seen in the field, and thus, the test provides an upper limit on in-situ conditions. The soil samples used in this test are typically taken from remolded specimens and may not see similar structures as seen in-situ, and bigger particles (i.e. those that don't pass the number 10 sieve) are typically not used in the test. Due to these issues, the soil samples may not match what is seen in the field due to non-representation of the granular particles, and the wetting may not be uniform in the field. Finally, the secondary swell that exists within the test, as seen in Figure 2.6, can be a significant factor and may last a long duration. Therefore, these methods are typically not always done due to the time requirements.

2.3.2 Swell Pressure Testing

The swell pressure taken from ASTM D4546 Method A can also be determined via a different experimental method. The set-up and procedure is similar to Method A in the ASTM, but the sample height is held constant by increasing the load to ensure that the height does not change. The sample can typically reach equilibrium within 24 hours with the overburden stress at the end of the test considered the swell pressure. This method is preferred as the experiment requires only one sample as compared to the four or more samples required in the ASTM standard.

2.3.3 Centrifuge Testing of Expansive Soils

Previous research has indicated that the use of geotechnical centrifuges can be useful in the characterization of expansive soils. The use of centrifuges is beneficial as, even with swelling that is initially driven via the suction gradient, traditional tests with the oedometer can take longer for water to permeate the specimen fully and enter the microporous structure of the clay.

The first use of centrifuge technology came from Frydman and Weisburg's test on a highly expansive soil found in Israel, the Mizra clay. The specimen was compacted to an initial height of 300 mm in lifts of 20 mm in a soil column with 3 mm diameter steel balls between lifts. Additionally, transducers were place between lifts in order to determine the advancing water front. Water was ponded above the sample and held constant via a control system with sand at the base in order to have a freely draining system. The steel balls were able to measure the strain within the soil and moisture content via gamma rays. Stresses were determined via assuming steady state conditions, and the corresponding swell potential is shown in Figure 2.8.

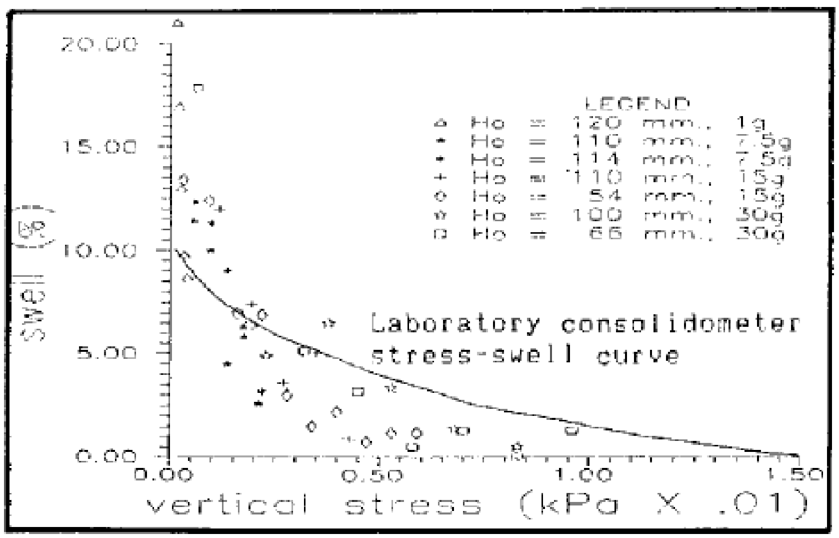

Figure 2.8: Swell versus Effective Stress for the Mizra Clay (Frydman and Weisburg 1991)

Further, Frydman and Weisburg noticed that differential swelling increased between the steel balls at the center of the specimen and the edges of the specimen as the overburden stress increased. Therefore, the difference in swell between the centrifuge and traditional test were attributed to side wall friction.

Gadre and Chandrasekaran also tested the swelling of a highly plastic clay, the Black Cotton soil (LL=71%, PI=32%) taken from a soil deposit near Bombay, India using centrifuge technology. Their samples consisted of the soil compacted to a density of 1.4 g/cc in a 75mm diameter consolidation ring with a thickness of 12.5 mm. Water was allowed to flow through the bottom of the sample at various g-levels, and the height was continuously monitored by a LVDT in the centrifuge apparatus. The apparatus set-up and swelling results over a variation of layer thickness are shown in Figures 2.9 and 2.10. Note that the layer thickness was varied by an increase in the centrifuge acceleration, i.e. higher g-levels would produce a “thicker” layer for their calculations. This layer thickness can also be thought of as a surcharge stress in the 1-G testing program.

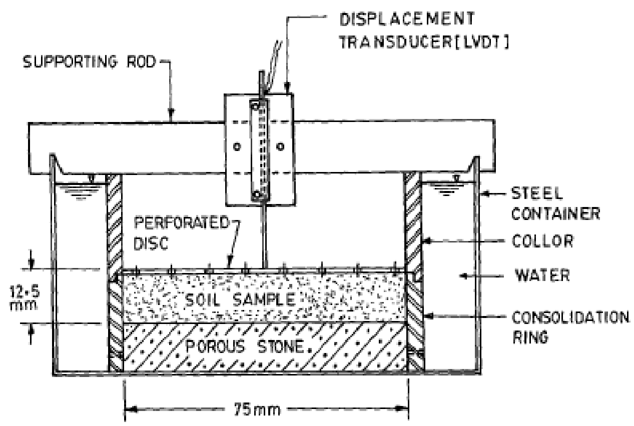

Figure 2.9: Experimental Setup for Centrifuge Testing (Garde and Chandrasekaran 1994)

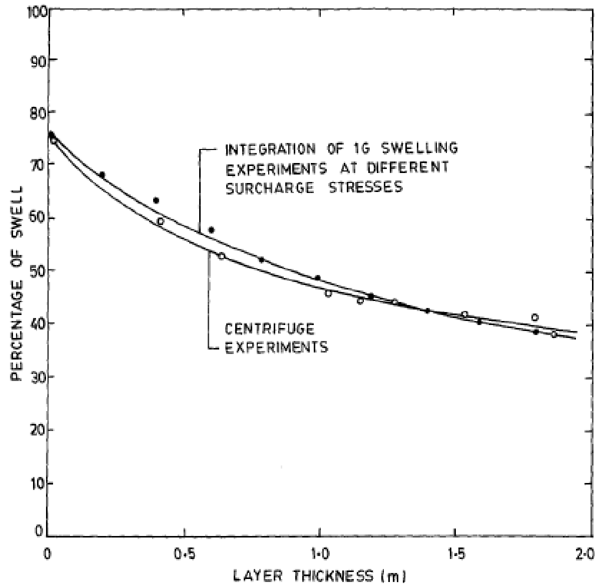

Figure 2.10: Swelling Potential versus Layer Thickness (Garde and Chandrasekaran 1994)

The soil swelled very rapidly for this experiment as most of the swell was seen within 30 minutes of the addition of water. While the results are not thoroughly expanded upon, the authors were able to demonstrate that centrifuge testing using an LVDT was possible and that the results were very similar to results taken from the 1-G swelling test.

Work previously completed at the University of Texas at Austin by Plaisted (2009), Kuhn (2011), and Walker (2012) has demonstrated the capability to characterize the swelling potential of a soil using a small centrifuge set-up with an in-flight data acquisition system. Plaisted's research involved testing reconstituted specimens of the Eagle Ford Shale within a centrifuge. The specimens were compacted to the optimum moisture content of 24% and a dry density of 1.55 g/cc, corresponding to a relative compaction of 100% of the standard proctor compaction dry density. The samples were run at heights of 1 and 2 cm at various g-levels and overburden. Water was infiltrated through the top portion of the specimen with an initial height of water of 2 cm, and the specimens were run for 3 days and measured for their final heights at the end of the test via a mounted caliper. The set-up for this centrifuge method is shown in Figure 2.11, and the swelling versus time is shown between the centrifuge and free swell data in Figure 2.12.

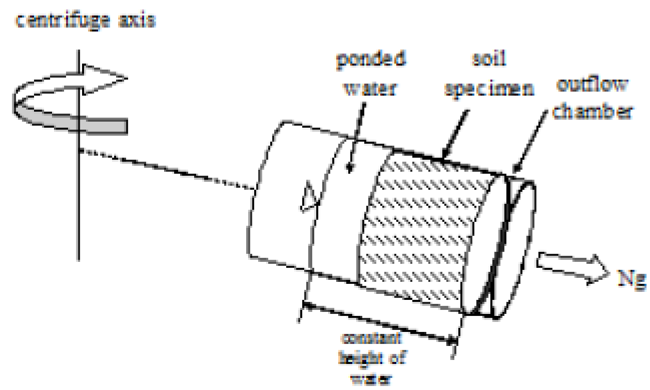

Figure 2.11: Testing Set-up for Centrifuge Swelling of Eagle Ford Shale (Plaisted 2009)

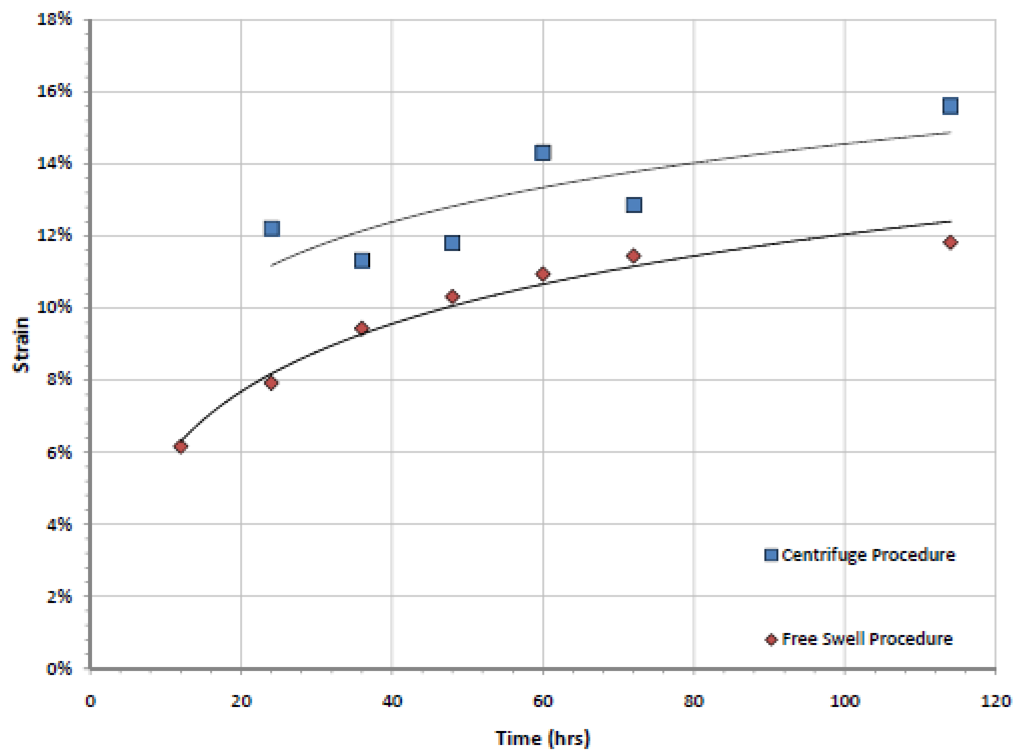

Figure 2.12: Swelling versus Time between Test Methods (Plaisted 2009)

Note that the centrifuge procedure produced more scatter and a higher swell than the free swell (ASTM D4546) method. It is the author's opinion that this difference can be explained as the centrifuge samples had to be removed from their loaded condition and measured after being removed from the centrifuge. Thus, the sample could freely swell in the few minutes between the centrifuge powering down and the researcher measuring the swell of a sample. However, Plaisted was able to demonstrate that a set-up for testing the swell of a highly plastic clay could be achieved with the resources available at the University of Texas.

Kuhn in 2010 also researched the swelling behavior of the Eagle Ford Shale at similar compaction conditions but performed the research in a larger scale centrifuge that was designed by the University of Texas at Austin. This centrifuge was able to successfully measure the swelling of a soil during the testing process without having to remove the sample from its loading condition. Samples were run at 25, 50, and 100 g's for two scenarios. Scenario i) involved testing with samples that had a constant water height and surcharge mass, thereby leading to the only variable being the g-level. Scenario ii) involved testing where the surcharge mass and water height were modified to maintain a constant water pressure at 400 psf and a constant total stress. This scenario was achieved by doubling the mass of surcharge and height of water whenever the g-level was doubled. Results showing the final void ratio, a measure of swell as the samples began at the same initial void ratio, versus the total stress are shown in Figure 2.13 for both scenarios.

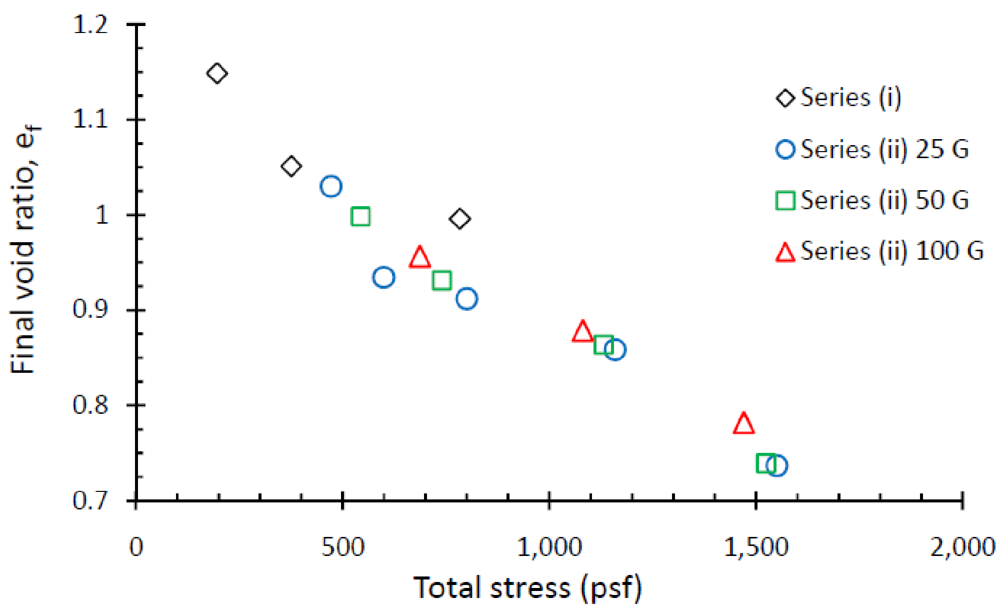

Figure 2.13: Final Void Ratio versus Total Stress for Large Centrifuge Testing (Kuhn 2010)

Both scenarios gave similar results and demonstrated that either method is useful in order to evaluate the swelling of a soil. Further, adding a linear position sensor allowed for direct measurement of the soil's swell during testing, allowing for comparisons between the ASTM D4546 test and centrifuge testing. Also, the rate of primary and secondary swell was shown to be correlated with the total stress in the sample and the g-level. Unfortunately, this testing was completed in a large centrifuge that was impractical for use in practice.

Walker's research (Walker 2012) focused on using a LPS in the testing set-up originally developed by Plaisted (2009). Walker was able to change the set-up in the centrifuge such that a linear position sensor was able to continuously measure the strain in the sample throughout the set-up. Further, the centrifuge was used to examine how the compaction conditions of a soil affected the final strain felt by a specimen. The relationship between swell and moisture content and the compaction dry density were then determined. Figures 2.14 and 2.15 detailed the compaction conditions versus swell for the Eagle Ford Shale.

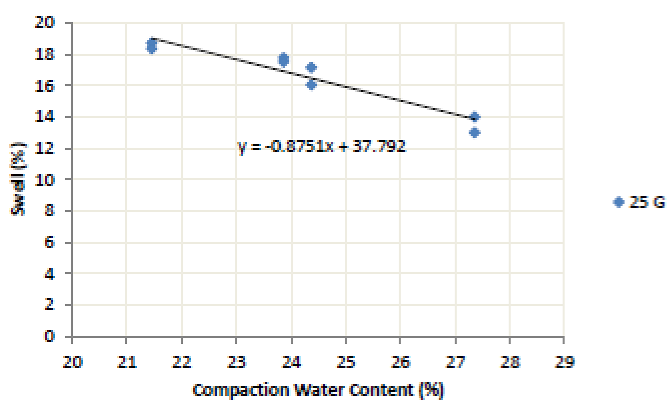

Figure 2.14: Swell versus Compaction Water Content under Constant Gravitational Acceleration for Eagle Ford Shale (Walker 2012)

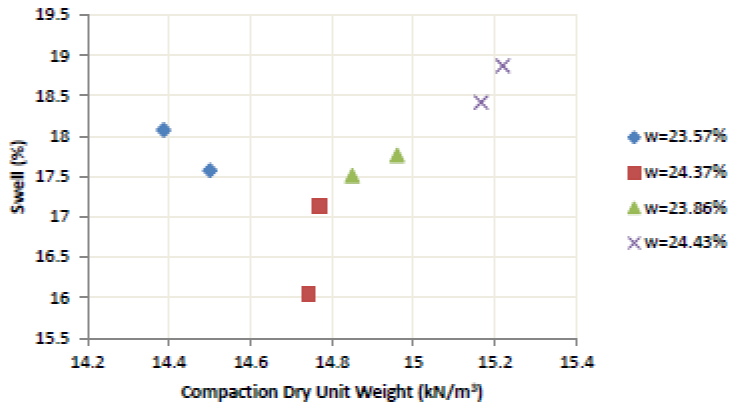

Figure 2.15: Swell versus Compaction Dry Unit Weight under Constant Gravitational Acceleration for Eagle Ford Shale (Walker 2012)

The correlation between swelling and the moisture content is very clear from Figure 2.14 as a 5% difference in the moisture content led to approximately a 4% difference in the swell of the Eagle Ford shale. However, the correlation between the dry unit weight and the swelling is not as clear as seen from Figure 2.15. Thus, Walker was able to demonstrate that a linear position sensor could be used in the small centrifuge and the effect of the initial moisture content on swelling.

2.4 Cyclic Wetting and Drying and Effects on Swelling

Some, but not enough, testing has been done to understand the effects that the cyclic wetting and drying has on the properties of expansive soils as generally most testing is done on recompacted, processed specimens. Initial test on understanding the effects of cyclic swelling and drying was done by Dif and Bluemel (1991) on undisturbed samples taken from the field (height 20-25 mm, diameter 70 mm) in a modified oedometer that allowed for shrinkage based on pumping in air from the top and bottom porous stone for the removal of water. The moisture content was then based on weighing the ring between cycles. The results for one of the clays are shown in Figure 2.16.

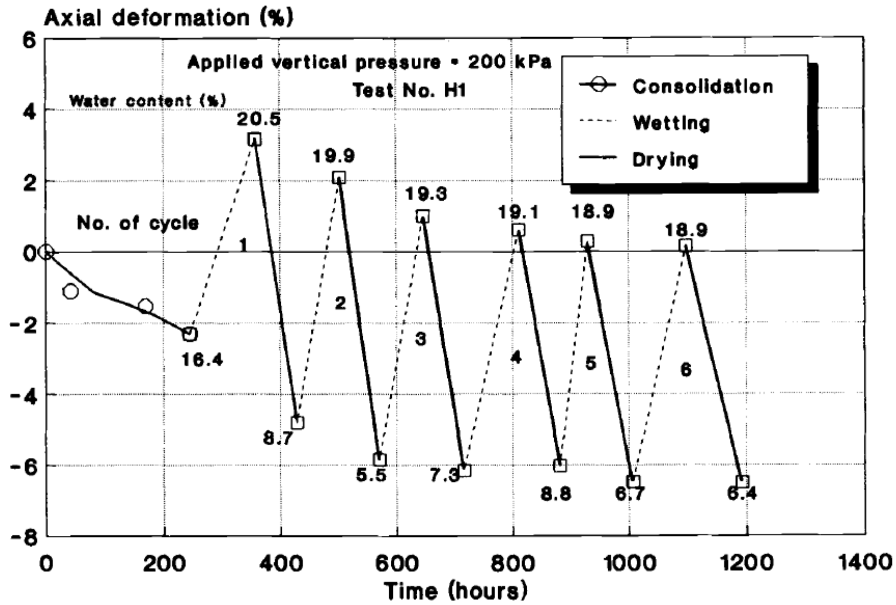

Figure 2.16: Effect of Cyclic Wetting and Drying on the Hohenggelsen Clay (Dif and Bluemel 1991)

As can be seen, the amount of swelling decreased after each cycle, and after about 3 cycles, an insignificant change in the axial deformation is seen for both drying and swelling. However, this amount is still significantly lower than the initial swelling and shrinking of the soil, showing that even undisturbed samples have effects from repeated cyclic moisture changes. Further testing from Zemenu, Martine, and Roger (2009) examined the effects that these cyclic cycles have on the drying-wetting path and the microstructure of the clay. As shown in Figure 2.17, the soil water retention curve is shown for the studied Parisian clay, the Argile verte de Romainville, on six separate samples. Note that the blue line indicates the swelling cycle and the pink line indicates the shrinkage cycle with Wr being the shrinkage limit of the soil.

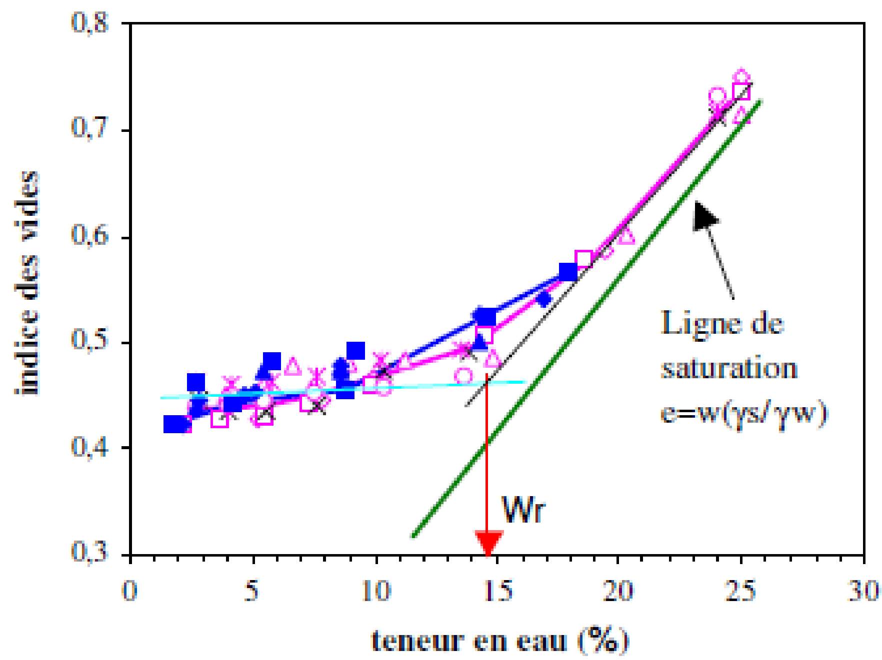

Figure 2.17: Moisture Content versus Void Ratio for an Expansive Soil (Zemenu et al. 2009).

As can be seen, the clay can remain near saturated for extended periods of moisture contents above the shrinkage limit of the soil, and below the limit, the void ratio remains nearly constant. The researchers were also able to view the soil structure of an expansive clay at the maximum swelling by removing the soil, cutting samples, freezing the samples immediately in liquid nitrogen and then using sublimation. The scanning electron microscope photos are shown in Figure 2.18 at its natural state (a), and after 1 (b), 3 (c), and 5 (d) cycles of swelling. The photos illustrate that the natural state of a soil remains a very layered structure that sees the plates of the soil remain close to each other, whereas increased amounts of free swelling leads to a more distributed structure that sees the micro-pores become macro-pores with dispersed structures.

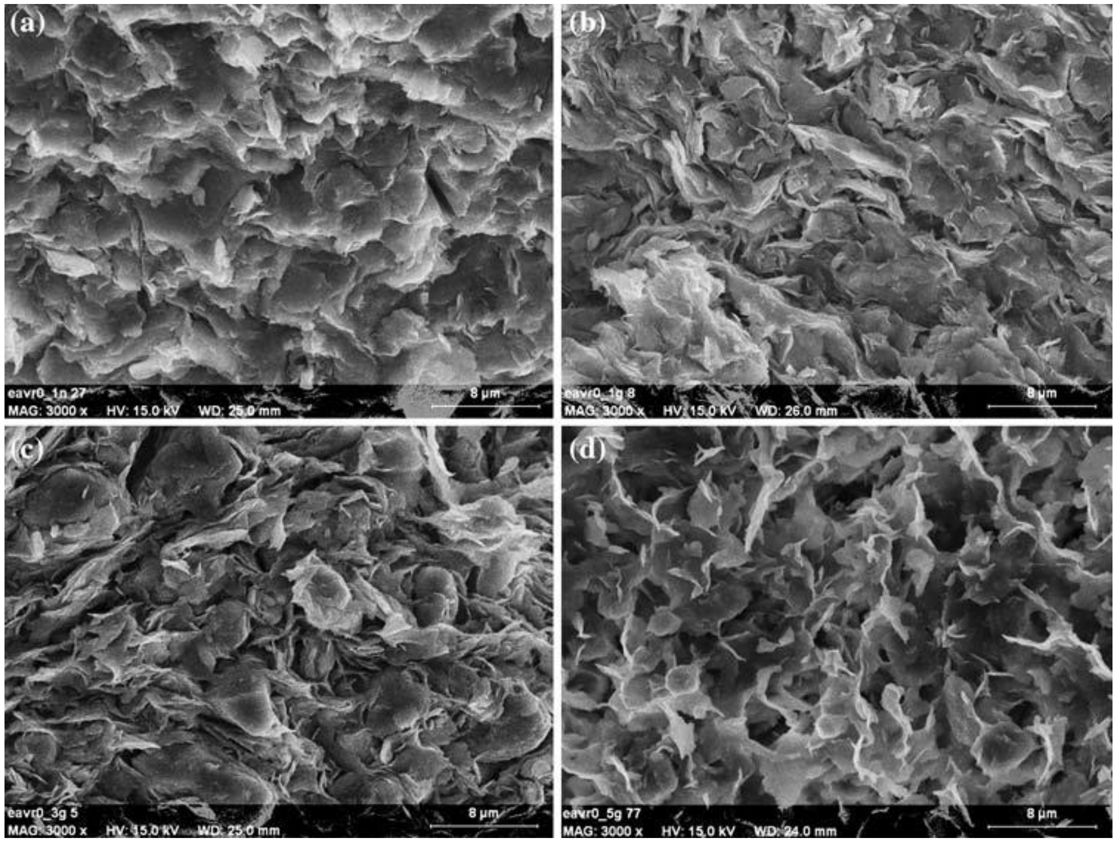

Figure 2.18: SEM Photos of Swelling of Argile verte de Romainville after 0, 1, 3, and 5 Cycles of Swelling (Zemenu et al. 2009)

Cyclic moisture changes in the soil also have significant impacts on the soil water retention curve of a soil (SWRC) that drive the suction of soil into the micro-pores of the soil. Lin and Cerato (2013) examined the effect of cyclic shrink-swell for a hysteretic soil water characteristic curve (HSWCC) of the Eagle Ford clay compacted at the optimum moisture content and maximum dry density as determined by the standard proctor test. The HSWCC of the Eagle Ford is shown in Figure 2.19. Hysteresis was important between the primary drying and swelling curves as the macro-pores in the structure decrease significantly during drying, changing the fabric of the structure such that soil would not be able to take in as much water into its pores at low suction values. Another change in the curve came between the primary wetting and secondary drying curve as the clay particles rearranged themselves during the wetting cycle allowing for a more homogenous structure. However, hysteresis tends to decrease after the initial swelling and drying cycle, but the initial change between cycles is significant. Thus, cyclic swelling and drying shows that there are significant impacts past the initial swelling and drying of a soil that is not captured via the swelling of recompacted specimens

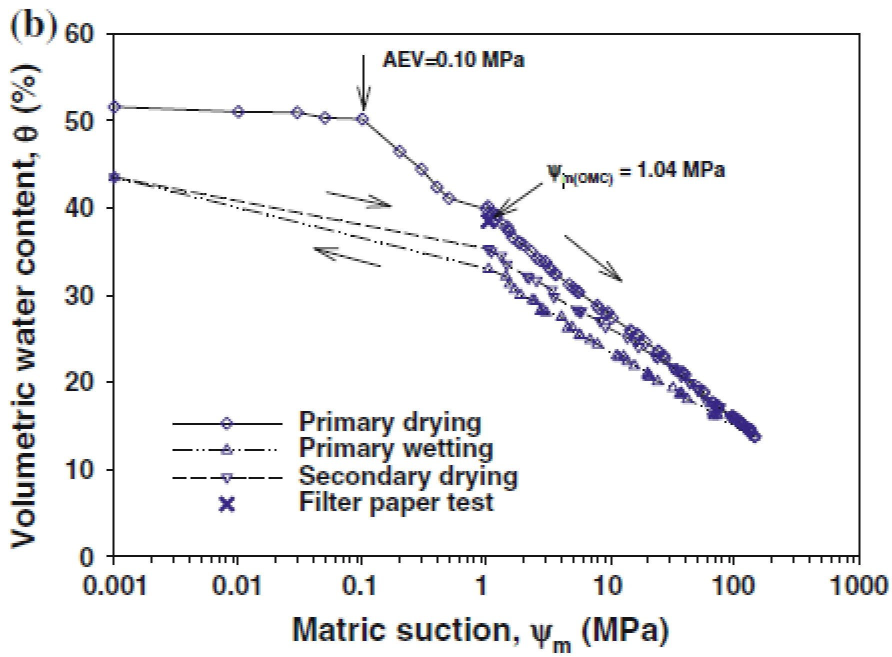

Figure 2.19: Hysteresis Soil Characteristic Curve of Eagle Ford Clay (Lin and Cerato 2012)

2.5 Effect of Sample Preparation on Swelling

Another key factor in the swelling of a soil is the preparation method for swelling. Attom, Abu-Zreig, and Obaidat (2001) examined the effect that the preparation of a soil sample influenced the swelling by comparing the swelling potential between samples that were compacted statically by applying a vertical static load, kneaded with a pneumatic compactor, and dynamically via the standard proctor test against the results from an undisturbed sample. The results from the test are shown in Figure 2.20.

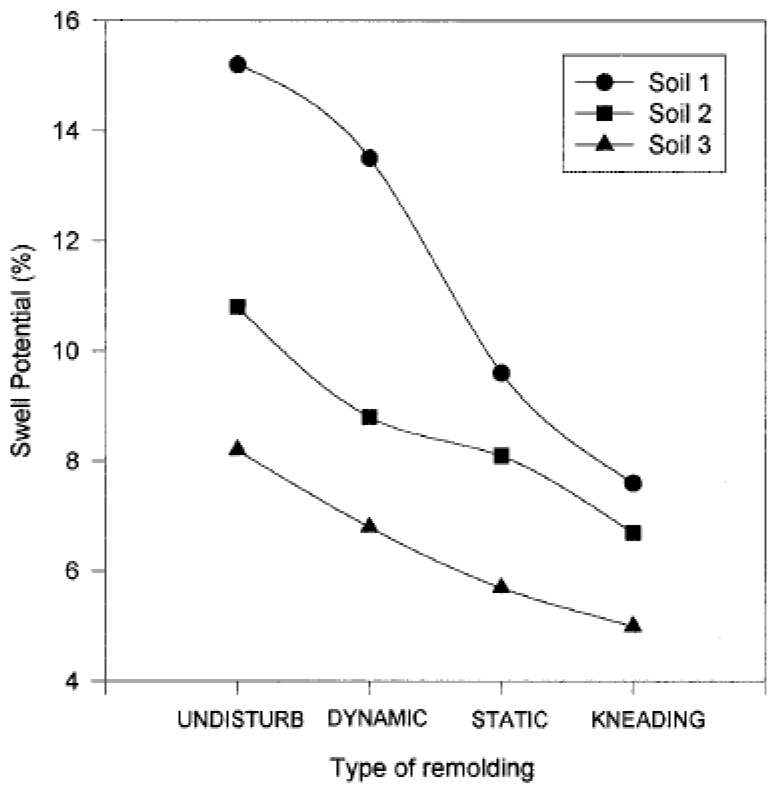

Figure 2.20: Swelling Potential versus Compaction Method (Attom et al. 2001)

The undisturbed sample had the highest amount of swelling for all three soils as the same prepared moisture content and density for the compacted tests based upon the undisturbed samples. Further, the type of compaction showed a significant influence on the swelling of a soil. Since the densities were the same, the difference in the swell can be explained by the difference in the fabric of the clays based on their microstructures. As the undisturbed sample had a significant amount of time to sediment and form, thixotropy could have caused the micropores to begin at a much smaller value, leading to an increased amount of swell. Thus, recompacted specimens may not accurately depict the conditions in the field to determine the vertical strain of a soil.

2.6 Effect of Impact Compaction on Soil Structure

Lambe (1958) examined at the structure of clay soils after impact compaction for soils compacted both dry and wet of the optimum moisture content. Their findings are that soils that are compacted dry of the optimum moisture content tend to have flocculated structures, or more random clay plate orientation, due to the inability of the diffuse double layer to be fully developed, whereas soils that are compacted wet of the optimum moisture content tend to have a dispersed structure, or more uniform distribution of clay plate orientation, due an increase in repulsion from the diffuse double layer. A visual representation of these structures along with the compaction curve is shown in Figure 2.21.

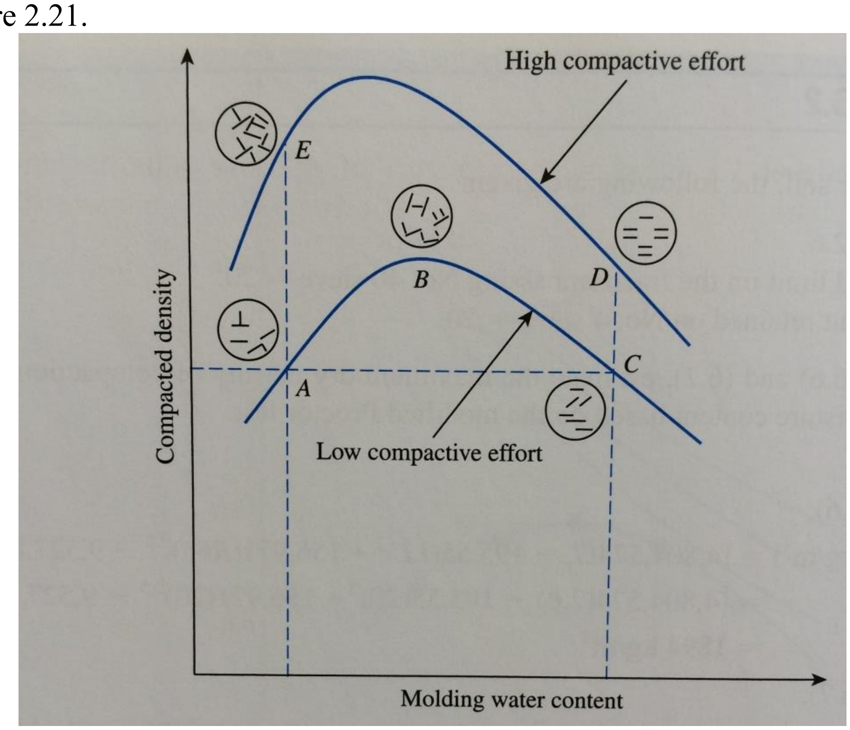

Figure 2.21: Structure of Impact Compacted Clays (Reconstructed from Lambe 1958)

This structure of the clay can dramatically change the mechanical properties of the soil, namely the shear strength, stiffness, hydraulic conductivity, and swelling and shrinking properties (Zornberg 2012). For the shear strength, the soils compacted dry of optimum tend to have a higher shear strength due to the flocculated structure and an increase in the effective stresses from the suction of the soil as compared to those soils compacted wet of optimum. For stiffness, soils compacted dry of optimum tend to be stiffer, but also more brittle, when compared to those soils compacted wet of optimum for impact compaction. For the hydraulic conductivity, soils compacted dry of optimum tend to have a higher hydraulic conductivity as compared to those compacted wet of optimum due to piping effect of larger inter particle voids which can transmit water more easily. Finally, soils compacted dry of optimum tend to swell more upon wetting and shrink less upon drying as compared to those compacted wet of optimum. As such, the structure of the soil after impact compaction is important in analyzing the mechanical and hydraulic behavior of soils.

Chapter 3: Soil Characterization

The soil used in this study was taken from a reconstruction of a roadway near Paige, TX. The soil was taken from open cuts during the extension of SH-21 and was sampled at eight locations. The site is approximately 45 miles to the east of Austin, TX in Bastrop County and is shown in Figure 3.1. A view of the Cook Mountain formation is shown in Figure 3.2 as observed in a cut conducted during field installation of moisture sensors.

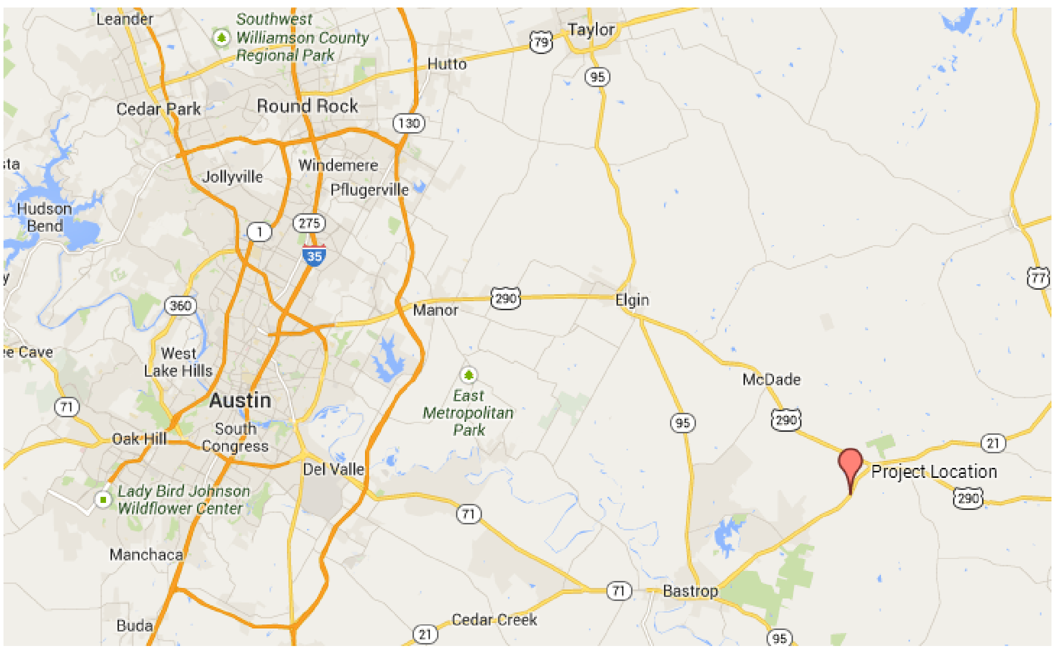

Figure 3.1: Location of Soil Sampling Site

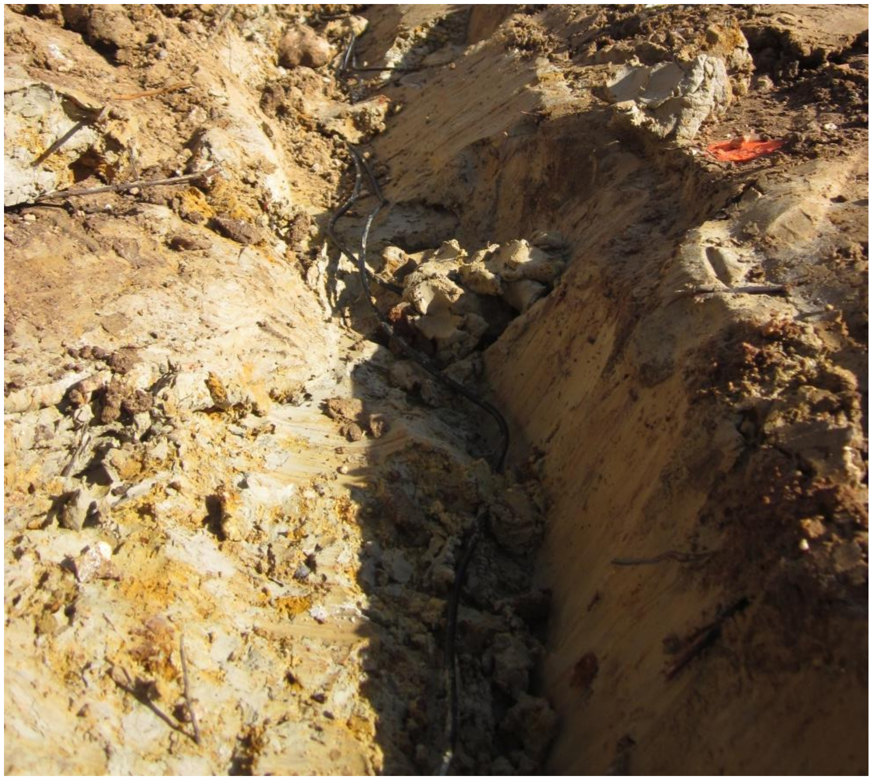

Figure 3.2: Exposed Cut of Cook Mountain Formation during Installation of Moisture Sensors

The soils were combined after an analysis determined that similar soils existed at seven of the eight sites, and the combined soils were air-dried according to ASTM D698-00a. The air-dried soil was then processed by passing the soil through a rock crusher twice, and the portion of the soil that passed the No. 10 sieve was used for characterization unless otherwise noted. All moisture contents are gravimetric and taken according to ASTM D1226.

3.1 Sampling and Geologic Setting

The soil deposit contained a clay that was colored with a mottled yellow, reddish brown, and red stained hue. A picture of the soils taken from the site is shown in Figure 3.3(a). Figured 3.3(b) shows a portion of the soil after the processing steps.

Figure 3.3: Cook Mountain Formation (a) view prior to processing and (b) view after post-processing (right)

The area near the construction site has a complex geologic history. The deposit was originally deposited in the Eocene era in a marine environment that consisted of either a marine-shelf or marginal marine environment that was preceded by a delta complex for the surrounding Sparta Sand (Hackley 2012). However, this formation has somewhat of an issue of the time of deposition, leading to some calling it the “Marine Yegua” formation or the Crockett Formation (Ewing 1994). While the formation may vary from a sandstone to a marine shale, the name of the soil will be referred to the Cook Mountain clay due to inadequate information on what member this portion of the Cook Mountain outcrop lays. A map of the geology in the area is shown in Figure 3.4 as taken from the 1:250,000 Geologic Atlas of Texas, Austin Sheet (Barnes 1981).

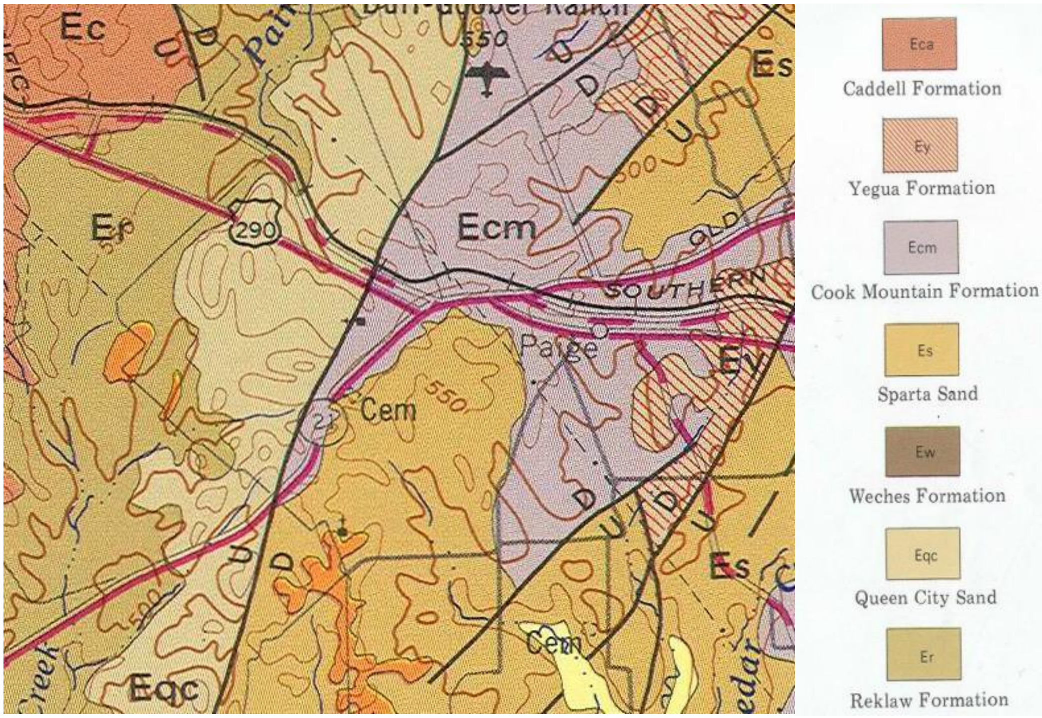

Figure 3.4: Geologic Map of the SH-21 Site (Barnes 1981)

3.2 ATTERBERG LIMITS AND USCS CLASSIFICATION

Atterberg Limits tests were conducted in accordance to ASTM D4318 using soil samples sieved through the No. 40 sieve. In order to verify that the blend was consistent, four separate buckets were prepared with equal amount by weight of soil from the seven similar sections. The Liquid Limit test procedure produced results that were consistent within ± 2% for three operators, thereby confirming that the blend produced consistent, repeatable results. The results indicated a Liquid Limit (LL) of 58%, a Plastic Limit of 17%, thereby leading to a Plasticity Index (PI) of 41%. The soil classification according to the Unified Soil Classification System (USCS) was determined to be a Fat Clay (CH) according to ASTM D2487. A summary of the results is shown in Table 3.1.

Table 3.1: Summary of Atterberg Limits and Soil Classification for the Cook Mountain Formation

Liquid Limit (LL)	58
Plastic Limit (PL)	17
Plasticity Index (PI)	41
USCS Classification	CH

3.3 Standard Proctor Test Results

In order to determine the optimum moisture content and maximum dry unit weight, the Standard Proctor test was done according to ASTM D698. The soil was mixed at a pre-determined moisture content in a large mixer prior to the test being performed. Figure 3.5 displays the compaction curve using the energy generated by the Standard Proctor test.

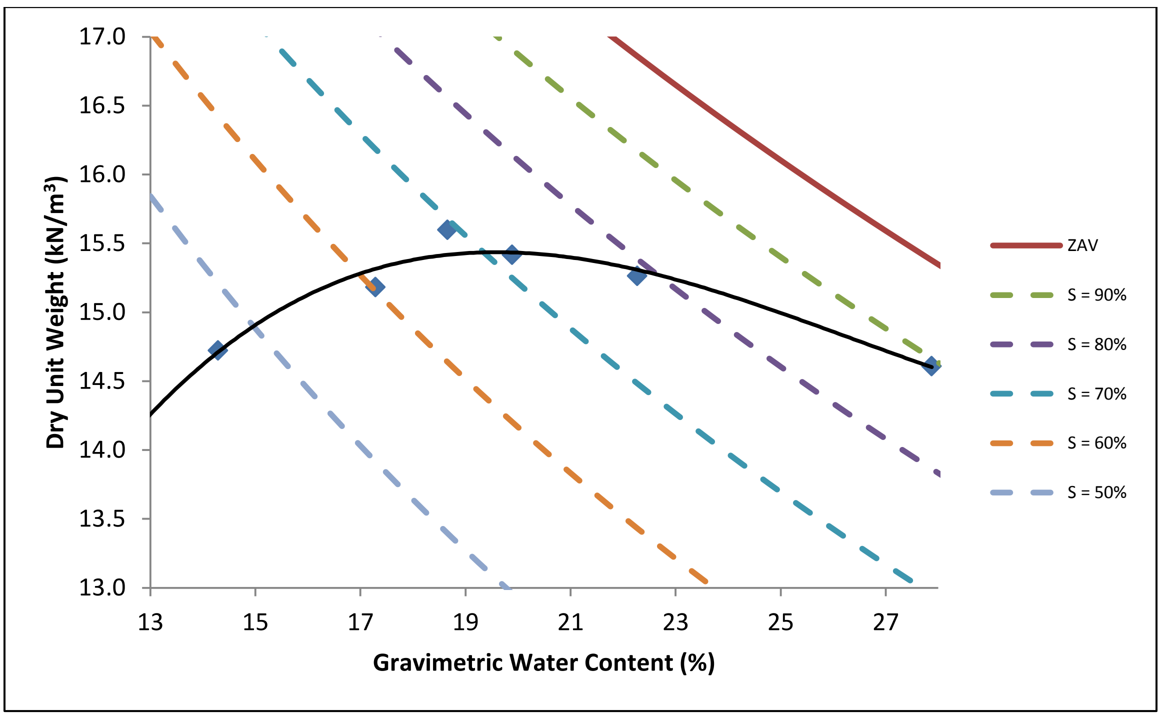

Figure 3.5: Compaction Curve for Standard Proctor Test of Cook Mountain Formation

According to the compaction curve, the optimum moisture content, $\omega_{opt,}$ is 20.0% with a maximum dry unit weight, γ_d, of 15.42 kN/m^3.

3.4 Specific Gravity

A set of specific gravity tests were performed on the processed soil that passed the No. 10 sieve. The tests were performed according to ASTM D854-10 using a 50 mL pycnometer and the boiling method of de-airing. The specific gravities at 20°C of the four tests were 2.761, 2.794, 2.782, and 2.798. The average specific gravity at 20°C used for the rest of the testing data was 2.784.

3.5 Grain Size Distribution

The grain size distribution of the Cook Mountain formation was obtained in accordance to ASTM D422-63 using the hydrometer method. The processed soil was first passed through the No. 10 sieve, with approximately 84% of the soil passing, and the hydrometer test was then performed. Figure 3.6 displays the results from the hydrometer test. According to the results of the hydrometer testing, the clay fraction for the processed soil is approximately 40%, and the activity of the soil is 0.59.

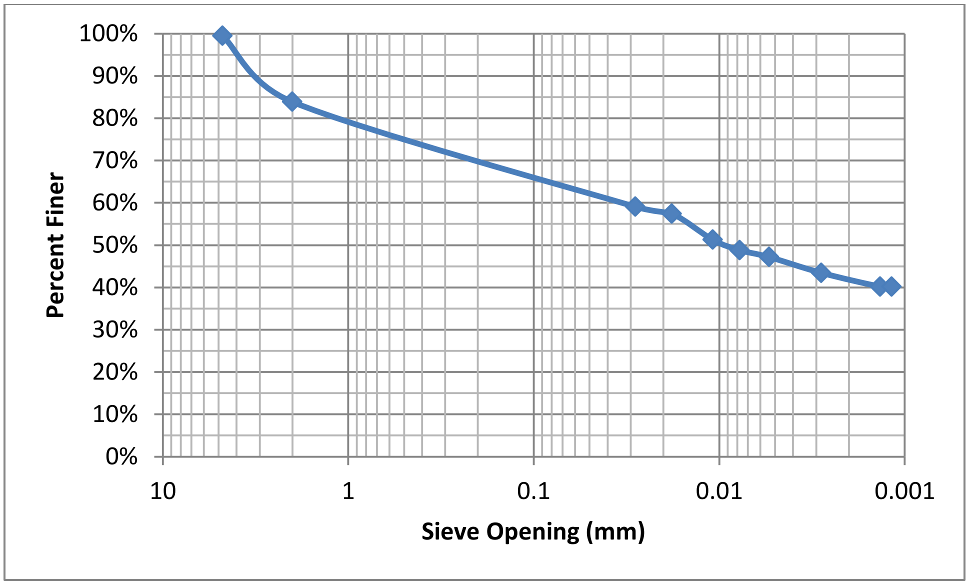

Figure 3.6: Grain Size Distribution for Cook Mountain Formation from Hydrometer Testing

3.6 Sulfate Content

In order to measure the soluble sulfate content of the soil, Oklahoma DOT method OHD L-49 was run. This method is turbidmetric and utilizes an Orion AQ4000 Colorimeter. The soil was sieved through the #10 sieve and then oven dried for 24 hours. A dilution ratio of 40 was used and yielded sulfate contents of 1288 and 524 ppm. Due to this result, the soil is considered to have a negligible amount of sulfates.

3.7 Consolidation Test Results

In order to examine the consolidation properties and how the soil changed under increased loads and rebounding, a reconstituted portion of the Cook Mountain was put through consolidation testing according to ASTM D2435 Method A. This consolidation testing consisted of loading a specimen to approximately 8000 psf of effective stress, rebounding the specimen to 500 psf, loading the specimen from that 500 psf to 64,000 psf, and rebounding the specimen to 250 psf. The soil was compacted at an initial moisture content of 20.1% and at a dry density of approximately 1.57 g/cm^3. The void ratio versus axial effective stress in psf is shown in Figure 3.7.

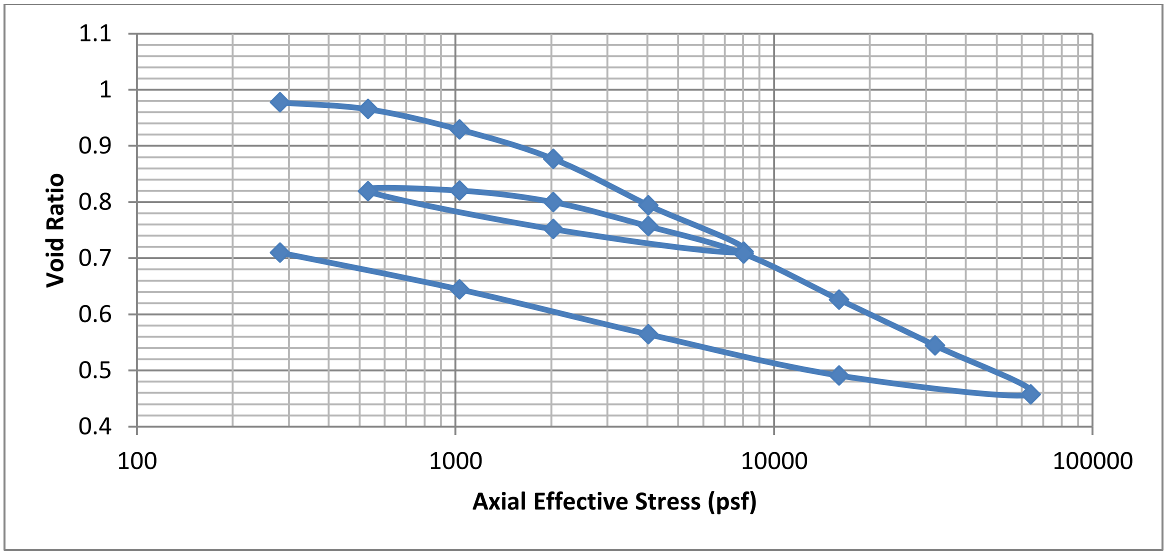

Figure 3.7: Void Ratio versus Effective Stress obtained from Consolidation Test

Based on this information, the compression index, C_c, was determined to be 0.281, the first swell index, C_{s1} was determined to be 0.90, and the second swell index, C_{s2}, was determined to be 0.121. This data was used to determine that the change of head during the single infiltration centrifuge test was a negligible cause for the secondary swelling in the infiltration method of centrifuge testing.

3.8 Scanning Electron Microscope Imaging

In order to get a better understanding of the Cook Mountain formation at the micro-level, a scanning electron microscope (SEM) at the Microscopy and Imaging Facility of the Institute for Cellular and Molecular Biology at The University of Texas at Austin was used. This SEM has the advantage of being able to get clear visualization of soil particles that tend to have a charging effect on them by providing clear imaging at a lower accelerating voltage, 5 kV, as compared to the typical voltage of 15 kV. Samples were taken from the processed soil, and a platinum coating of 10 nm was applied prior to testing to prevent charging from occurring too rapidly. SEM images taken are shown in Figures 3.8 and 3.9.

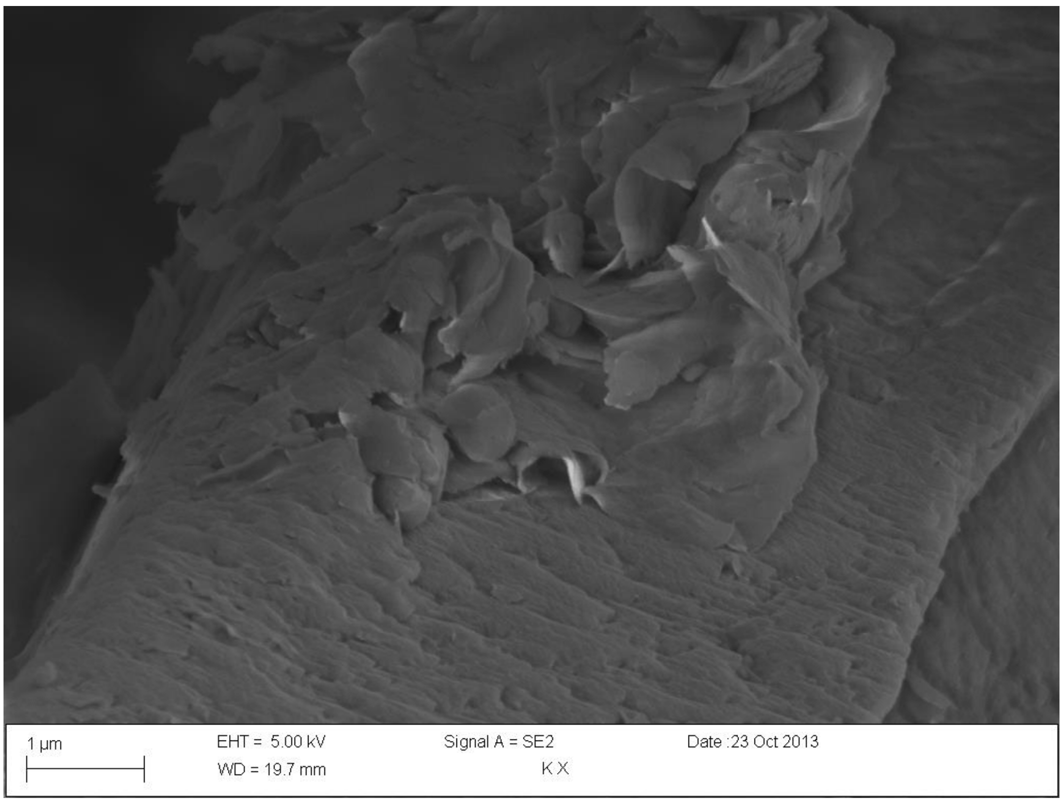

Figure 3.8: SEM Image of Montmorillonite in a Sample of Cook Mountain Clay

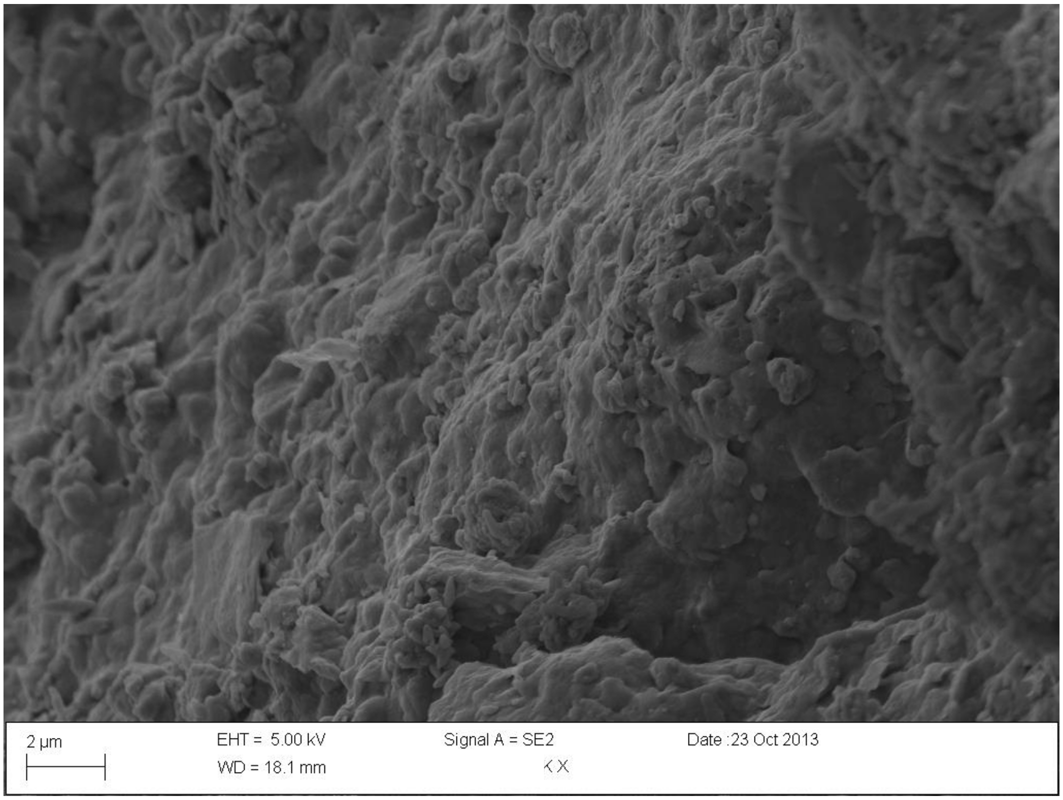

Figure 3.9: SEM Image of Fabric of Processed Cook Mountain Soil

From the imaging, the montmorillonite located at high magnifications on the Cook Mountain are a good indicator that the soil will swell significantly. The bedding pattern within them indicates that at a micro-level, the soil has significantly dispersed to the point at which the diffuse double layer was prevalent prior to sampling from the field. Further, combining the knowledge that this soil was originally a sedimentary deposit from a marine environment, the presence of illite can be seen in Figure 3.9 through some of the larger plates.

Chapter 4: Equipment, Materials and Procedures

4.1 CENTRIFUGE TESTING SET-UP

4.1.1 Centrifuges

The first centrifuge used in this project is the Damon IEC CRU-500 Centrifuge. The centrifuge consists of a Model 259 rotor that has a capacity of six centrifuge cups and a control board. The control board has knobs for speed, temperature and a timer as well as buttons to start and stop the centrifuge and a switch to change the rate at which the centrifuge stops. Pictures of the centrifuge and centrifuge control board are shown in Figure 4.1. This centrifuge was the main centrifuge for testing as it allows for the direct application of the seating load as well as has the capability of reaching g-levels up to 200 g's.

Figure 4.1: Damon IEC CRU-500 Centrifuge and Control Board (Walker 2012)

The second centrifuge used in the project is a Damon IEC EXD Centrifuge. The centrifuge is floor mounted and also has a Model 249 Rotor. This centrifuge is different in that the rotational velocity is controlled by a power knob located on the centrifuge that ranges from 0 to 100 and correlates to a power level for the motor. However, an issue with the too much vibration from an excessive power level indicates that this centrifuge can only be used for g-levels that range from approximately 5 to 40 g's. Thus, the seating load that was applied to specimens had to be correlated based on the longer start up time for the centrifuge. These issues led to this centrifuge only being used for reconstituted specimens in the original set-up for the characterization of the stress-swell curve at baseline conditions. The centrifuge is displayed in Figure 4.2.

Figure 4.2: Damon IEC XRD Centrifuge (Plaisted 2009)

4.1.2 Centrifuge Buckets and Data Acquisition System

The Model 249 Rotor has six arms on which centrifuge cups can be placed. Metal centrifuge buckets are placed in all six arms. Two centrifuge cups are used for the data acquisition system (DAS) and its battery supply, and the other four cups are used for testing of specimens. The rotor in the Damon IEC CRU-500 centrifuge is shown below in Figure 4.3.

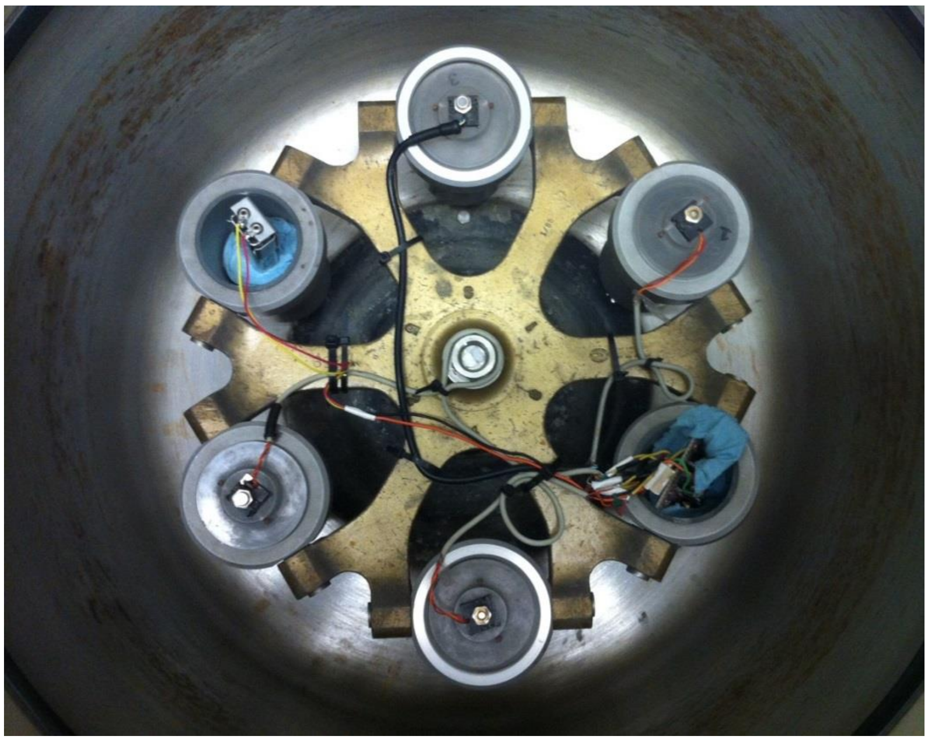

Figure 4.3: Model 249 Rotor in the IEC CRU-500 Centrifuge

Two separate types of metal buckets are used during testing of the reconstituted specimens in the original set-up, IEC Models CAT 384 and 384S. Model 384 buckets weigh approximately 457.5g and contains a smooth interior, which is used to place a permeameter cup to hold the DAS and power source. These buckets had holes drilled in the bottom of them to prevent a vacuum from being generated, thereby allowed the permeameter cups to be removed more quickly. Therefore, these buckets were only used in the testing of reconstituted specimens as well as for housing the DAS and power supply source. Model 384S buckets weigh between 434 and 434.5 g and did not contain holes at the bottom of the cups. By not having holes at the bottom, the buckets were allowed to create a constant head during double infiltration centrifuge testing to prevent moisture from leaving the centrifuge buckets. Further, to prevent a vacuum, the buckets were milled out an additional 0.1" from the inner diameter to prevent water from being forced out via capillarity. This model was only used during the double infiltration centrifuge testing. Both models contain manufactured notches at the top portion of the cup to fit into the hangers of the rotor, and, therefore, let the cups spin perpendicular to axis of rotation of the centrifuge. The two models are shown in Figure 4.4.

Figure 4.4: IEC Models CAT 384 (top left) and interior (bottom left) and 834s (top right) and interior (bottom right)

The DAS works by using Linear Position Sensors (LPS) that are placed on the top portion of the centrifuge cups prior to testing as shown in Figure 4.5.

Figure 4.5: Linear Position Sensor (LPS) used in DAS (Walker 2012)

These LPS can monitor the heights of the soil samples during the testing process which are relayed back to a computer by an internal JeeNode Arduino with an analog-to-digital converter (ADC) along with readings from an accelerometer that measures the g-level at approximately the radius of the middle of the soil. The internal JeeNode Arduino transmits this information to the computer via an external JeeNode Arduino which is connected to the computer with an USB connection. A LabView program is used to write the raw voltage data from the LPS sensors and accelerometer to text files.

4.1.3 Permeameter Set-up for Single Infiltration Procedure

For the single infiltration set-up, a permeameter cup with a top and bottom portion, two acrylic porous disks and filter papers, and overburden weight applied via washers were needed. The top (a) and bottom (b) portions of the permeameter cup, filter papers (c) and acrylic porous disks (d) are shown in Figure 4.6.

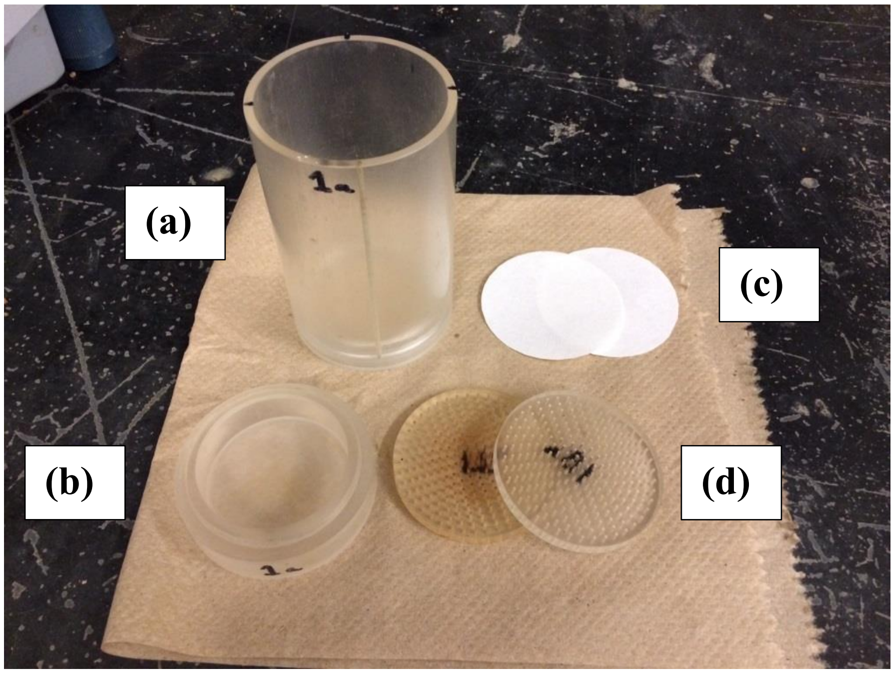

Figure 4.6: Parts of the Permeameter Set-up for Infiltration Set-up

The top portion of the permeameter cup is the portion where the soil is compacted in between two porous disk and filter paper, and the bottom portion acts as an outflow chamber for the water that passes through the soil. The bottom portion becomes very important for the calculation of stresses as the final height of water is back-calculated based on the amount of water in the chamber in conjunction with the water in the total permeameter set-up and the final moisture content of the soil. The permeameter cup allows for a specimen with a diameter of 2.26 inches and a height between 0.5 and 2 cm, though 1 cm tall samples are preferred for the a balance of speed of testing and accuracy. The acrylic porous disks are approximately 0.5 cm in height with 199 1/32” holes to allow for water to freely enter and exit the soil specimen. A picture with an assembled version of the permeameter cup for both a 1 cm and 2 cm specimen is shown in Figure 4.7.

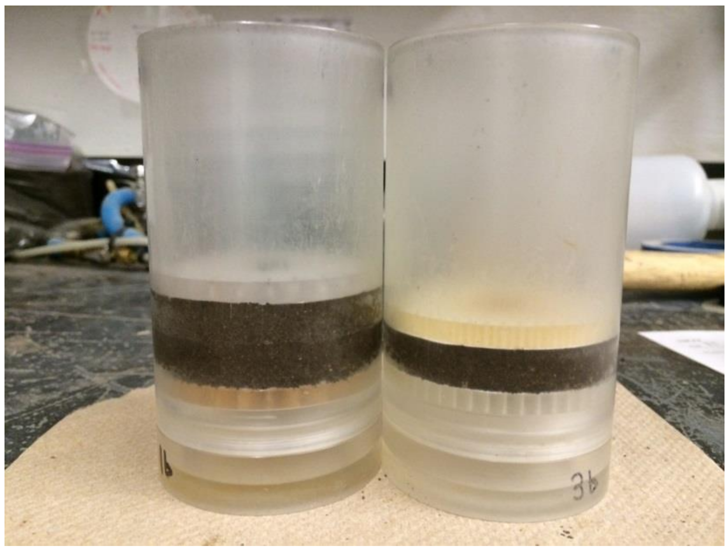

Figure 4.7: Assembled Permeameter Cups for Single Infiltration Testing

4.1.4 Permeameter Set-up for Double Infiltration Procedures

For the double infiltration test set-up, a permeameter cup with a top and bottom portion, a cutting ring, and two brass porous disks and filter paper are needed. The top (a) and bottom (b) portions of the permeameter cup, porous disks (c), filter paper (d), and a cutting ring (e) are shown in Figure 4.8.

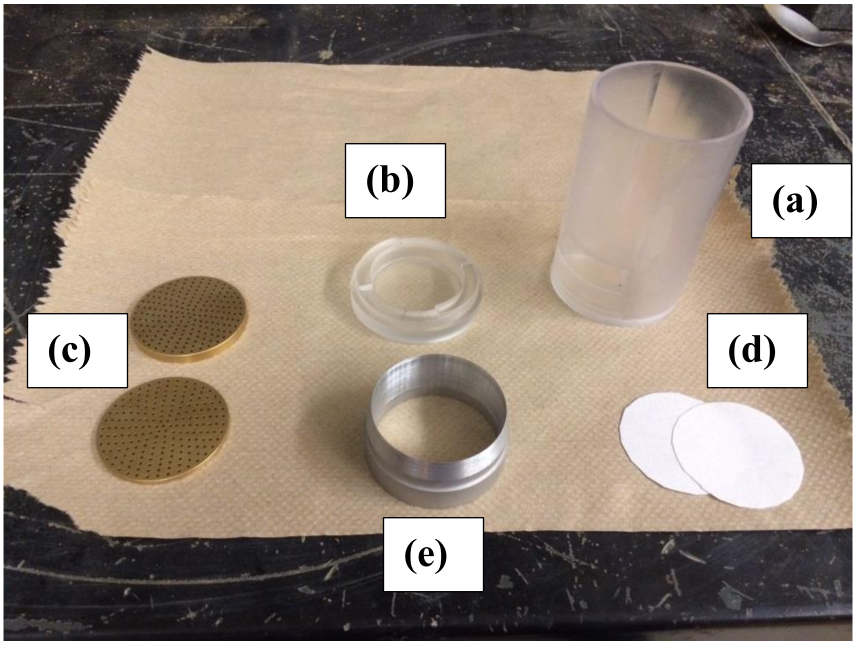

Figure 4.8: Parts of the Permeameter Set-up for Double Infiltration Set-up

The top portion of the permeameter cup contains a ledge in order to fit the cutting ring and soil specimen in through the bottom of the top portion of the permeameter cup. Further, in order to allow water from above the specimen, half of the top portion of the permeameter cup was milled out to allow for water to go past the cutting ring and enter the bottom portion of the cup. These features are shown in Figure 4.9.

Figure 4.9: Top View of Top Portion of Permeameter Cup for Double Infiltration Centrifuge Set-up

The bottom portion of the permeameter cup is similar to that from the single infiltration test but was no longer an outflow chamber. Instead, the bottom portion of the permeameter cup was notched above the threading to allow for direct access of water between the top and bottom portions of the cup. This notched feature is shown in Figure 4.10. Thus, the pore water pressure is known at the top and bottom portion of the soil sample, thereby eliminating complications in the derivation of stresses and allowing for a constant head of water after the end of primary swelling.

Figure 4.10: View of Notches in Bottom Portion of New Permeameter Cup

The porous disks vary in height with one being 0.5 cm in height, which was used for allowing water to enter the soil via the top, take an average height of swelling of the soil specimen, and the application of an overburden weight, and the other being 0.25 cm in height, which was used for the base of the set-up. The porous disks were made from naval brass which allowed for a much higher submerged weight for use as an overburden during test as compared to acrylic or aluminum due to its high specific gravity and were approximately 2 inches in diameter. Approximately 199 1/32" holes were drilled to allow for water to enter the soil specimen.

The cutting ring is approximately 2.67 cm in height, with a 2.00 inch inner diameter, and a 2.24 inch outer diameter. The ring was made from aluminum and allows for the testing of either 1 or 2 cm high soil samples from either reconstituted, compacted, or in-situ specimens. These dimensions were based on the minimum diameter and height as prescribed by ASTM D4546 for laboratory specimen. An assembled permeameter cup for the double infiltration centrifuge set-up is shown in Figure 4.11.

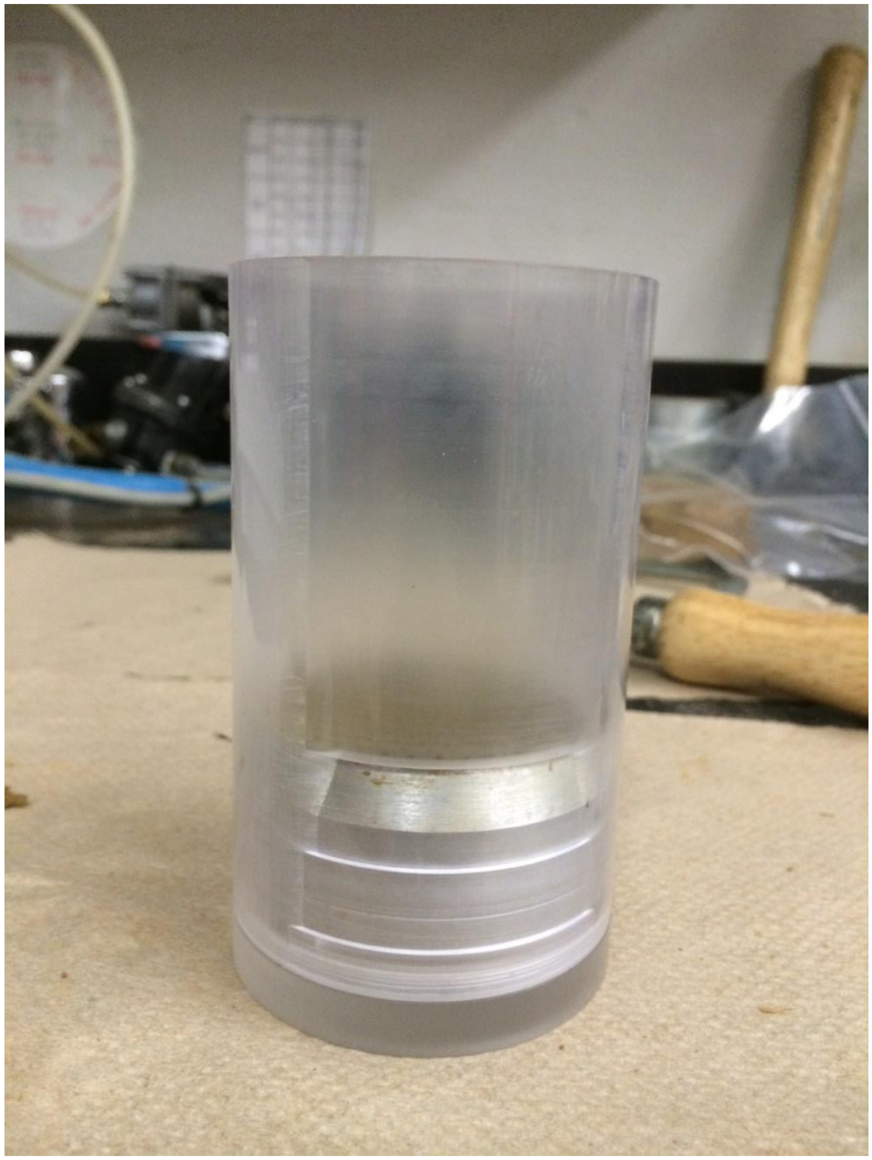

Figure 4.11: Assembled Permeameter Cup for Double Infiltration Centrifuge Set-up

4.2 ASTM D4546 EQUIPMENT

For the ASTM D4546, a standard consolidation frame from Wykeham Farrance Engineering Ltd. was used along with standard consolidation cell components outlined in Figure 2.5. A picture of the set-up in the process of testing a compacted specimen is shown in Figure 4.12. Standard weights were used to apply pressure during the compression and testing stages via the loading arm.

Figure 4.12: Consolidation Frame used for ASTM D4546 Testing

Readings for the sample height were taken via both a dial gauge and a linear variable differential transformer (LVDT). The readings from the dial gauge were used to create a linear correlation between the raw voltage readings in order to generate swell versus time curves.

4.3 Initial Soil Moisture Preparation

After processing, the soil is passed through the No. 10 sieve in order to remove large clods that may still remain. This air-dried soil had its gravimetric moisture content taken, which was approximately 6%. The soil is then mixed by adding an appropriate amount of distilled water by use of a spray bottle in a minimum of four separate watering cycles of adding water and mixing soil to ensure the soil was thoroughly and evenly distributed with moisture. The amount of water targets a moisture content that was 0.5% higher than the desired moisture content to make up for losses during the mixing process. Once the water is added, the soil is placed in an air-tight zip lock bag for at least 48 hours at which the moisture content is checked and adjusted. The total mass of soil prepared in each bag was approximately two kilograms in order to prepare enough for the soil compaction in the standard proctor mold and have a reasonable time frame for the soil's moisture content to come to equilibrium.

4.4 Soil Compaction and Sample Preparation

For the testing process with the new centrifuge method and for the ASTM D4546 comparison testing, the soil is compacted according to ASTM D698 with standard effort (i.e. 12,400 ft-lbf/ft^3). After the soil is prepared at desired compaction moisture content, compaction is done in three separate lifts with 25 blows per layer using a 5.5 lb compaction hammer and a drop height of 12 inches. Compaction results in a 4.584 in high, 4 in diameter soil specimen. Any additional soil above the top of the proctor mold is trimmed using a straight edge piece of iron. After extruding the sample, the sample is quartered using a hand saw and wire saw in order to create four specimens to test. Testing was conducted using an initial test moisture content that could be equal to the sample's as-compacted moisture content or at a different moisture content. Moisture conditioning was needed if the initial test moisture content was different than the as-compacted moisture content. For the moisture conditioned samples, the sample either had its moisture content lowered or raised. If moisture conditioning was required to lower the as-compacted moisture, the sample was cut into the cutting ring for either the ASTM D4546 tests or the new double infiltration method and allowed to dry for enough time to reach the desired moisture content, typically going from a wet moisture condition to a dry moisture conditions within 24 to 36 hours. After samples had dried out, they are placed in air tight zip lock bags and sealed until testing. If moisture conditioning was required to raise the as-compacted moisture, the samples were trimmed to a slightly wider diameter than the cutting ring and had distilled water added. The distilled water was added in approximately 3 separate sprays in order to allow for the moisture to absorb into the soil as opposed to ponding on top of the trimmed soil. The samples are then sealed in air tight zip lock bags until testing. Issues arising from the change in moisture conditions are expanded upon in Chapter 6.

4.5 ASTM D4546 Test Procedure

The testing based on the swelling of a soil in the consolidation frame was done according to a modified version of ASTM D4546-08. The following is a summary of the testing methodology for the reconstituted specimens. Note that the difference for trimmed specimen's preparation was only the trimming into the cutting ring as opposed to compaction within the cutting ring for the reconstituted specimen.

The mass of the cutting ring along with the vacuum grease and two filter papers is first weighed. Then soil is first added to the cutting ring, whether that is through a reconstituted specimen being compacted within it or by trimming a compacted specimen into it. The weight of cutting ring and soil is then noted. The cutting ring is then placed in the consolidation cell, underlain by a porous disk and overlain by a top porous disk and loading point. The consolidation frame's arm is then leveled, and the zero height is taken via both a dial gage indicator and a LVDT. The program TestNet is then started, and the compression of the specimen begins by applying a 125 psf load as a seating load akin to the seating load in the centrifuge test with the height taken. The desired stress is then applied, and the specimen is allowed to compress until the change in compression is negligible, typically after 40 to 60 minutes. The height is then taken, and then the specimen is inundated with water and allowed to freely swell. Once swelling is completed after 48 hours, the final height is noted, and the specimen is removed and weighed for its gravimetric moisture contents both at the beginning and end of the test.

The measured variables during the test are the masses of the initial wet soil, the final wet soil, and the dry soil after oven drying as well as the height of the sample during compaction or trimming and during the test. From these masses and the height measurements, the variables that can be calculated from the test results are the strain, the moisture content at the beginning and end of the test, the void ratio and saturation. The stress was taken by the stress applied via the weights during testing as well as including the mass of the top porous stone and loading ball.

4.6 Single Infiltration Centrifuge Procedures

For the swell testing on the reconstituted specimens, the methodology follows that which was reported by Zornberg et al. (2013). A summary of the testing method is presented here.

- After the soil is prepared according to Section 4.3, the top and bottom portion of the permeameter cup are weighed separately, and then together assembled with the bottom porous disk, filter paper, and vacuum grease placed to a height of 1 cm above the bottom porous disk.
- The height of the partially assembled cup is taken using a caliper and a metal plate to create an average height of the overlaying area.
- The target height of the specimen, corresponding to a specimen with a height of 1 cm, is then calculated, and a specified amount of soil is added to achieve a relative density of 100% at the optimum moisture content. A

small portion of soil from the zip lock bag is then weighed to determine the initial moisture content.

- The soil is initially compacted by slightly applying pressure via the author's thumb to create a semi-uniform surface, and then compacted using a small diameter kneading compactor to densify the soil further. This compactor creates an uneven surface; therefore, a large kneading compactor with a rubber mallet is used to create an even surface. The surface is then measured at 5 locations on the soil's surface as shown in Figure 4.13 using the metal plate, and the process is repeated until a uniform surface at the desired height is achieved.

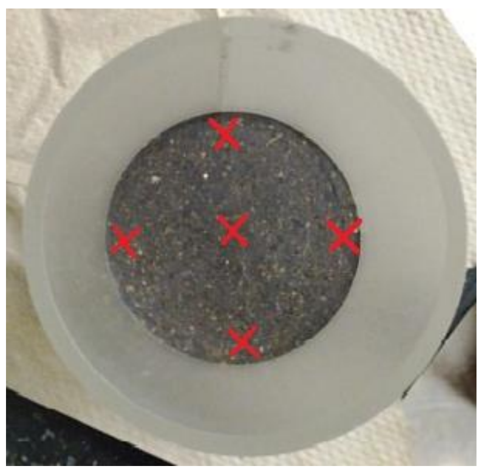

Figure 4.13: Locations of the Height Measurements in the Permeameter Cup (Walker 2012)

- The mass of the cup and compacted soil is then taken to determine the actual amount of soil added to the cup.
- The top filter paper and porous disks are then added, and the sample is then weighed again along with taking the height at the center of specimen.

- Two sets of overburden washers are weighed and added with the first set being the overburden applied only during the compression cycle to take into account the stress from the water during the swelling test and the second set being the overburden washers that were applied throughout the testing process.
- The permeameter cups are then taken to the centrifuge where the LPS are placed on the top of the permeameter cups through the middle of the washers. The LabView program is then turned on that measured the LPS readings. A screenshot of the LabView program is shown below in Figure 4.14.

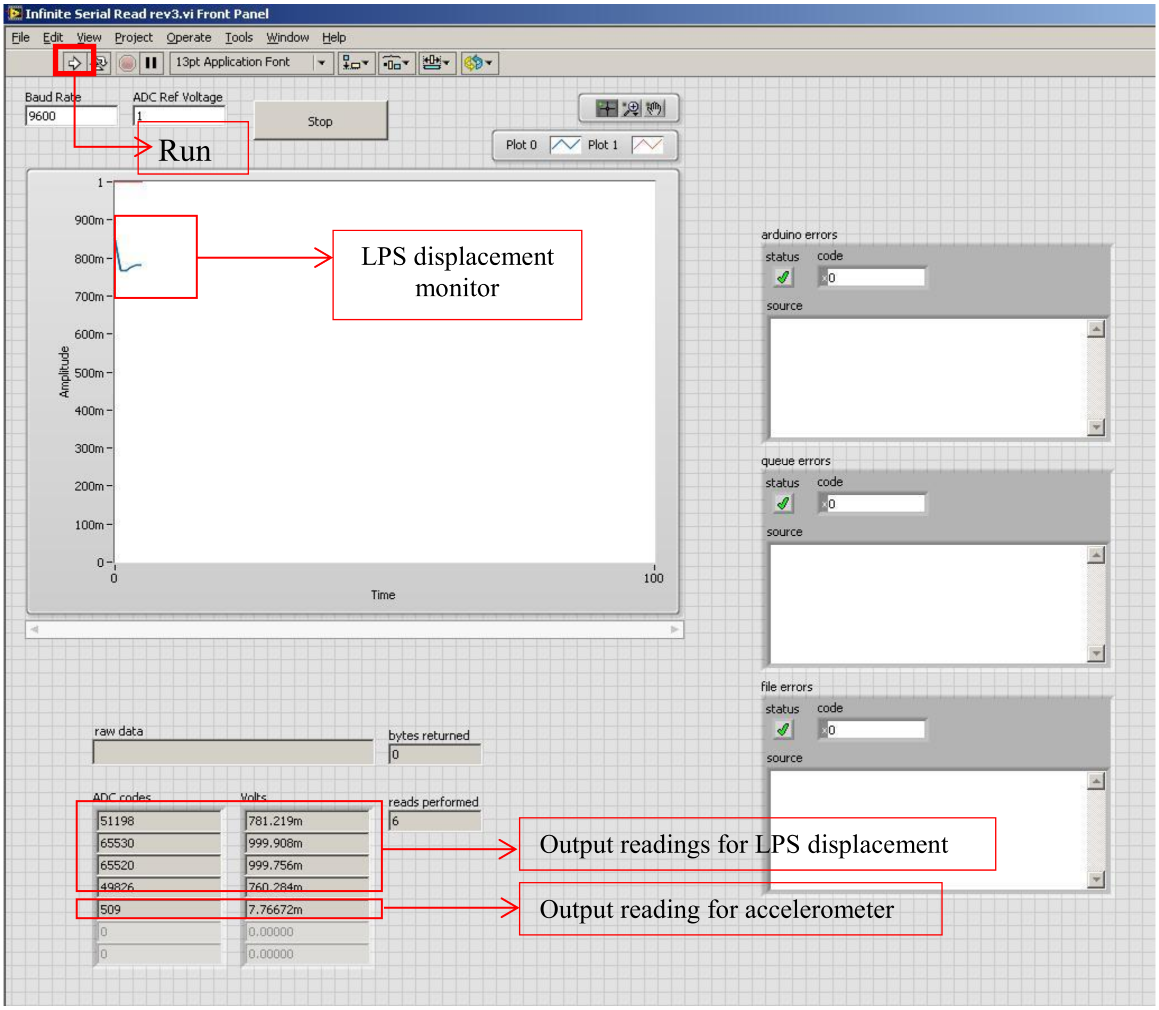

Figure 4.14: Screenshot of the LabView Program (Zornberg et al. 2013)

- The centrifuge's RPMs were then adjusted to apply only 2-3 g's for the seating load. The seating load is done to ensure that full contact was taking place between the porous disk, filter paper, and soil specimen. The centrifuge is then turned on while staying at this seating load for approximately 5 minutes.

- After the seating load cycle had completed, the RPMs were then adjusted to those for the desired testing g-level, and the soil is allowed to compress for approximately an hour.
- After the compression cycle is completed, the specimens are removed and distilled water corresponding to a 2 cm height, or 51.3 grams, is then added.
- The permeameter cups are then returned to the centrifuge, and the centrifuge is started and allowed to spin for approximately 24 – 48 hours depending on the applied stress.
- After the testing period, the centrifuge and LabView program are stopped, and the specimens are removed with the full set-up and bottom portion of the permeameter cup weighed to determine the final height of water and any loss of water. Any water at the bottom of the centrifuge buckets or centrifuge is noted. The specimens are then weighed, and their gravimetric moisture contents taken.

4.7 Double Infiltration Centrifuge Procedures

For the swell testing using the new double infiltration set-up, the specimens can either be reconstituted or compacted. For this testing to examine the fabric of the soil samples, only compacted specimens were used, thus their methodology is examined in the following sections.

4.7.1 Trimming of Soil into the Cutting Ring and Assembly of Permeameter Cup

The following list describes how a soil sample is trimmed into the cutting ring of the permeameter cup and how the assembly of the permeameter cup takes place:

- The mass of the top and bottom portion of the permeameter cup combined is taken.
- Two pieces of filter paper are carefully trimmed to the diameter of the porous disks.
- The bottom height of the cutting ring, 0.25 cm porous disk, and filter paper is measured using the caliper and metal plate from Section 4.6.
- The mass of the top 0.5 cm porous disk and filter paper combined is taken. This is considered the overburden during the testing procedure.
- Vacuum grease is added to the inner portion of the cutting ring by spreading it using one's index finger.
- The mass of the cutting ring with vacuum grease and filter papers is taken, and then the mass of the ring, filter papers, and both porous disks is taken.
- After the soil is compacted, extruded, quartered, and any additional adjustments to the moisture content has taken place as described in Section 4.4, the soil is then trimmed into the cutting ring.
    - This cutting is done careful beginning with a small insertion of the soil sample as shown below in Figure 4.15.

Figure 4.15: Insertion of Cutting Ring into Soil Sample.

- After the cutting ring is slightly inserted, the sides of the soil sample are removed via a wire saw as shown in Figure 4.16. The cutting ring is slowly inserted into the soil, and the sides of the soil are slowly removed until the cutting ring is fully inserted.

Figure 4.16: Cutting of Excess Soil during Insertion of Cutting Ring

- After the cutting ring is fully inserted, the bottom portion of the soil is trimmed in order to create a flat base.
- The soil is then extruded via the 0.5 cm porous disk and 0.25 cm in conjunction as shown in Figure 4.17. This excess soil is then trimmed, completing the process.

Figure 4.17: Extrusion of Excess Soil during Trimming

- The soil is then extruded back downwards with the 0.25 cm porous disk as the base and the 0.5 cm porous disk as the extrusion device from the top portion of the cutting ring.
- The top porous disk and filter paper is then removed, and the height of the sample is taken using the metal plate and caliper.
- The top porous disk and filter paper is re-inserted, and the mass of the complete cutting ring is taken.

- The cutting ring is then inserted into the bottom portion of the top permeameter cup and then sealed with the bottom of the permeameter cup. The completed assembly is shown in Figure 4.11.
- The mass of the completed assembly is then taken, along with the mass of the centrifuge bucket.

4.7.2 Compression Cycle and Centrifuge Testing

After all the permeameter cups are assembled in a similar fashion, the cups are then ready to be placed in centrifuge for testing. The following describes the testing procedure.

- The permeameter cups are inserted into the centrifuge buckets and placed in the centrifuge with the LPS being placed on the top portion of the permeameter cups.
- The LabView program is then started, and the samples go through a compression cycle as described in Section 4.6.
- After approximately five minutes of the seating loading and 40 minutes of compression, the centrifuge is stopped, and the samples are removed.
- Distilled water corresponding to a 2 cm height of water above the soil sample which accounts for water in the bottom portion of the permeameter cup and sides, or 78.3 g, is then added, and the cups are returned to the centrifuge. The amount of water added is noted for each test.
- The specimens are then allowed to swell for 36-48 hours or until primary swelling is completed.
- After the test is done, the centrifuge is stopped, and the centrifuge buckets and permeameter cups are removed.

- The permeameter cup within the centrifuge bucket, the permeameter cup alone, and the centrifuge bucket alone are then measured for each specimen.
- The water is removed from the permeameter cup, and the cutting ring is removed from the permeameter cup.
- The porous disks are then removed, and the cutting ring, wet sample, and filter paper are then placed in a weighing tray and placed in an oven at a temperature of 110°C in order to determine the dry mass of solids.

After testing was completed, the raw voltage data from the LPSs and accelerometer recorded from the LabView program was converted into height measurements and artificial gravitational levels using a Python script developed by Michael Plaisted and tweaked by the author. This corrected data was exported in a text file that was then used in an excel spreadsheet to process and breakdown the testing data.

4.7.3 Measured Variables and Calculated Properties

The variables that are measured during testing are the mass of the assembly, the mass of the soil prior to and after testing, the height of the soil after compaction, the change in height of the sample during the testing, and the g-level at the accelerometer in the centrifuge. From these measured variables, the calculated properties are the swelling of a sample at a given time, the initial and final moisture content, the initial and final void ratio, the initial and final saturation, the initial dry unit weight and density, the initial and final volume, the slope of the primary and secondary slopes, and the equivalent stress felt in the soil. Table 4.1 lists the calculated variables and the equations used to calculate them. Note that the equations used to calculate the stresses felt within the sample are derived and explained in Chapter 6.

Table 4.1: Equations for Calculated Variables

Property	Equation	Variables
Initial Height, h_i	$h_i = h_c + (\Delta h_{cs} - \Delta h_s)$	h_c Height of sample at compaction Δh_{cs} Change in height of sample at the end of compression Δh_s Change in height of sample at end of seating load
Strain or Swelling, S	$S = \frac{\Delta h_t}{h_i} * 100\%$	Δh_t Change in height of sample at time, t
Volume, V	$V = (h_c + \Delta h_t) * A$	A Area of sample
Dry Density of Soil, ρ_d	$\rho_d = \frac{\frac{m_s}{1+\omega_i}}{V_f}$	m_s Mass of soil at beginning of the test ω_i Initial moisture content of soil V_f Final Volume
Void Ratio, e	$e = \frac{SG * \rho_w}{\rho_d} - 1$	SG Specific Gravity of the Soil ρ_w Density of Water
Saturation, S	$S = \frac{SG * \omega}{e}$	
Slope of Swelling Curve, s	$s = \frac{\Delta h_{t2} - \Delta h_{t1}}{\ln(t_2) - \ln(t_1)} * \ln(10)$	Δh_{ti} Change in height at time *i* t_i Time *i*

4.7.4 Typical Results

After the data was processed in the excel spreadsheet, a swell versus time graph could be generated in lognormal space. A typical one, shown for a test that was run on a sample that was compacted and tested dry of optimum, is shown below in Figure 4.18.

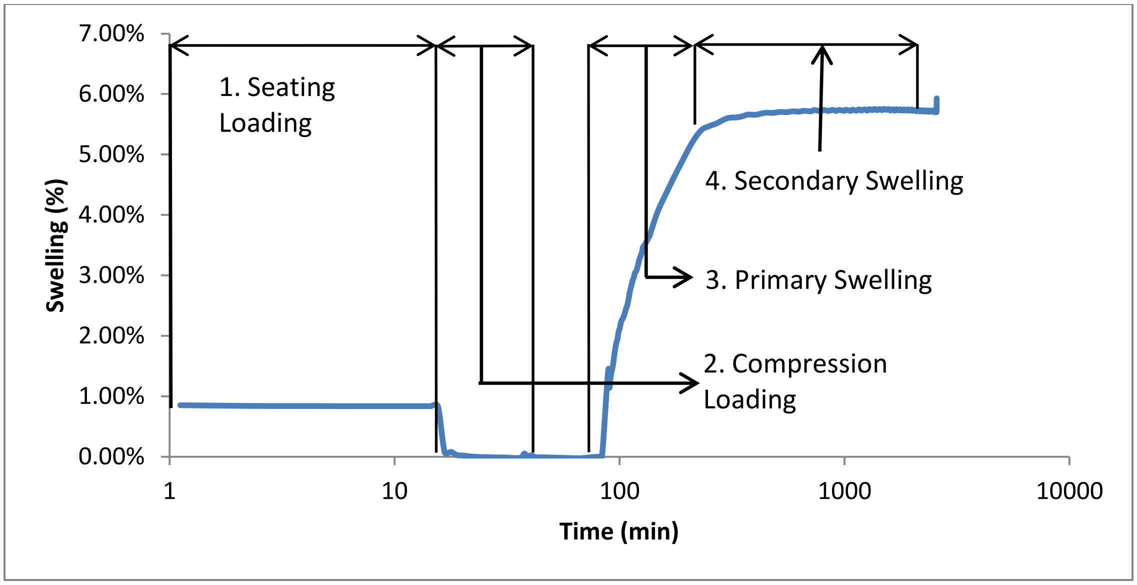

Figure 4.18: Typical Results from Double Infiltration Centrifuge Testing

As can be seen, there are four general regions in the centrifuge sample as labeled in Figure 4.18. The first region is the application of the seating load at which there is very little change in strain observed due to the small amount of stresses applied. The second region is the application of the compression load at which there is a significant amount of compression. Note that the strain in this region is nearly zero due to the initial height being located in this region as opposed to the compacted height at the beginning of the test. Thus, this compression cycle is very important as it conditions the soil for its load prior to the testing process. A gap exists between the second and third region during which the specimen is removed from the centrifuge in order to add water to the sample. After the sample is returned to the centrifuge environment, the third region is where the specimen undergoes swelling, initially due to the high suction gradient and a decrease in the macro-voids and increase in the micro-voids. The primary swelling slope is taken in this region closer towards the end of the region in order to determine how much a soil swells in a log cycle during this process as the initial stages of primary swelling will be heavily dominated by the removal of the soil from the centrifuge environment for the application of water. At the end of the third region is the inflection point, or the end of primary swelling in the soil. This point is used to define the swelling of a soil as opposed to the maximum swell felt in the soil as soils within the active zone in the field will be unlikely to feel the secondary portion of the swell versus stress curve as the soils are unlikely to be completely inundated for such a time period. The fourth region is where secondary swelling occurs at which the slope or rate of swelling is significantly decreased and fairly constant. At the end of testing, the soil does experience some additional swelling due to the centrifuge being stopped and stresses being relaxed.

Chapter 5: Testing Program and Results

The testing program involved two series. Series I involved testing of reconstituted specimens compacted at the optimum moisture content and at a density corresponding to the maximum dry unit weight according to the Standard Proctor test. Tests were conducted using the single infiltration centrifuge test and the ASTM D4546 test on 1 cm tall samples. Series II involved testing done on trimmed specimens at both as-compacted (Series IIa) and moisture conditioned moisture contents (Series IIb) using the ASTM D4546 test and the new double infiltration centrifuge test. Tables 5.1 and 5.2 show the scope of testing done in each series. In total, 12 tests were performed for the first series, whereas 34 tests were performed for the second series.

Table 5.1: Testing Matrix for Reconstituted Specimens

Testing Procedure	Amount of Tests
Centrifuge	9
ASTM D4546	3
Total	**12**

Table 5.2: Testing Matrix for Trimmed Specimens

		ASTM D4546	Centrifuge
ω_c	ω_i	Number of Tests	Number of Tests
Dry	Dry	5	2
Wet	Wet	3	2
OPT	OPT	2	2
Dry	Wet	4	2
Wet	Dry	6	2
OPT	Dry	1	1
OPT	Wet	1	1
	Total:	**22**	**12**

5.1 Results from Reconstituted Specimens

Results from tests listed on Table 5.1 are plotted in Figure 5.1 which shows the vertical swelling at the end of primary swelling versus vertical effective stress along with a curve fitting of the experimental centrifuge results. Results for each individual test can be found in Appendix A. These tests results define a baseline swelling curve that can be used as reference for comparison against tests from Table 5.2 to examine the effects of fabric and compaction techniques.

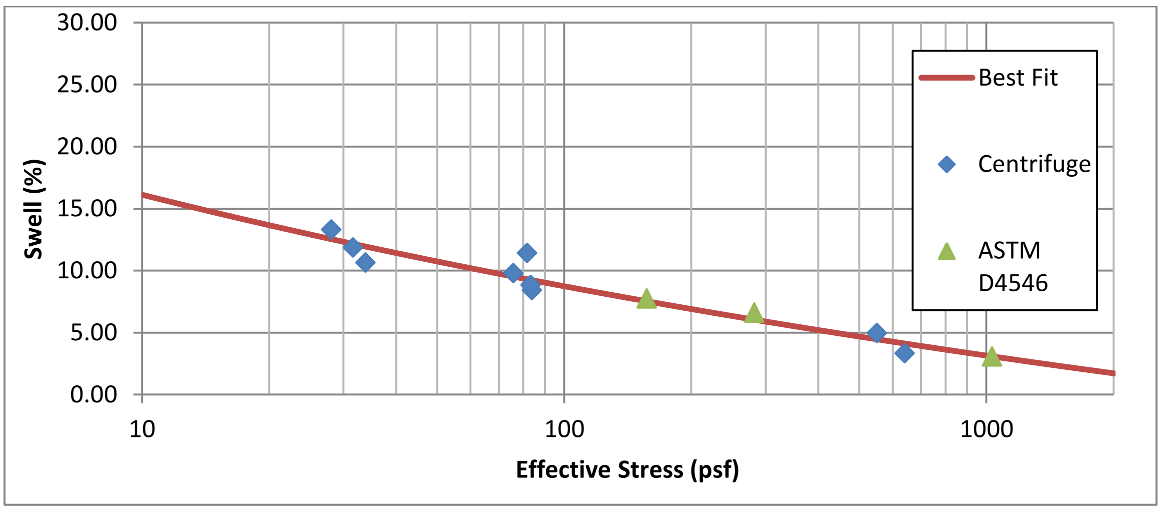

Figure 5.1: Effective Stress vs. Swell Results for Reconstituted Cook Mountain Specimens

The first observation to note is that the centrifuge testing data matches well with results from the ASTM D4546 tests. Thus, as Walker (2012) showed, the single infiltration centrifuge data produces results that are comparable to the ASTM D4546 tests, even though the infiltration is coming from the top of the soil specimen as opposed to the top and bottom of the soil specimen. Using the results from both methods, Figure 5.1 shows that the relationship between swell and effective stress is approximately log linear for the range of stresses used in this testing program. Also, significant swell can still occur beyond 1000 psf. This behavior indicates that this soil will be especially problematic for transportation projects as the soil will swell significantly in the active zone, even if the active zone extends beyond the assumed depth of 8 ft.

One of the issues with the single infiltration centrifuge set-up, the relatively small range of stresses that can be tested, is seen in Figure 5.1. For example, the first cluster of tests at approximately an effective stress of 30 psf corresponds to 5 g tests, the second cluster of tests at approximately 80 psf correspond to 25 g tests, and the last cluster of points at approximately 600 psf correspond to 200 g tests. This distribution of stresses as a function of the imposed g-level is a limitation of the original single infiltration centrifuge method as the range of stresses that can be achieved is limited due to the small amount of overburden from the acrylic porous disk and iron washers. The g-level corresponding to the same stresses for the new double infiltration centrifuge based method are much lower as the range of stresses can go from approximately 45 psf for a 5 g tests to 1800 psf for a 200 g test. Thus, an added benefit of the double infiltration centrifuge method is the ability to reach higher effective stresses that were not previously reachable in the original single infiltration centrifuge set-up as well as utilizing lower g-levels for the same stress conditions from the original centrifuge method.

Overall, the results from testing on reconstituted specimens confirmed that the Cook Mountain clay has a high capacity to swell upon wetting and produced consistent results between testing methodologies.

5.2 Results from Trimmed Specimens

To select a basis for the trimmed specimens, a target dry unit weight was selected for a consistent target between tests. In order to have a wide range in moisture content, a dry unit weight that corresponded to a relative compaction of 96%, or 14.8 kN/m^3, was selected. From the compaction curve in Chapter 3, the moisture content for a specimen compacted dry of optimum, or "dry", corresponding to this density is 15% whereas the moisture content for a specimen compacted wet of optimum, or "wet", corresponding to this density is 25.5%. Figure 5.2 illustrates the compaction curve with the target dry unit weight as a line along with the results from the proctors compacted which were used in testing of Series II.

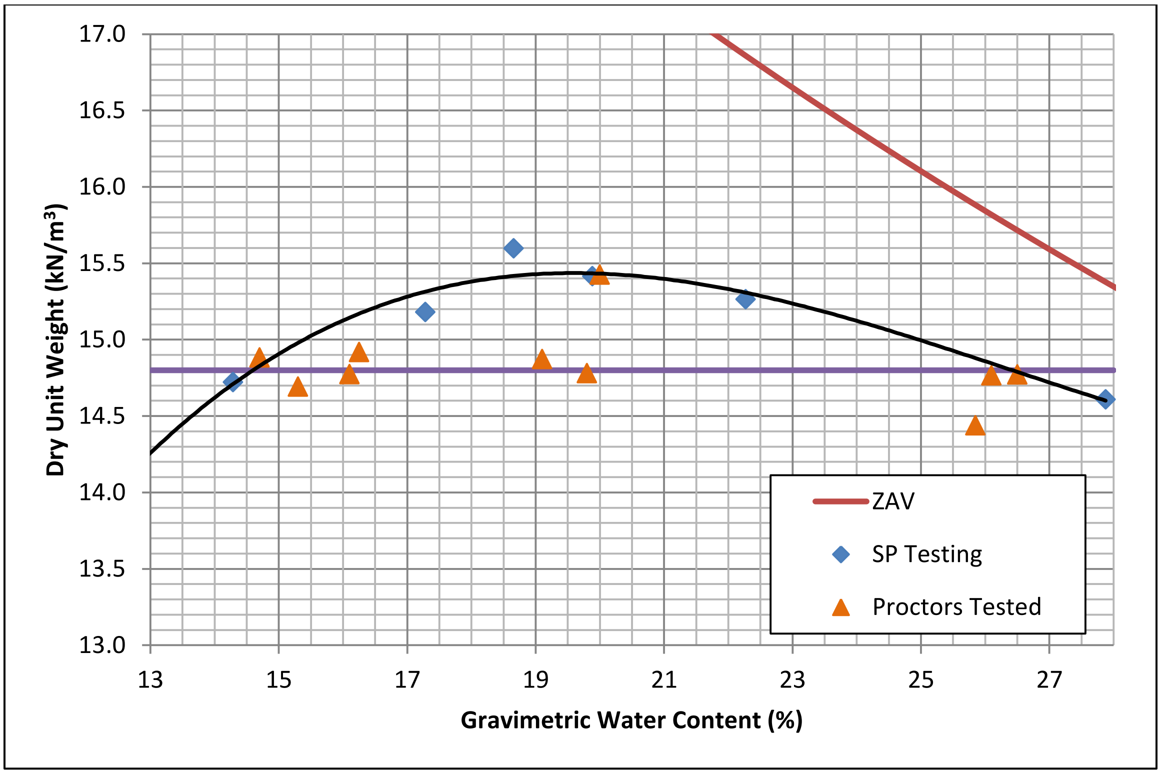

Figure 5.2: Compaction Curve and As-Compacted Conditions of Specimens Tested in Series II

As shown in Figure 5.2, there is some variability with the moisture contents of the compacted samples for testing in Series II. An issue with the compaction conditions of the specimens tested in Series II comes from the use of only one moisture content for use in the determination of the average moisture content in the specimen as opposed to the specimens from the Standard Proctor tests which used three separate moisture contents to determine an average moisture content of the compacted soil. Despite this issue, the actual dry densities of the samples from the proctor molds are all between relative compactions of 94 and 97%, which is close to the targeted relative compaction. However, issues with the dry densities of specific locations within the soil mass are expanded upon in Chapter 6. Note that there are two proctor tests that were compacted at the target dry density at the optimum moisture content due to additional sieving of the air dried particles prior to testing. These specimens were used in order to compare against specimens initially compacted at the same dry density but either dry or wet of optimum as well as a specimen compacted at the optimum conditions.

Testing of the trimmed specimens was divided in Series IIa or Series IIb. Some of the specimens were tested using an initial moisture content equal to the at compaction moisture content which composed tests for Series IIa. Other specimens were tested using an initial moisture content that was moisture conditioned from the as-compacted moisture content, which composed tests for Series IIb, in order to separate the effect of fabric on the swelling of soil with the effect of the initial moisture content. Samples that had their moisture contents raised had moisture of a calculated amount added via a spray bottle and were left to wet and reach equilibrium for approximately 24 to 48 hours in sealed zip lock bags. Samples that had their moisture contents lowered were initially trimmed into the cutting ring and subsequently extruded in order to air dry. After 12-24 hours when the samples had reached the approximate mass that corresponded to the desired moisture content, the specimens were placed in sealed zip lock bags until testing. Issues stemming from these methods of moisture conditioning are expanded upon in Chapter 6. An effective stress of 280 psf was targeted in all tests based on the stress applied in the consolidation frames via the 250 psf loading weight and porous stone. This target effective stress corresponded to a target g-level of approximately 28 g's for the double infiltration centrifuge tests. Results between a typical ASTM D4546 test and a double infiltration centrifuge test, both compacted and tested at the dry condition, are shown in Figure 5.3.

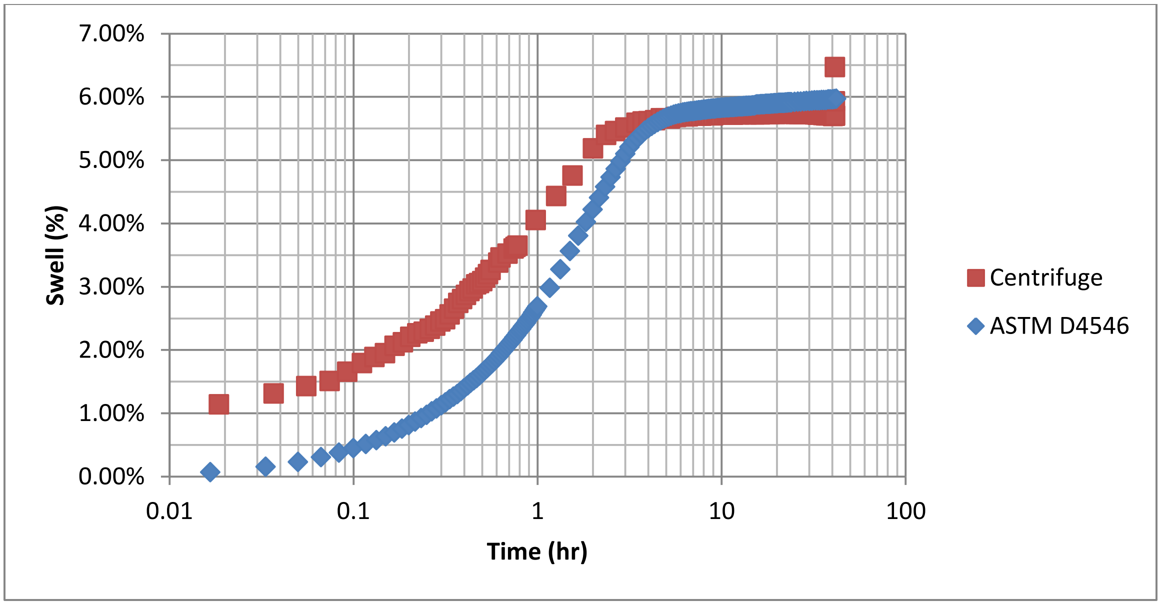

Figure 5.3: Comparison of Swell vs. Time Curves between Double Infiltration Centrifuge and ASTM D4546 Tests

Note that the portion of the swell versus time curve for the centrifuge test corresponding to the compaction cycle was removed in order to examine only the swelling portion of the curves. This shift results in an initial amount of swell of approximately 1% due to stress relaxation and a small portion of swelling from the addition of water outside of the centrifuge environment. The tests were performed at a similar effective stress of approximately 282 psf for the ASTM D4546 test and 258 psf for the centrifuge test. Results from these tests match well. Specifically, the maximum amount of primary swelling from both of these tests is both close to 5.6%, indicating that the new double infiltration centrifuge method produces similar maximum swelling results to those obtained using ASTM D4546. However, some difference can be reported. The benefits of the centrifuge test can be seen as the result comes at a slightly faster time, and a clear reduction in the secondary swelling can be observed. These observations are further addressed in Section 6.5. Therefore, the results from the centrifuge match up well with those from the ASTM D4546 tests, validating the testing procedure.

5.2.1 Results from Trimmed Specimens Tested at As-Compacted Moisture Content

The results, or vertical swell at the end of primary swelling versus vertical effective strain, from Series IIa tests on specimens that were tested at their compacted moisture content are shown in Figure 5.4. Note that the target effective stress and target dry density was the same between tests and that the initial moisture content was the same as the as-compacted moisture content. Results from both ASTM D4546 and the double infiltration method are shown together and are not separated. The results from these tests can also be seen for each individual test in Appendix B.

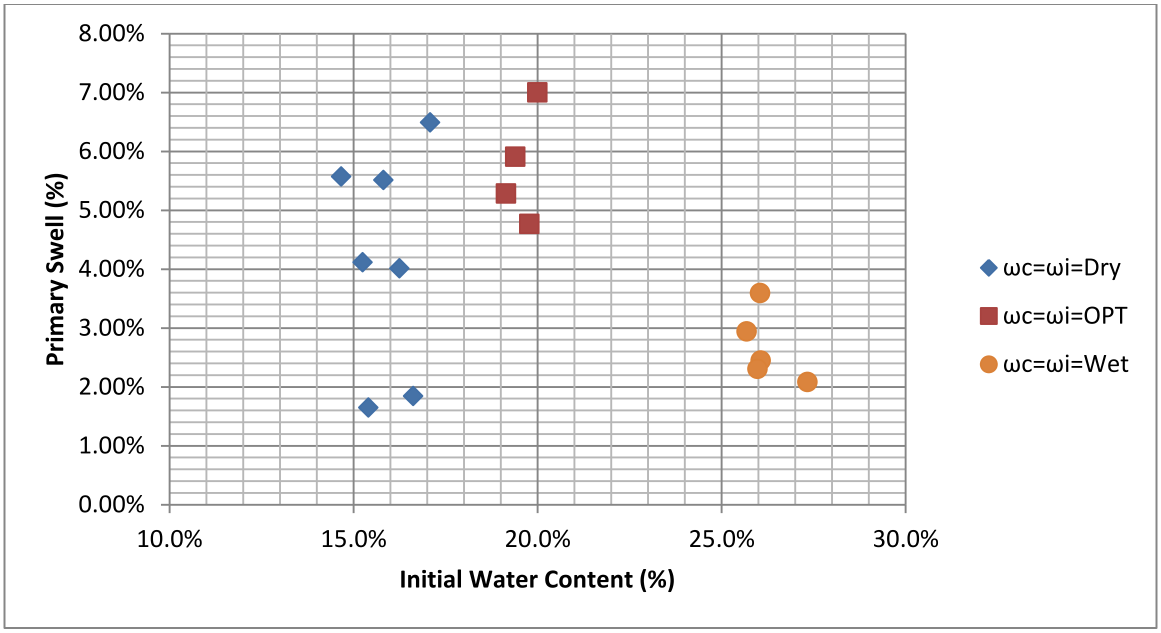

Figure 5.4: Results from Testing of Trimmed Specimens at As-Compacted Moisture Contents

The results indicate that drier samples tend to have a higher amount of primary swelling than those that are compacted wet at the as-compacted moisture content. However, a large amount of variability exists for the samples that are compacted dry of optimum which will be explored further in Chapter 6. Overall, the general trend matches previously reported by Walker (2012) that the initial moisture content affects significantly the swelling of a soil specimen. Note that there is a discrepancy for the tests on the specimens compacted at optimum which is explained in Section 6.2.1.

5.2.2 Results from Trimmed Specimens Tested at Moisture Conditioned Moisture Content

The results from Series IIb tests on specimens that were tested at a moisture conditioned moisture content that was different than the as-compacted moisture content are shown in Figure 5.5. The results from these tests can also be seen for each individual test in Appendix B.

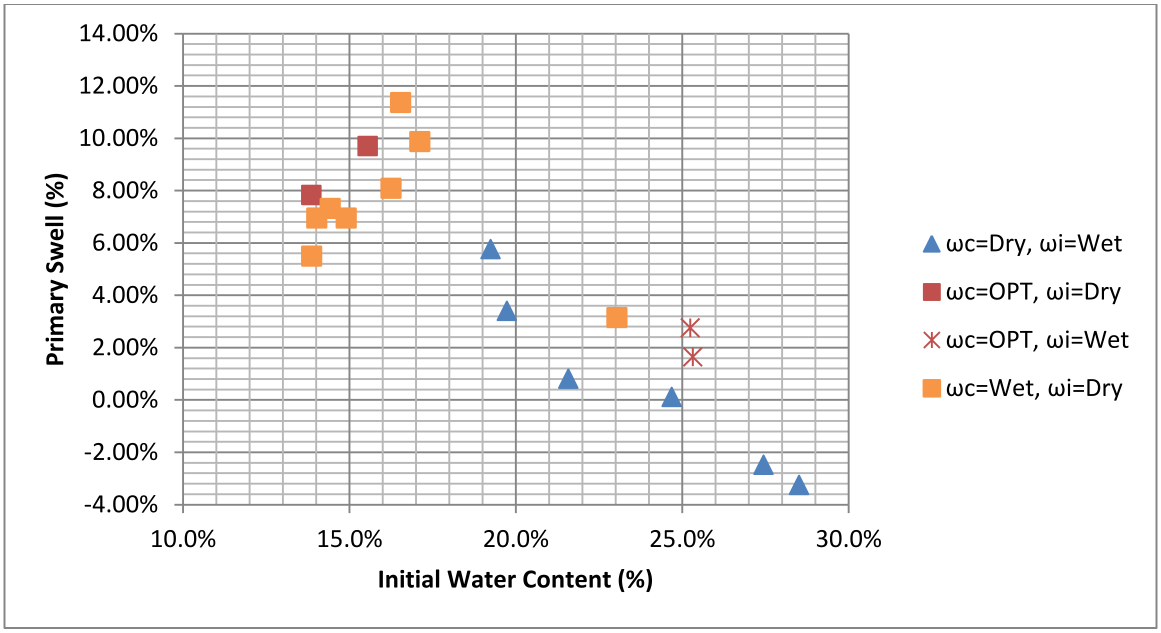

Figure 5.5: Results from Testing of Trimmed Specimens at Moisture Conditioned Moisture Contents

The results in Figure 5.5 indicate the same correlation between the vertical swelling at the end of primary swelling and initial moisture content, albeit with a few differences. Specimens that were moisture conditioned from an as-compacted moisture content that was dry to a moisture content that was wet of optimum saw little to no swell or collapse upon being wetted, whereas specimens that were moisture conditioned from a wet condition to a dry condition saw a higher amount of swell than those originally compacted dry of optimum. Analysis of these results is discussed in Chapter 6.

Chapter 6: Analysis of Results

6.1 Stresses in Double Infiltration Centrifuge Testing Set-up

In order to provide a comparison to existing methods as well as convey results that are usable for TxDOT, a representative effective stress within the samples from the double infiltration centrifuge tests needs to be calculated. The framework for the stresses in the centrifuge was obtained based on those presented by Plaisted (2009) and Dell'Avanzi et al. (2004). The Dell'Avanzi et al. paper was originally done to examine one-dimensional unsaturated flow through an increased gravitational gradient. In order to simplify the derivation and reduce the need of knowledge of the suction of an unsaturated specimen, the sample in the new centrifuge method was assumed to be saturated with Darcian flow at the end of primary swelling. This assumption also led to the fluid potential being dependent solely on the gravitational gradient imposed on the specimen by assuming that the discharge velocity was negligible and the suction at the end of primary swelling is equal to zero.

In order to account for the increased gravitational gradient, the centripetal acceleration in the sample was calculated as follows:

$$a_c = \omega^2 * r = N * g \tag{6.1}$$

with a_c as the centripetal acceleration, ω as the angular velocity, r as the radial distance from the central axis in the centrifuge, N being the scalar factor between the centripetal acceleration and the standard acceleration of gravity or the artificial g-level, and g being the standard acceleration of gravity.

6.1.1 Soil Stresses

In order to calculate the stress coming from the weight of the soil, the unit weight of the soil was needed. However, since the gravitational acceleration varies with the radius, the unit weight varies along the specimen's height as follows:

$$\gamma = \rho_s a_c = \rho_s \omega^2 r \tag{6.2}$$

In order to calculate this unit weight, the density was assumed to be constant throughout the specimen and was calculated as follows:

$$\rho_s = \frac{\left[\left(V_f - V_d\right) * \rho_w + SG_{CM} * \rho_w * V_d\right]}{V_f} \tag{6.3}$$

with V_f being the final volume of the soil specimen, V_d being the dry volume of the soil specimen, SG_{CM} being the specific gravity of the Cook Mountain clay, and ρ_w being the density of water, taken to be 1 g/cm^3. With this assumption, the total stress caused by the soil at any point through the soil mass can be calculated by integrating the unit weight as follows:

$$P(r) = P_t + \int_{r_t}^{r} \rho_s \omega^2 r dr = \frac{1}{2}\rho_s \omega^2 (r^2 - r_t^2) + P_t \tag{6.4}$$

with P_t being the pressure exerted at the top of the soil sample that takes into account both the overburden from the LVDT and porous disk as well as the column of water above. A comparison between this method and a method that only accounts for the artificial g-level from the accelerometer with a correction for a different radius at any given point as compared to the radius of the accelerometer is shown in Figure 6.1 for a Cook Mountain specimen at an imposed g-level of 25 g's.

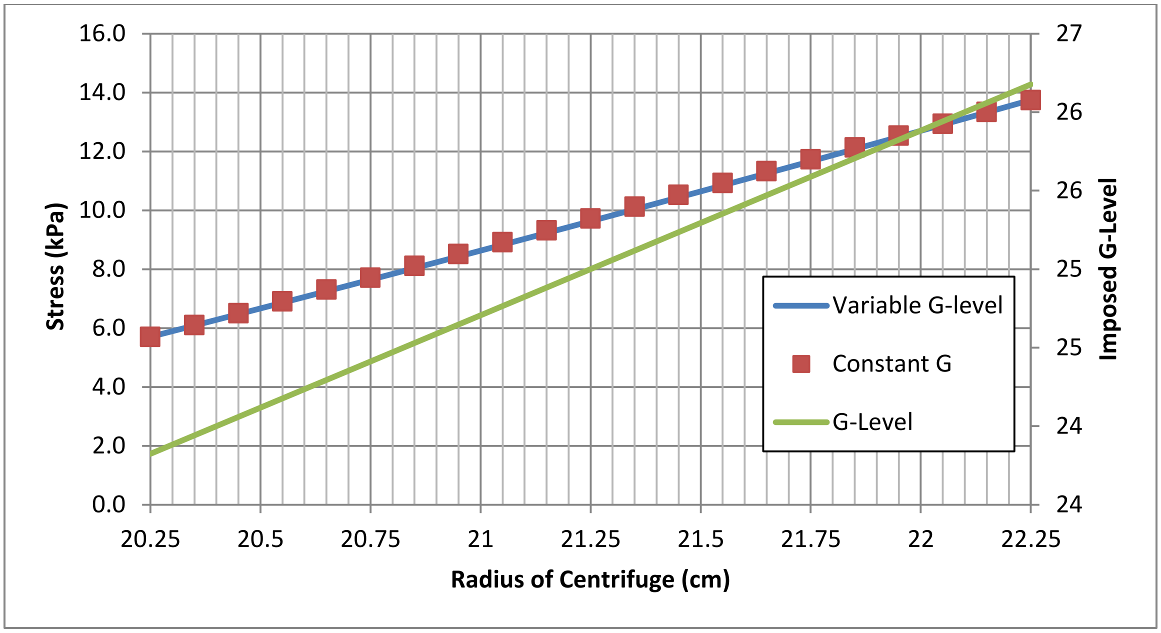

Figure 6.1: Stresses from the Soil and Overburden in the Double Infiltration Centrifuge Set-up

Note that for the soil pressures, the difference is fairly insignificant when correcting based on the different radius for the constant g-level case. This assumption can be used through the range of imposed g-levels used in testing as the error at 200 g's is less than 1%.

6.1.2 Pore Water Pressures

Pore water pressures can be predicted by assuming steady state, the validity of Darcy's law, and a saturated sample at the end of primary swelling. Using Dell'Avanzi et al. (2004), the discharge velocity of water through the soil sample can be calculated as follows:

$$v_c = -\frac{k_s}{g} * \frac{\delta \Phi_c}{\delta r} \tag{6.5}$$

with v_c being the discharge velocity through the sample, k_s being the saturated hydraulic conductivity of the sample, and $\frac{\delta \Phi_c}{\delta r}$ being the gradient in the water potential at a radius, r. If the base of the sample, r_b, was taken to be the datum, the fluid potential, Φ_c, can be calculated as follows:

$$\Phi_c = \frac{1}{2} * \omega^2 * (r_b^2 - r^2) + \frac{P_w(r)}{\rho_w} \tag{6.6}$$

With $P_w(r)$ being the pore water pressure in the sample at a radius r. Therefore, the gradient of the soil can be taken by taking the derivative with respect to the radius of Equation 6.6 as follows:

$$\frac{\delta \Phi_c}{\delta r} = -\rho_w \omega^2 r + \frac{\delta P_w(r)}{\delta r} \tag{6.7}$$

Using this, the discharge velocity equation is now as follows:

$$v_c = -\frac{k_s}{g} * \left(-\rho_w \omega^2 r + \frac{\delta P_w(r)}{\delta r}\right) \tag{6.8}$$

Assuming that the discharge velocity remains constant over the radius as the volumetric moisture content stays the same with time due to saturation, the derivative of Equation 6.8 with respect to the radius becomes as follows:

$$\frac{\delta v_c}{\delta r} = 0 = \frac{k_s \rho_w \omega^2}{g} - \frac{k_s}{g} * \frac{\delta^2 P_w(r)}{\delta r^2} \tag{6.9}$$

The saturated hydraulic conductivity and the acceleration of gravity both cancel out, thus Equation 6.9 is left with:

$$\rho_w * \omega^2 = \frac{\delta^2 P_w(r)}{\delta r^2} \tag{6.10}$$

which, when integrated, becomes:

$$P_w(r) = \frac{1}{2} \rho_w \omega^2 r^2 + C_1 r + C_2 \tag{6.11}$$

Using the boundary conditions of a known pore water pressure at the top and bottom of the specimen since they are connected in the permeameter cup, we can impose boundary conditions for C_1 and C_2 using the Equations 6.12 and 6.13 for the water pressure at any given point:

$$P_1 = \frac{1}{2}\rho_w\omega^2({r_t}^2 - r_0^2) = P_w(r_t) \quad (6.12)$$

$$P_2 = \frac{1}{2}\rho_w\omega^2({r_b}^2 - r_0^2) = P_w(r_b) \quad (6.13)$$

Note that r_0 is taken as the radius from the central axis for the top of the water. Thus, C_1 and C_2 are determined to be as follows:

$$C_1 = \frac{P_2 - P_1 + \frac{1}{2}\rho_w\omega^2(r_t^2 - r_b^2)}{r_b - r_t} \quad (6.14)$$

$$C_2 = P_1 - \frac{1}{2}\rho_w\omega^2 r_t^2 - C_1 r_t \quad (6.15)$$

Finally, the final equation to calculate the pore water pressures through the specimen is as follows:

$$P_w(r) = \frac{1}{2}\rho_w\omega^2(r^2 - r_t^2) + \frac{P_2 - P_1 + \frac{1}{2}\rho_w\omega^2(r_t^2 - r_b^2)}{r_b - r_t}(r - r_t) + P_1 \quad (6.16)$$

The predicted pore water pressures across the soil specimen are shown in Figure 6.2. These results were obtained for the case of a 2 cm head of water above the top of a 2 cm soil specimen using for two cases, one using the above equation and other using a constant g-level and radius correction described in Section 6.1.1.

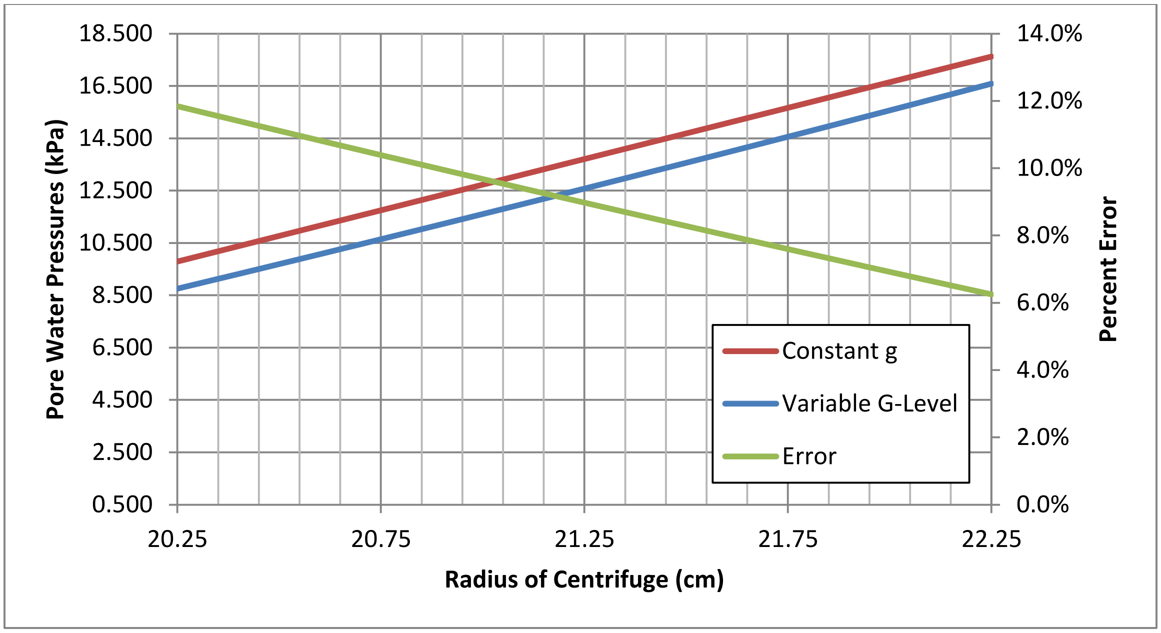

Figure 6.2: Pore Water Pressures through the Soil Specimen in the Double Infiltration Centrifuge Set-up

For the pore water pressures, there is a significant difference between the case of a constant g-level and the case using the equations for a variable g-level through the specimen. Unlike the soil stress condition, a much greater range of g-levels through the entirety of the water column leads to this difference. For example, in this case, the g-level at the top of the water column is 20 g's whereas at the bottom of the soil specimen, the g-level is approximately 26.5 g's. Therefore, the pore water pressure through a specimen needs to be calculated using a variable g-level.

6.1.3 Effective Overburden Stresses

In order to predict the stresses at the top of the specimen, the overburden must be calculated via the applied weight from the porous disk and the weight from the LVDTs. Since the cutting ring is submerged, the effective stress must take into account the buoyant, and not total, weight of the overburden. For the LVDT rod, the overburden mass is taken as follows:

$$m_{rod,b} = \frac{\pi d_{rod}^2}{4} * ((h_{rod} - h_w) * SG_{al} * \rho_w - h_{rod} * (SG_{al} - 1) * p_w \quad (6.17)$$

with d_{rod} being the diameter of the rod at 0.495 cm, h_{rod} being the height of the rod at 13.1 cm, h_w being the height of water, and SG_{al} being the specific gravity of aluminum taken to be 2.7.

For the overburden mass of the porous disk, first the volume of the porous disk had to be calculated by taking the mass of the dry porous disk and dividing it by the specific gravity of brass, 8.42. After this, the submerged mass can be calculated as follows:

$$m_{pd,b} = (SG_{brass} - 1) * V_{brass} \quad (6.18)$$

Thus, the effective stress at the top of sample from the overburden can be calculated as follows:

$$\sigma'_{ob} = \frac{m_{ob} * a_c}{A_s} = \frac{(m_{rod,b} + m_{pd,b})\omega^2 r_t}{A_s} \quad (6.19)$$

with A_s being the area of the soil specimen. Note that the stress was assumed to be applied at a singular point and was not assumed to vary over the radius. This assumption will cause some error due to the height of the LVDT extending over a fairly large radius, but this error is minimal due to the relatively small mass of the LVDT as opposed to the water and porous disk.

6.1.4 Effective Stresses in the Soil Specimen

The soil effective stresses are obtained by subtracting the pore water pressure at any point from the total stresses. Thus, the effective stress, σ', becomes:

$$\sigma'(r) = P(r) - P_w(r) + \sigma'_{ob} \quad (6.20)$$

In order to calculate the equivalent stress through the soil sample, the effective stress at the top and bottom of the sample can be calculated as follows:

$$\sigma'_t = \sigma'_{ob} \tag{6.21}$$

$$\sigma'_b = \sigma'_{ob} + \frac{1}{2}\rho_s\omega^2({r_b}^2 - r_t^2) - \frac{1}{2}\rho_w\omega^2({r_b}^2 - r_t^2) \tag{6.22}$$

Note that the final radius of the top of specimen was taken at the point of inflection on the swelling curves and that the pore water pressure at the top portion of the sample cancels out due to the entire sample being submerged. An examination of the total stresses, effective stresses, and pore water pressures is shown in Figure 6.3 for an example with the Cook Mountain soil compacted at optimum moisture content, at a relative compaction of 100%, with an overburden mass of 46.0 g, with a height of water above the top of the soil sample of 2 cm, and at an artificial g-level of 25 g's at the accelerometer that is used to determine the variable g-level through the sample.

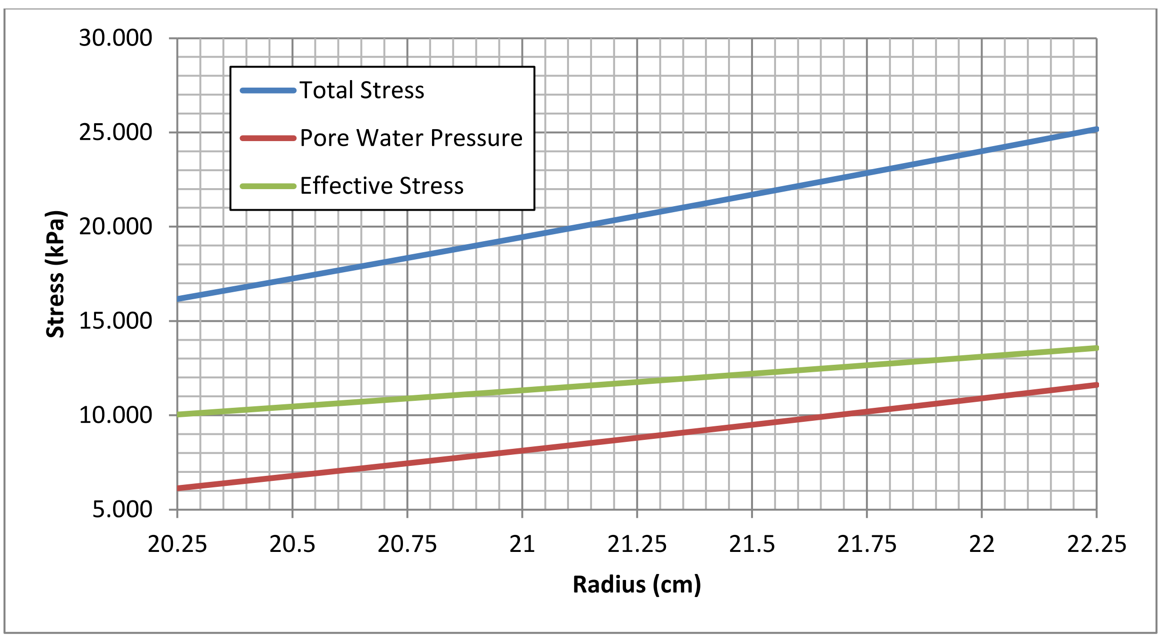

Figure 6.3: Stresses in a Soil Specimen in Double Infiltration Centrifuge Set-up

6.1.5 Determination of Equivalent Effective Stresses

In order to compare the results from the centrifuge testing to those obtained using from the ASTM D4546 testing, an average value for effective stress had to be determined. In order to calculate this, a simplified method using a stress ratio and log-linearly interpolating between the top and bottom stress was used based on Zornberg et al. (2013). A summary of the method is presented below.

Between the top and the bottom stress of the sample, a log-linear curve can be fit based on the following equation shown by Plaisted (2009):

$$\varepsilon = A * \ln(\sigma') + B \tag{6.23}$$

With A and B being fitting coefficients. From this, there exists an equivalent stress through the sample that is equal to the stress at which the average swelling of the sample occurs. Results from the infiltration testing indicate that the value of the equivalent stress relative to the stress ratio, or the ratio between the bottom and top effective stress, was independent of the A and B fitting coefficients. Thus, the stress ratio (SR) can be calculated as follows:

$$SR = \frac{\sigma'_b}{\sigma'_t} \tag{6.24}$$

Using this stress ratio and the log-linear assumption, an interpolation value (IV) can be defined as follows:

$$IV = \frac{\sigma'_t - \sigma'_{equivalent}}{\sigma'_b - \sigma'_t} \tag{6.25}$$

Using the assumption of log-linearity and that the equivalent stress occurs at the average portion of the curve where the average strain occurs, the IV becomes:

$$IV = \frac{\frac{1}{e} SR^{\left(\frac{1}{SR-1}+1\right)} - 1}{SR - 1} \tag{6.26}$$

Thus, the IV can be calculated based on a known top and bottom effective stress, and the equivalent, or average, effective stress can be calculated as follows:

$$\sigma'_{equivalent} = (\sigma'_b - \sigma'_t) * IV + \sigma'_t \tag{6.27}$$

6.2 OVERVIEW OF RESULTS FROM TRIMMED SPECIMENS

Specimens were grouped into three conditions for Series IIa and four conditions for Series IIb. Series IIa, those specimens that had the initial moisture content (ω_i) equal to the as-compacted moisture content (ω_c), were grouped into a dry condition (i.e. ω_i=ω_c=Dry), a wet condition (i.e. ω_i=ω_c=Wet), and an optimum condition (i.e. ω_i=ω_c=OPT). Series IIb, those specimens that had a moisture conditioned initial moisture content that was not equal to the as-compacted moisture content, were grouped into a dry to wet condition (i.e. ω_c=Dry, ω_i=Wet), a wet to dry condition (i.e. ω_c=Wet, ω_i=Dry), an optimum to dry condition (i.e. ω_c=OPT, ω_i=Dry), and an optimum to wet condition (i.e. ω_c=OPT, ω_i=Wet). In terms of general structure, the dry and dry to wet conditions had a flocculated structure, wet and wet to dry had a dispersed structure, and optimum, optimum to dry and optimum to wet all had a partially dispersed structure. Table 6.1 has the list of tests for the trimmed specimens with their results.

Table 6.1: Results of Testing on Trimmed Specimens

Date	Initial Height (cm)	Final Height (cm)	e,i	e,f	ω,i	ω,f	Δw	Mass wet soild added(g)	ρd (g/cm3)	ρd,SPT (g/cm3)	ρ (g/cm3)	S,i	S,f	Rate, P (%/log cycle)	Rate, S (%/log cycle)	Swell (%)	Time to Swell (hr)	Stress (psf)	Method	As-Compacted Moisture Condition	Initial Moisture Condition
3/19/14	1.989	2.035	1.243	1.267	16.6%	39.9%	23.3%	92.19	1.240	1.435	1.446	37.2%	87.5%	1.886%	0.126%	1.843%	2.33	282	ASTM D4546	Dry	Dry
3/19/14	2.007	2.139	0.919	1.046	17.1%	35.5%	18.4%	107.74	1.449	1.435	1.696	51.7%	94.1%	5.850%	0.374%	6.487%	12.67	282	ASTM D4546	Dry	Dry
3/23/14	2.018	2.131	1.036	1.140	14.7%	38.8%	24.1%	100.54	1.365	1.518	1.565	39.3%	94.6%	4.979%	0.218%	5.568%	4.33	282	ASTM D4546	Dry	Dry
3/24/14	2.085	2.118	1.214	1.220	15.4%	40.0%	24.6%	96.94	1.256	1.507	1.449	35.3%	91.1%	2.046%	0.128%	1.647%	4.33	282	ASTM D4546	Dry	Dry
3/26/14	2.032	2.144	0.840	0.941	15.8%	37.6%	21.7%	66.86	1.513	1.507	1.753	52.4%	100.0%	13.061%	-0.009%	5.512%	4.49	258	Centrifuge	Dry	Dry
3/26/14	1.936	2.013	0.981	1.061	16.3%	42.1%	25.9%	59.37	1.405	1.507	1.634	46.1%	100.0%	6.331%	-0.105%	4.013%	1.73	250	Centrifuge	Dry	Dry
3/28/14	2.023	2.106	1.078	1.141	15.3%	40.3%	25.1%	99.83	1.338	1.507	1.542	39.3%	98.2%	4.121%	0.185%	4.113%	1.83	282	ASTM D4546	Dry	Dry
3/20/14	1.974	1.904	1.706	1.542	28.5%	46.0%	17.4%	84.76	1.027	1.435	1.320	46.5%	82.8%	-0.077%	-0.124%	-3.252%	16.83	282	ASTM D4546	Dry	Wet
3/24/14	1.932	2.040	1.018	1.096	19.2%	37.2%	17.9%	102.18	1.377	1.445	1.642	52.5%	94.2%	5.102%	0.520%	5.755%	6.83	282	ASTM D4546	Dry	Wet
3/28/14	1.773	1.728	1.914	1.650	27.5%	48.5%	21.0%	73.17	0.954	1.445	1.216	39.9%	81.6%	-0.350%	-0.045%	-2.486%	0.75	282	ASTM D4546	Dry	Wet
3/28/14	2.005	1.786	1.280	1.005	24.7%	41.0%	16.3%	97.81	1.219	1.445	1.520	53.6%	100.0%	0.061%	0.009%	0.105%	0.58	282	ASTM D4546	Dry	Wet
3/30/14	1.643	1.657	0.944	0.960	21.6%	39.3%	17.7%	53.73	1.432	1.507	1.741	63.7%	100.0%	0.340%	-0.090%	0.805%	4.87	353	Centrifuge	Dry	Wet
3/30/14	1.710	1.768	1.093	1.164	19.7%	35.7%	16.0%	51.14	1.330	1.507	1.593	50.3%	85.4%	4.667%	0.349%	3.404%	1.93	351	Centrifuge	Dry	Wet
3/14/14	2.057	2.166	0.868	0.954	19.1%	32.8%	13.7%	116.23	1.488	1.516	1.773	61.3%	95.4%	4.147%	0.659%	5.285%	26.00	282	ASTM D4546	OPT	OPT
3/25/14	1.936	2.074	0.903	1.026	20.0%	34.8%	14.8%	108.14	1.461	1.573	1.753	61.6%	94.0%	7.000%	1.000%	7.000%	8.00	282	ASTM D4546	OPT	OPT
4/2/14	1.950	2.065	0.717	0.818	19.4%	33.5%	14.1%	70.90	1.622	1.507	1.936	75.4%	100.0%	2.892%	0.888%	5.906%	13.50	226	Centrifuge	OPT	OPT
4/2/14	1.819	1.905	0.731	0.814	19.8%	33.0%	13.3%	65.77	1.608	1.507	1.926	75.3%	100.0%	3.397%	0.116%	4.766%	7.43	226	Centrifuge	OPT	OPT
3/26/14	1.880	2.031	0.712	0.845	13.9%	31.5%	17.6%	110.34	1.751	1.573	1.849	54.1%	100.0%	5.876%	2.577%	7.826%	31.00	282	ASTM D4546	OPT	Dry
4/2/14	1.755	1.925	0.609	0.765	15.6%	32.1%	16.5%	65.89	1.731	1.507	2.000	71.2%	100.0%	7.747%	1.103%	9.698%	17.91	227	Centrifuge	OPT	Dry
3/26/14	1.975	2.029	0.953	0.991	25.2%	34.4%	9.2%	112.36	1.423	1.573	1.783	73.6%	96.3%	2.269%	0.538%	2.752%	13.50	282	ASTM D4546	OPT	Wet
4/2/14	1.872	1.902	0.841	0.871	25.3%	35.0%	9.7%	66.60	1.512	1.507	1.895	83.8%	100.0%	0.633%	-0.318%	1.635%	25.70	224	Centrifuge	OPT	Wet
3/16/14	1.944	1.984	0.889	0.923	27.3%	32.8%	5.5%	115.68	1.471	1.506	1.873	85.4%	98.7%	1.495%	0.543%	2.084%	23.50	282	ASTM D4546	Wet	Wet
3/21/14	1.918	1.964	0.893	0.932	26.1%	32.4%	6.3%	112.83	1.469	1.506	1.851	81.2%	96.4%	1.741%	0.797%	2.447%	25.00	282	ASTM D4546	Wet	Wet
3/26/14	1.719	1.770	0.726	0.777	25.7%	34.4%	8.7%	65.43	1.613	1.472	2.027	98.4%	100.0%	2.815%	1.143%	2.942%	14.01	256	Centrifuge	Wet	Wet
3/26/14	1.798	1.839	0.687	0.726	26.0%	33.0%	7.0%	70.17	1.650	1.472	2.079	105.2%	100.0%	2.259%	0.755%	2.304%	13.08	259	Centrifuge	Wet	Wet
3/31/14	1.873	1.941	0.838	0.873	26.0%	31.2%	5.2%	115.02	1.513	1.526	0.865	86.5%	99.2%	4.136%	1.614%	3.591%	31.00	282	ASTM D4546	Wet	Wet
3/17/14	1.934	1.987	0.784	0.836	23.0%	31.3%	8.3%	117.24	1.559	1.506	1.918	81.8%	100.0%	2.442%	1.183%	3.138%	23.50	282	ASTM D4546	Wet	Dry
3/22/14	1.776	2.073	0.751	1.003	16.3%	31.2%	15.0%	105.93	1.782	1.506	1.846	60.2%	86.4%	4.914%	2.096%	8.081%	31.00	282	ASTM D4546	Wet	Dry
3/22/14	1.808	1.935	0.767	0.875	14.9%	31.7%	16.8%	104.40	1.783	1.506	1.808	54.1%	100.0%	3.619%	1.588%	6.940%	29.00	282	ASTM D4546	Wet	Dry
3/30/14	1.781	1.904	0.580	0.690	14.0%	29.9%	15.9%	67.16	1.762	1.472	2.009	67.3%	100.0%	4.487%	1.715%	6.950%	31.48	360	Centrifuge	Wet	Dry
3/30/14	1.780	1.910	0.598	0.715	14.4%	30.3%	15.9%	66.63	1.742	1.472	1.994	67.2%	100.0%	4.611%	1.720%	7.309%	30.54	358	Centrifuge	Wet	Dry
4/1/14	2.029	2.231	0.619	0.771	17.1%	28.4%	11.2%	129.95	1.717	1.526	0.769	70.3%	100.0%	6.141%	-	9.872%	46.00	282	ASTM D4546	Wet	Dry
4/1/14	2.083	2.214	0.635	0.722	16.6%	28.5%	12.0%	131.90	1.700	1.526	0.725	68.2%	100.0%	8.322%	-	11.354%	47.00	282	ASTM D4546	Wet	Dry
4/2/14	1.839	1.953	0.758	0.846	13.9%	31.4%	17.5%	106.03	1.807	1.526	0.509	53.1%	100.0%	3.606%	-	5.488%	20.17	282	ASTM D4546	Wet	Dry

As can be seen from Table 6.1, some variability exists within the data, especially for results from specimens compacted dry of the optimum moisture content. In order to examine the cause of this variability, Table 6.2 lists the average swell result for each of the seven conditions along with their standard deviations.

Table 6.2: Average Result for Each Test Condition on Trimmed Specimens

ω_c	ω_i	Avg. Swell (%)	σ (%)
Dry	Dry	4.17%	1.87%
Wet	Wet	2.67%	0.60%
Opt	Opt	5.74%	0.96%
Dry	Wet	0.72%	3.44%
Wet	Dry	7.39%	2.52%
OPT	Dry	8.76%	1.32%
OPT	Wet	2.19%	0.79%

The samples that were initially compacted dry tend to have a significant variation in their maximum primary swelling for both Series IIa and IIb. Section 6.2.1 will expand on this as the issue lies in the variability of the dry density of the soil as compared to those compacted wet. Also note that samples from Series IIb have higher variability between results, again an issue expanded upon in Section 6.2.1 as well as in Section 6.2.2.

6.2.1 Variation in Density between Trimmed Specimens

When examining the reasoning behind the high variation of swelling characteristics in certain test conditions, the difference in dry density between the trimmed specimen and the soil from the compaction mold was shown to be a key factor. Figure 6.4 shows the dry density of the specimens that were trimmed and tested versus the dry density of the entire compacted soil mass from the Standard Proctor mold for each test with the target dry density shown as a line. The average dry density and relative compaction, standard deviation between specimens, and average percent difference from the targeted dry density are shown in Table 6.3.

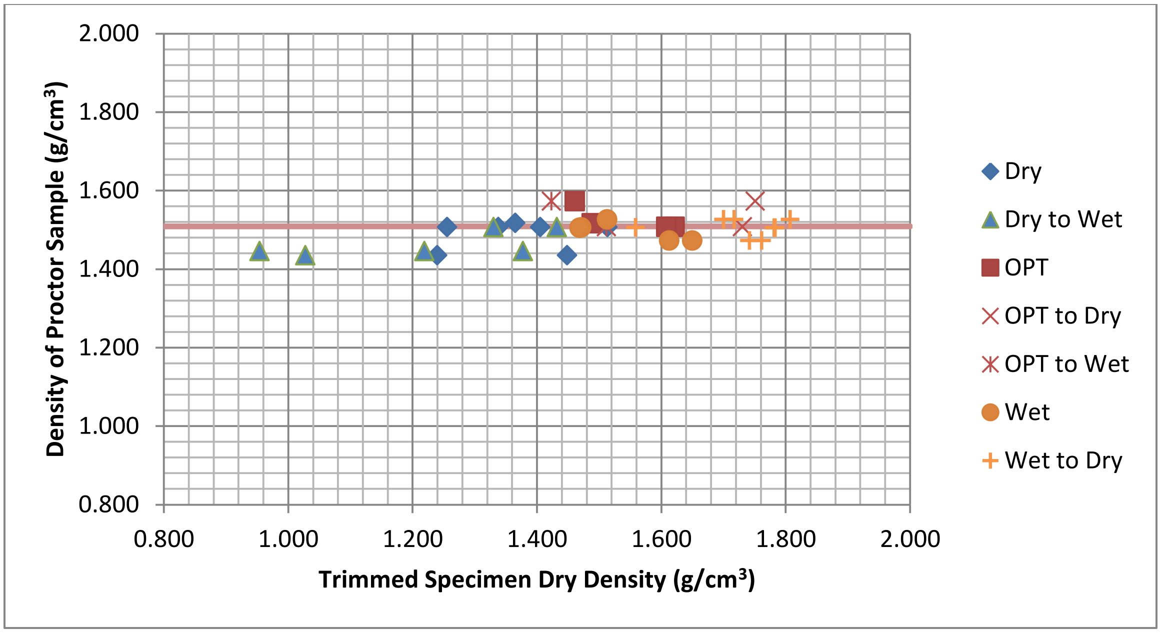

Figure 6.4: Comparison between Tested and Compacted Densities

Table 6.3: Average Dry Density and Deviation for Each Condition

ω_c	ω_i	Avg. $\rho_{,d}$ (g/cm3)	RC (%)	σ (g/cm3)	Density Difference (%)
Dry	Dry	1.37	87%	0.10	-9%
Wet	Wet	1.54	98%	0.08	2%
OPT	OPT	1.54	98%	0.08	2%
Dry	Wet	1.22	78%	0.19	-19%
Wet	Dry	1.73	110%	0.08	15%
OPT	Dry	1.74	111%	0.01	15%
OPT	Wet	1.47	93%	0.06	-3%

For specimens that were compacted dry, the densities varied significantly for both the Series IIa and Series IIb specimens, typically at a lower dry density that the targeted dry density. This difference stems from the macro-voids that are prevalent within this soil structure from the compaction of the drier clods, thereby leading to local points within the soil mass where the dry density may be significantly lower. As the structure of the soil is flocculated, these voids tend to be much more prevalent as compared to those specimens compacted with more a dispersed structure. When dry specimens are wetted under loading conditions, these macro-voids tend to decrease, but, as the specimen is unconfined during wetting, the macro-voids will increase thereby leading to a significant decrease in the dry density. Therefore, the densities of the dry and dry to wet specimens are important to its overall swelling and swelling characteristics as they will vary significantly. This vast range in swells and densities illustrates why in-situ specimens are a necessity as the fissures and discontinuities within the soil mass leads to changes in how a soil responds when in contact with water.

For specimens that were compacted wet and at optimum, the initial moisture condition leads to comparable dry densities to the targeted dry density. However, after the moisture conditioning, the specimens increase in density. A possible explanation for this lies at the micro level. Since these specimens have a dispersed structure, removal of moisture from the voids via suction tends to reduce the diffuse double layer, leading to a decrease in the repelling force between particles. This decrease in the repelling force will lead to the clay plates rearranging themselves closer together as moisture is sucked out via suction in the air. Thus, the structure tends to lead to a much stronger, denser specimen that swells more as the clay particles are spaced closer together. However, issues with these specimens are examined in Section 6.2.2 due to the difficulties resulting from the increase in strength and dry density of the specimens.

Using this variation in the dry densities of sample with the same initial fabric and initial moisture content, the effect of the density of a specimen on swelling characteristics can be resolved. When comparing specimens at the same testing moisture content and fabric but a different dry density, the specimen that is denser will swell more. An explanation for this increase in swell may come from the micro-level. This increase in swell stems from the increase in the potential repulsing forces during the influx of water as the clay plates are spaced closer together will have their diffuse double layers overlap more frequently as opposed to looser specimens. Therefore, the density has an effect on swelling, although the effect is not as significant as the influence of the initial moisture content or, as will be seen later, the fabric.

6.2.2 Issues with Moisture Conditioned Specimens

Another reason for the source of variability in the results stems from the adjustment of the moisture condition of already compacted specimens leading to the introduction of cracks and fissures. These cracks and fissures exist for both dry specimens going to a higher moisture content and for wet specimens going to a lower moisture content.

For specimens that were compacted dry and had their moisture contents raised, the macro-voids within the soil increased during the equilibrium of the moisture content through the soil. Figure 6.5 shows the cracking that existed in two specimens at the end of raising the moisture content.

Figure 6.5: Cracks in Specimens Compacted Dry after Moisture Conditioning

During the addition of water, the moisture was able to more rapidly enter the specimen via the macro-voids present after compaction which helped speed the process of reaching equilibrium through the specimen. However, the addition of moisture was added under no load or confinement. Therefore, the lack of confinement allowed for the soil to swell unconfined both laterally and vertically which increased the macro-voids within the specimen. Further, the dry density of the specimen also decreased as the clay plates would see a decrease in suction, thereby leading to a lower effective stress which would loosen the soil during the moisture adjustment. Therefore, this decrease in the effective stress and increase in the macro-voids explains how the specimens that were adjusted from a dry condition to a wet condition had significantly lower dry density than those initially compacted wet.

For specimens that were compacted wet and then dried out, cracking and a significant increase in the strength of the soil became a major issue. Figure 6.6 illustrates the cracking prevalent in a specimen left to air dry (left) and the relative lack of cracking in a specimen that was trimmed prior to air drying (right).

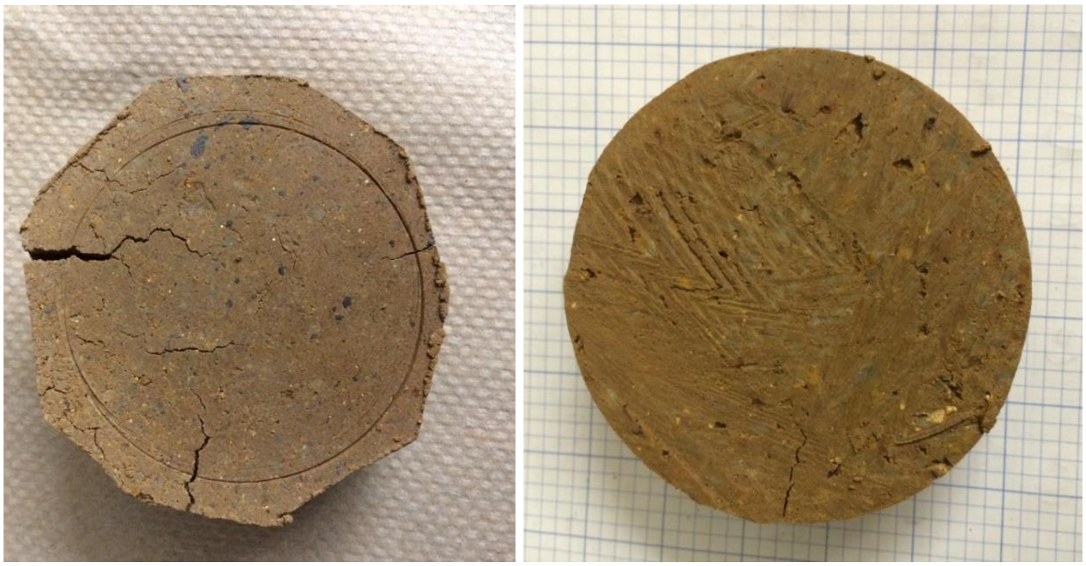

Figure 6.6: Cracks in Specimens Compacted Wet after Moisture Conditioning

When the specimen initially air dried from the wet condition, the cracking distorted the specimen to the point at which the specimen would crumble during trimming as the amount of effort to trim the specimen increased significantly. This effort increased due to the significant increase of the dry density in the sample during the drying, leading to a higher effective stress that led to a specimen with a higher shear strength. Due to the increased strength, the wire saw was unable to cut the specimen, and the hand saw took a significant amount of time, up to two hours, to slowly insert the soil into the cutting ring. In order to do the testing, the specimen was trimmed into a cutting ring prior to air drying with the grease used as a way to prevent the soil from cracking laterally. As the soils dried, the change in volume led to a decrease in volume due to a roughly 10% decrease in the diameter and a slight decrease in the height of the specimen. The difference in volumes is shown in Table 6.4 as the dried volume, Vol., Dried, as opposed to the volume for a specimen at the same height but assuming if the diameter would not have decreased, Vol., Full.

Table 6.4: Volume Differences for Specimens Dried

Specimen Date	ω_c	ω_i	Vol., Dried (cm^3)	Vol., Full (cm^3)	Vol. Difference (%)
3/26/14	OPT	Dry	55.339	59.670	-7%
3/22/14	Wet	Dry	51.145	57.386	-11%
3/22/14	Wet	Dry	50.943	57.740	-12%
4/2/14	Wet	Dry	51.518	58.882	-13%
3/30/14	Wet	Dry	32.014	33.433	-4%
3/30/14	Wet	Dry	31.924	33.423	-4%

Including this volumetric strain as a direct correction for the vertical volumetric strain led to significantly higher results than those compacted at dry. In order to determine how significant the effect of the trimming process prior to air drying was, additional tests were run by carefully trimming two specimens that were compacted wet and dried into testing for the ASTM D4546 test and comparing the results with a specimen that was trimmed prior to drying. Their results for their vertical strain versus time curves are shown below in Figure 6.7.

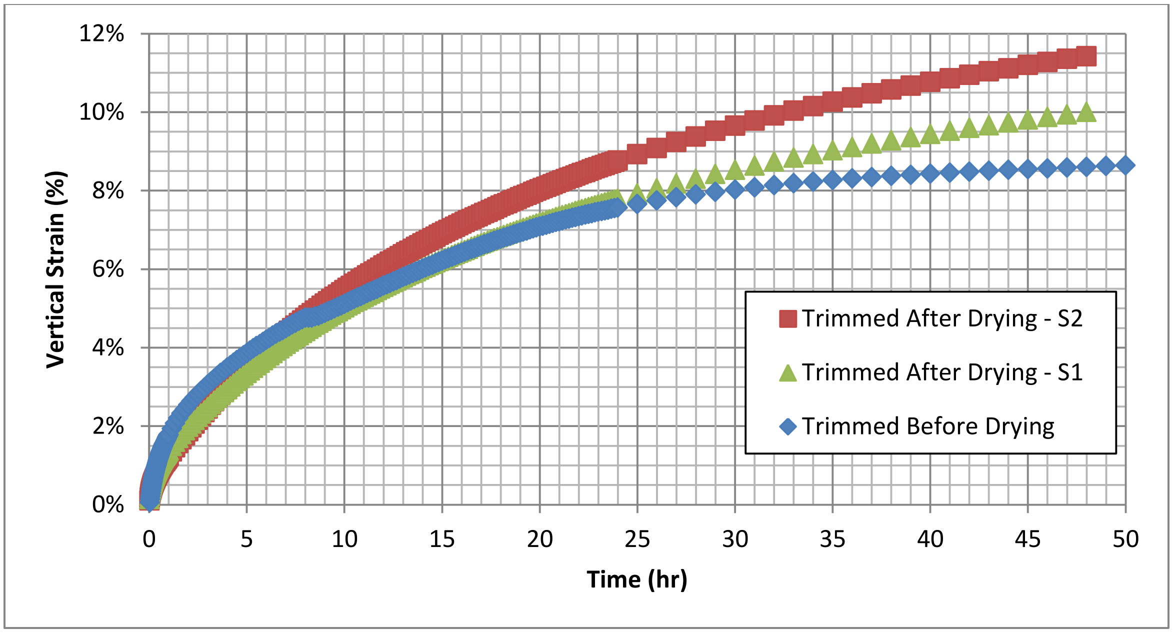

Figure 6.7: Results between Trimmed Prior and After for Wet to Dry Specimens

As can be seen, the specimen that are trimmed prior to testing show a higher amount of vertical strain than those that are trimmed prior to drying. However, the difference in the vertical strain between specimens is not equal to the amount of vertical strain assumed when correcting for the volumetric strain, in this case 10.5% for the specimen dried after trimming. Thus, the amount of error introduced in this test does not have an easy correction factor as there is an amount of free swell in the specimens that were trimmed prior to air-drying when they are inundated with water from the lack of lateral confinement until the specimen reaches the edge of the cutting ring. Also note that the primary swelling portion of the test is longer for specimens that are trimmed after drying as the moisture front has less surface area to enter the soil. However, the properties seen from typical wet to dry test are still observed as the specimens swell more and over a long time frame than those specimens initially compacted dry at the same moisture content. Results for tests that went from wet to dry or OPT to dry are presented henceforth without a correction factor as the results without the correction for volumetric strain are much closer than those with a correction for the lateral volumetric strain for use in comparing the general trends at the same moisture content.

6.3 Effect of Fabric on Specimens Tested at As-Compacted Moisture Contents

In order to examine the effect of fabric on the swelling of highly plastic clays, the vertical swell at the end of primary swelling, time to the end of primary swelling, rate of the primary and secondary swelling portions of the curve, and the initial vs. final void ratio were determined to examine the differences in the swelling properties and time dependent properties of the soil. Note that the effect of stress was controlled by testing specimens at or near the target vertical effective stress of 282 psf for both ASTM D4546 and submerged centrifuge tests.

For specimens that were tested at their compaction moisture contents, the compaction moisture content vs. swell at the end of primary swelling is shown in Figure 6.8.

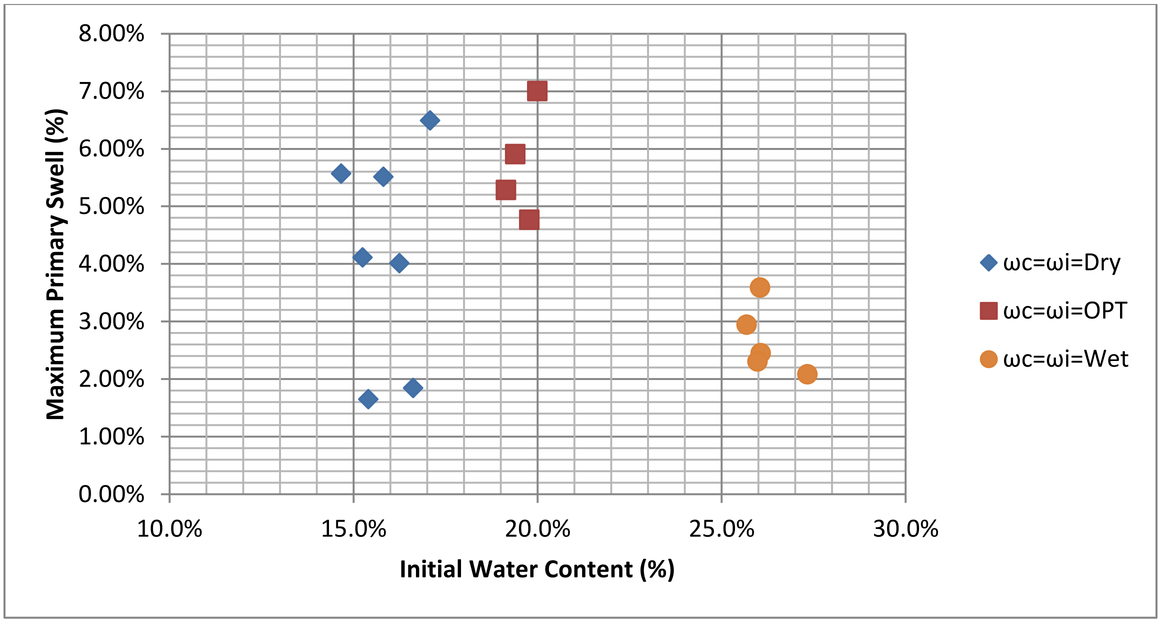

Figure 6.8: Compaction Moisture vs. Swell Results for Specimens Tested at As-Compacted Moisture Contents

The trend from the results indicates that, for specimens compacted and tested at the same moisture content, the vertical swell increases with decreasing moisture content. This is consistent with previously reported results. However, the scatter of test results is particularly high for dry and OPT specimens. The dry specimens' scatter can be explained by the significant amount of variation in the dry density as previously explained in Section 6.2.1. The optimum specimens are a different case as they were compacted with differently prepared soils that had a lower dry density for the lower three results and had a higher result for that which was compacted at the optimum dry density. This relationship between the optimum specimens and the results from Section 6.2.1 confirm the conclusion that soils that are denser at the same moisture content will swell slightly more. This relationship can be explained by denser specimens having a more tightly packed structure regardless of fabric. Thus, the denser soil tends to have a higher ability to swell when removing the effects of the initial moisture content and fabric.

The relationship between the compaction moisture content and time to the end of primary swelling is shown below in Figure 6.9.

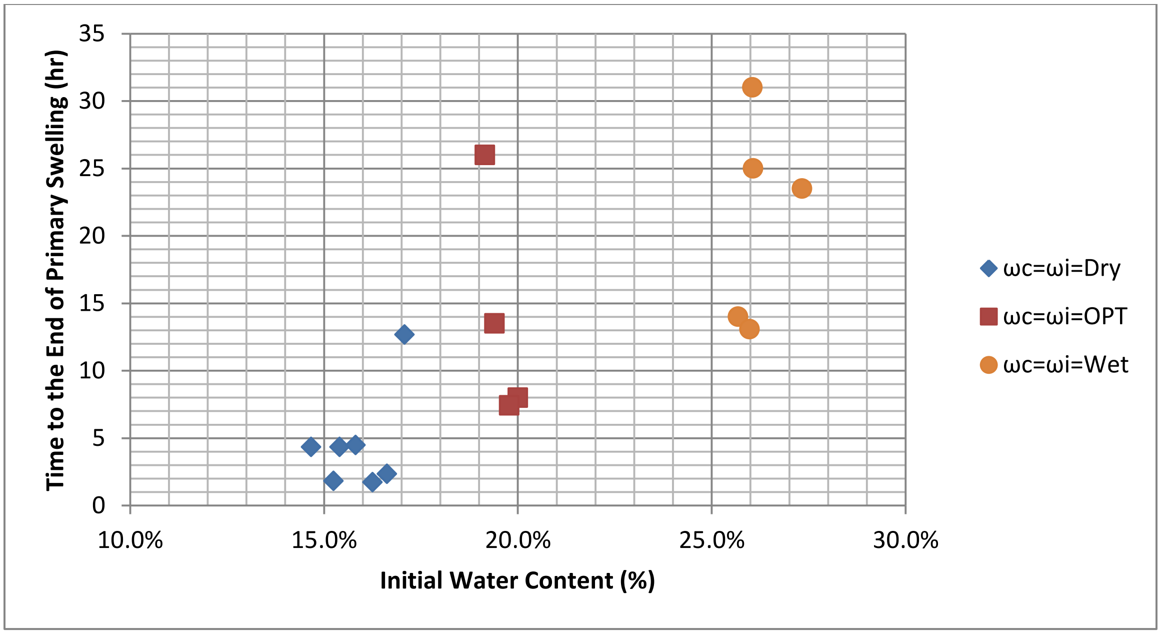

Figure 6.9: Compaction Moisture vs. Time to the End of Primary Swelling for Specimens Tested at As-Compacted Moisture Conditions

The relationship between the initial conditions and the time to the end of primary swelling is clearer than the results from the maximum primary swell. Specimens that are compacted dry will swell much more rapidly than those compacted wet. An explanation for this trend stems from the initial suction and the hydraulic conductivity of the samples. Since the specimens are drier, they have a higher amount of suction thereby leading to a high suction gradient that drives the initial swelling mechanism. Specimens that are compacted wet will have a lower suction, and thus, have a lower gradient that drives the swelling process. Drier specimens will also have a higher hydraulic conductivity that stems from the piping effect in the flocculated structure, or how water will go towards the area in the randomly oriented particles that are further away from the face of clay plates which allows for moisture to flow without becoming associated with the diffuse double layer, allowing for water to flow more rapidly through the specimen. Dispersed structures will force water to flow between the clay plates and in areas that are closer to the diffuse double layer, impeding flow. Thus, water is able to permeate through the flocculated specimens quicker, and the majority of the sample can receive moisture faster than specimens with a dispersed structure. This relationship is also shown in the rate of primary swelling versus moisture content as shown in Figure 6.10, albeit issues with this property are expanded upon in Section 6.4.

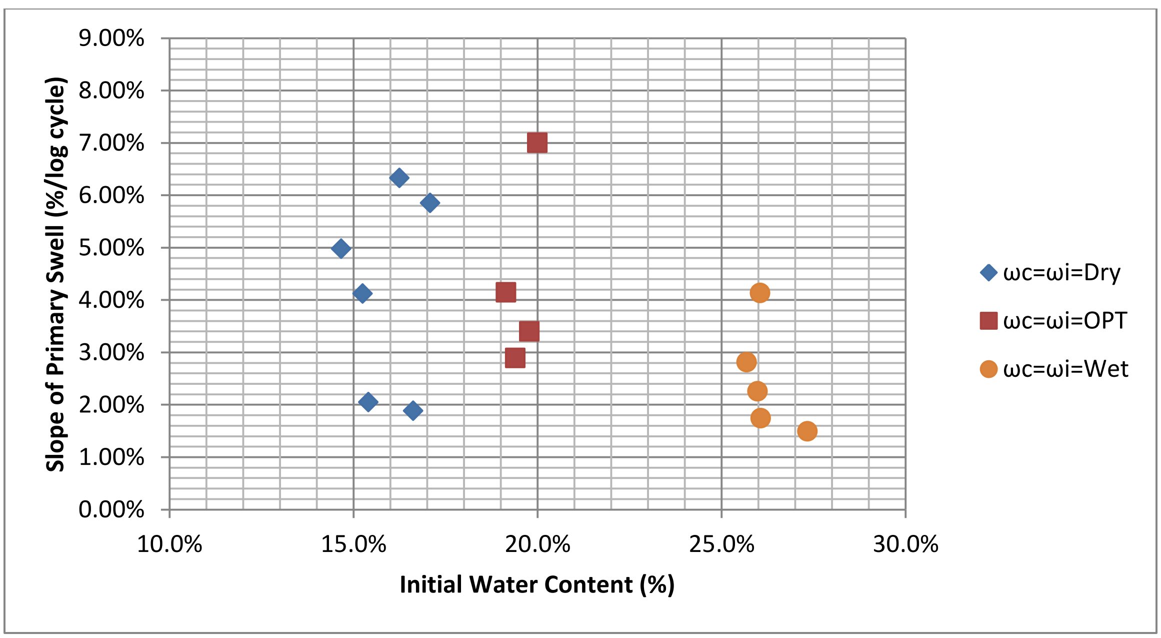

Figure 6.10: Compaction Moisture vs. Rate of Primary Swelling for Specimens Tested at As-Compacted Moisture Conditions

In order to examine the magnitude of the secondary swelling, the rate of secondary swelling versus moisture content is shown below in Figure 6.11.

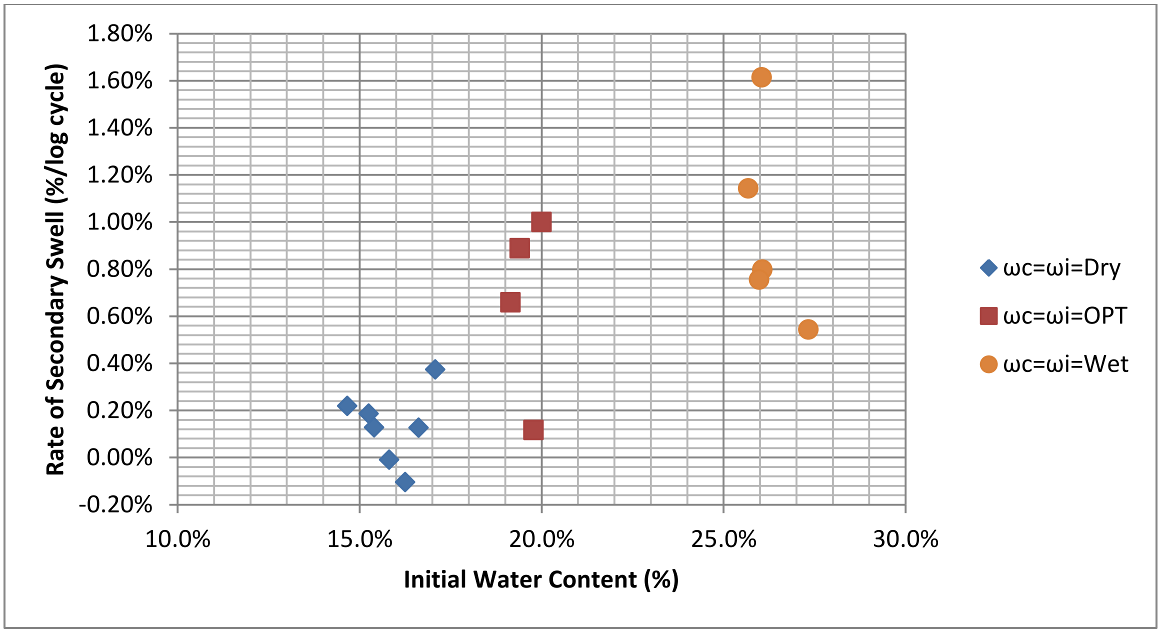

Figure 6.11: Compaction Moisture vs. Rate of Secondary Swelling for Specimens Tested at As-Compacted Moisture Conditions

The rate of secondary swelling increases with the compaction moisture content for specimens that are compacted dry tending to have little to no secondary swelling. Specimens that are compacted wet tend to see a higher amount of secondary swelling. A possible reasoning behind this higher amount of secondary swelling comes from how water, due to the dispersed fabric of the wet specimens, needs more time to reach the smaller portion of the micro-voids, thus, a higher capacity to swell is available after the primary swelling portion of the curve. Soils that have flocculated structures will have less of an issue as the amount of voids and the size of the voids between clay plates will typically be higher from the random orientation of clay plates. Thus, the soils with a dispersed structure have a higher capability to swell in the secondary swell portion of the swell curve than those soils with a flocculated structure.

The change in void ratio from the initial to final condition was the last property examined for the effect of fabric as shown in Figure 6.12.

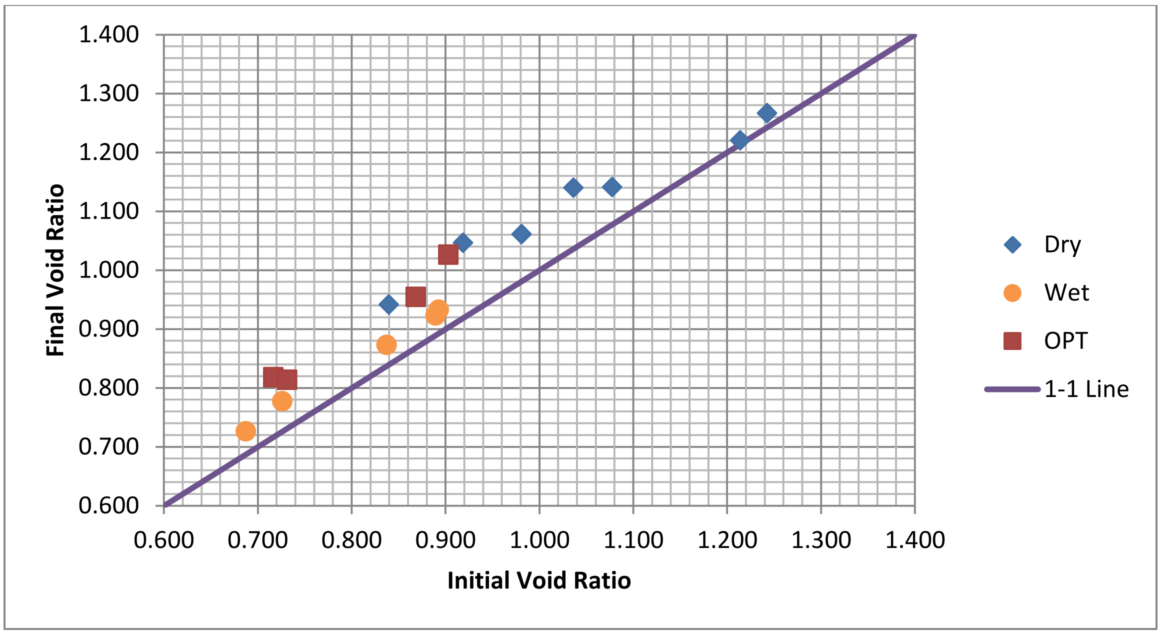

Figure 6.12: Initial vs. Final Void Ratio for Specimens Tested at As-Compacted Moisture Conditions

A nearly linear trend is observed. Specimens that are compacted dry tend to have a higher initial and final void ratio, whereas the initial and final void ratios for wet specimen tend to be lower. This higher void ratio is another factor in the variability of the dry unit weight from Section 6.2.1. Thus, the structures that are compacted with flocculated structures tend to have a greater amount of voids as compared to those compacted with dispersed structures as the random orientation of particles will lead to a higher propagation of voids even at similar dry densities.

By testing samples at the same initial moisture contents as their compaction moisture content, the effect of fabric and that of initial moisture could not be fully evaluated. In order to separate these effects, samples were tested at moisture conditioned moisture contents with the results compared against those tested at the as-compacted moisture contents to separate the effect of each variable.

6.4 Effect of Fabric on Specimens Tested at Moisture Conditioned Moisture Contents

To assess the effect of fabric, specimens should be tested using the same initial moisture content that is independent of the moisture used during compaction. Thus, results from Series IIb were analyzed to determine the effect of fabric on these adjusted specimens for the vertical swell at the end of primary swelling, time to the end of primary swelling, rate of the primary and secondary swelling portions of the curve, and the initial vs. final void ratio. Note that the effective stress was controlled again in order to remove the influence of the effective stress on swelling characteristics.

For specimens with adjusted moisture contents, the swell versus moisture content is shown below in Figure 6.13.

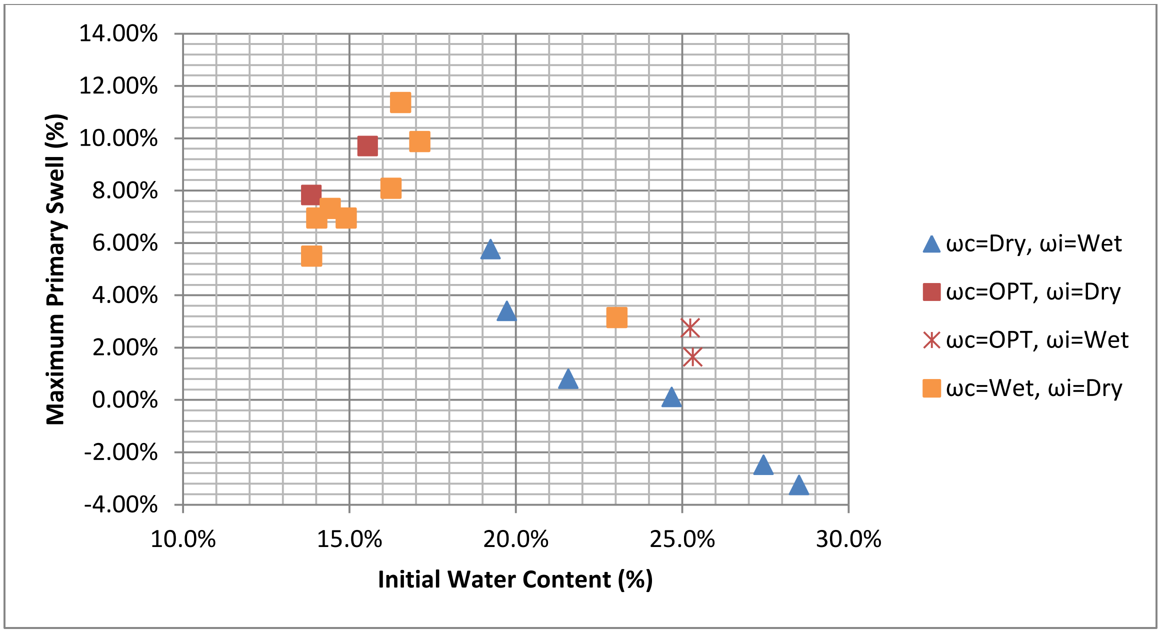

Figure 6.13: Initial Moisture Content vs. Vertical Swell for Specimens Tested at Moisture Conditioned Moisture Contents

The same trend of drier specimens swelling more than wetter specimens can be observed, consistent with previous results. In order to separate the effect of fabric on the swelling from the effect of the initial moisture content, results from Series IIa are shown in comparison to results from Series IIb in Figure 6.14.

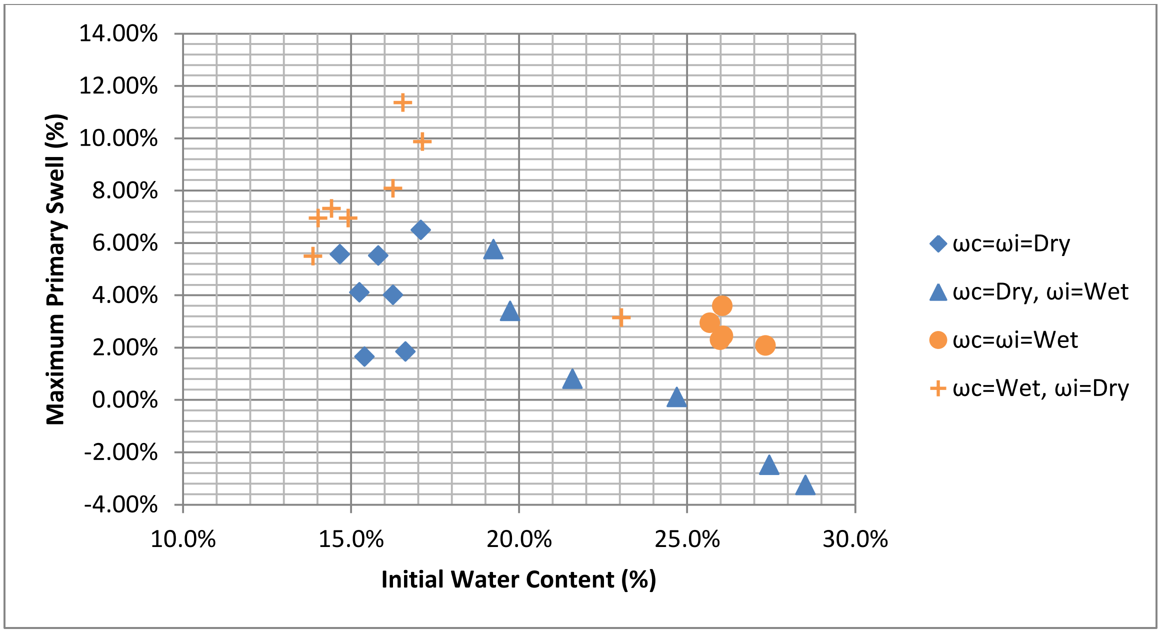

Figure 6.14: Initial Moisture Content vs. Vertical Swell for Flocculated and Dispersed Specimens

The specimens that are compacted with a dispersed structure and had their moisture contents lowered will swell more than those compacted with flocculated structure at the same moisture content. A possible reasoning behind this is that specimens that are dispersed have a higher capacity for the diffuse double layers between clay particles to intersect, thereby leading to a higher capacity to swell as opposed to those with a random particle orientation that may or may not have their diffuse double layers intersecting with the neighboring clay particle. On the other side, specimens that have a flocculated structure and wetted will collapse or experience little to no swell when tested as opposed to the specimens compacted with dispersed structure at the same moisture content. A possible reasoning behind this is that the specimens that are flocculated are in contact with each other during the compaction condition, and as the moisture is added, the clay plates tend to distance themselves in a random, non-uniform order as compared to the dispersed structure. With this distancing, the soil structure will tend to collapse or experience little swell as the clay particles will tend to re-arrange themselves under the addition of a load that allows for the minimum spacing that will not interact with a neighboring clay's diffuse double layer. Therefore, the initial orientation of clay plates becomes a key factor in the swelling of a clay, and specimens taken from in-situ will be highly effected by both their stress history and original depositional environment.

In terms of how quickly adjusted moisture specimens swelled, Figure 6.15 shows the time to the end of primary swelling vs. the initial moisture content.

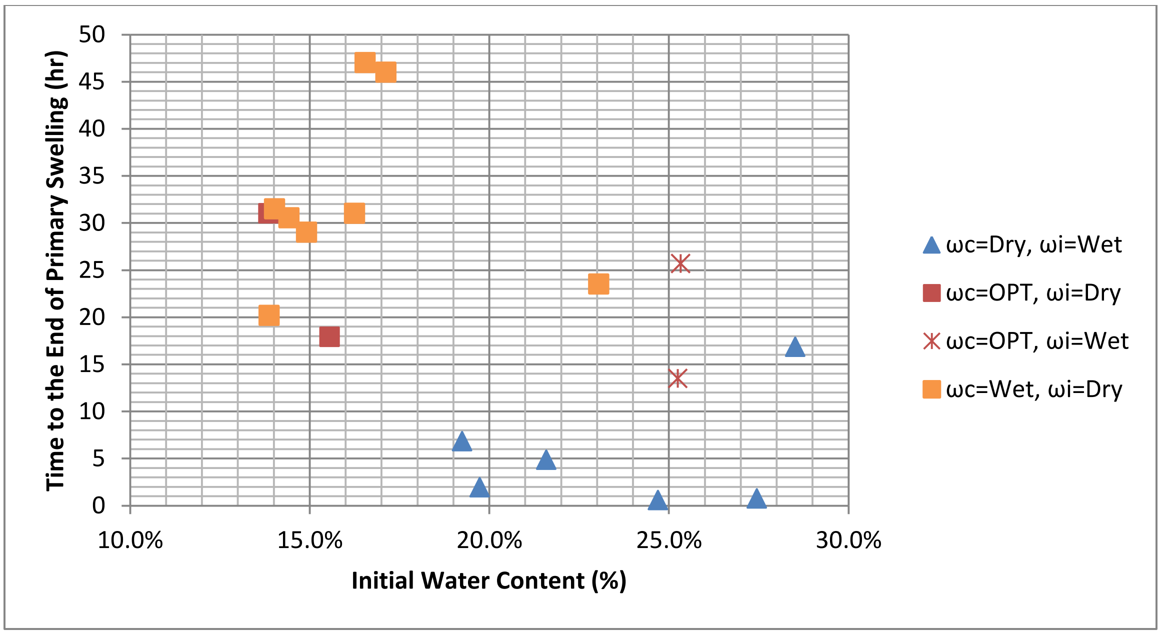

Figure 6.15: Initial Moisture Content vs. Time to End of Primary Swelling for Specimens Tested at Moisture Conditioned Moisture Contents

The same trend for specimens that were tested at their compacted moisture content can be observed where flocculated specimens will swell more rapidly than dispersed specimens. The same reasoning remains here where the effect of the hydraulic conductivity of the samples and flow paths being the reason why the specimens that are flocculated will swell more rapidly. Note that average time for a specimen to swell at the drier moisture content for dispersed specimens has actually increased in comparison to those at the compacted moisture content. Thus, the decrease in moisture content and increase in suction does not necessarily produce faster results as water will take longer to enter the voids between clay plates due to the decrease in spacing between particles from the air-drying process. For flocculated specimens, the end of primary swelling comes slightly faster than those at the compaction moisture content, but the issue of whether the dry densities are the main influence here cannot be distinguished. However, the role of fabric in the time for primary swelling to occur is seen, and thus, fabric is key for the time at which primary swelling is finished.

The rate at which swelling is the other variable that is necessary to monitor in regards to the effect of fabric. The rate of primary swelling vs. tested moisture content is shown in Figure 6.16.

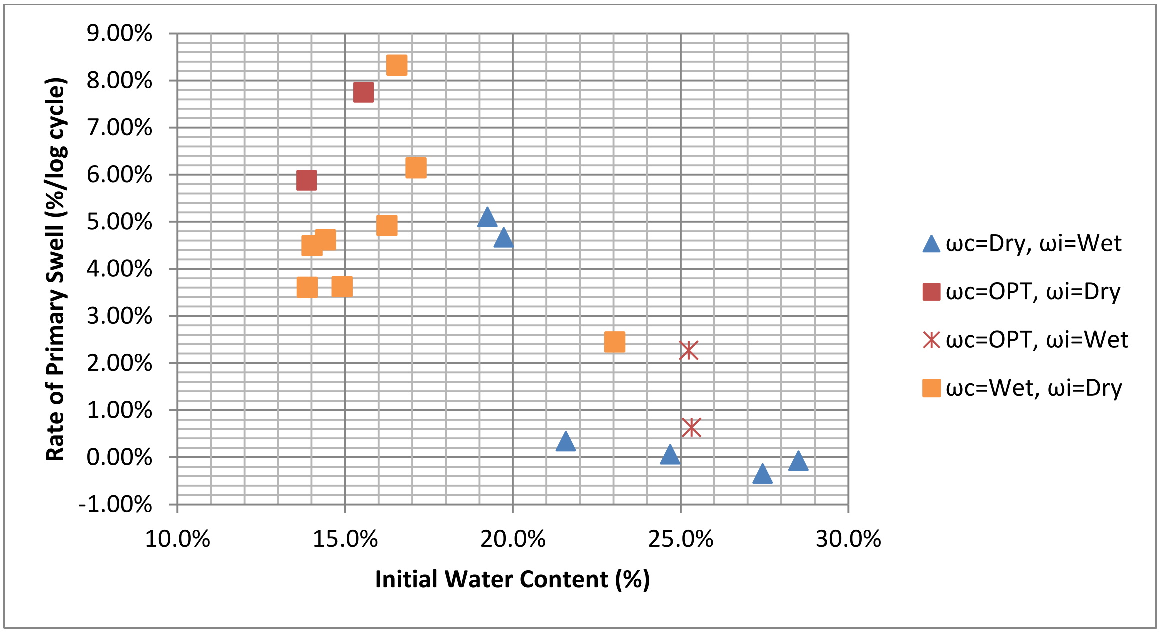

Figure 6.16: Initial Moisture Content vs. Rate of Primary Swelling for Specimens Tested at Moisture Conditioned Moisture Contents

In comparison to those tests tested at the as-compacted moisture conditions, the same general trend exists where those with lower moisture contents will tend to have higher rates of primary swelling due to the higher suction. However, the rate of primary swelling at the same moisture content for dispersed specimens will tend to be higher than those for flocculated specimens. A possible reasoning lies in the infiltration of water into the specimen. When water is flowing through the specimens, the dry specimen's flocculated structure will lead to piping of free water without having to deal with the effects of the diffuse double layer, thereby flowing through the specimens faster but at a smaller log cycle as compared to those for the dispersed specimen which will still see significant amount of swelling after ten hours. Thus, the rate of primary swell should not be focused too heavily upon as compared to the time to the end of primary swelling as dispersed and flocculated structures have different time frames over the log cycle of time at which they swell. Instead, for the time dependent properties of primary swelling, the time to the end of primary swelling will be a much better indicator of how quickly a soil will swell. However, as shown in Figure 6.17, the trend for the rate of secondary swell is not dependent on these issues with the log cycles.

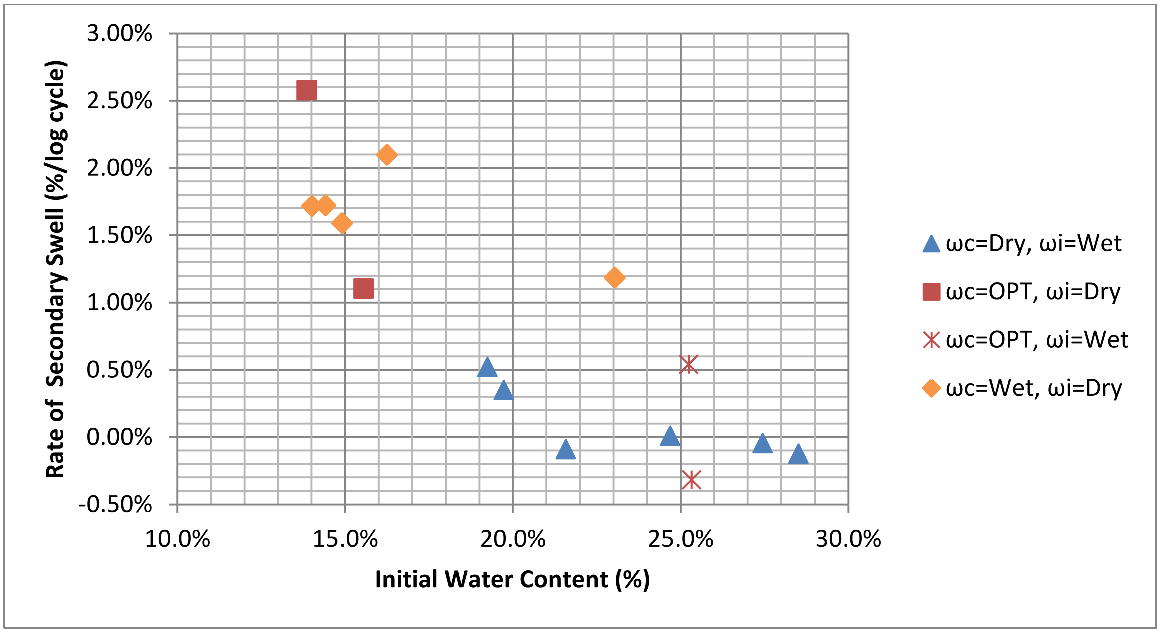

Figure 6.17: Initial Moisture Content vs. Rate of Secondary Swelling for Specimens Tested at Moisture Conditioned Moisture Contents

The trend from the compacted specimens here is the same where the dispersed specimens will see a higher rate of secondary swell as compared to the flocculated specimens. The same reasoning from the compacted specimens applies in which the more difficult portions of the soil to reach are more likely to be prevalent and have a significant amount of potential to swell for disperse specimen due to their lower hydraulic conductivity as opposed to the flocculated specimens. Thus, fabric is a very key issue for the secondary swelling of highly plastic clays as the more difficult regions of the soil to reach are dependent on the initial fabric of the soil as opposed to the initial moisture content.

The trend between the initial and final void ratio is shown in Figure 6.18.

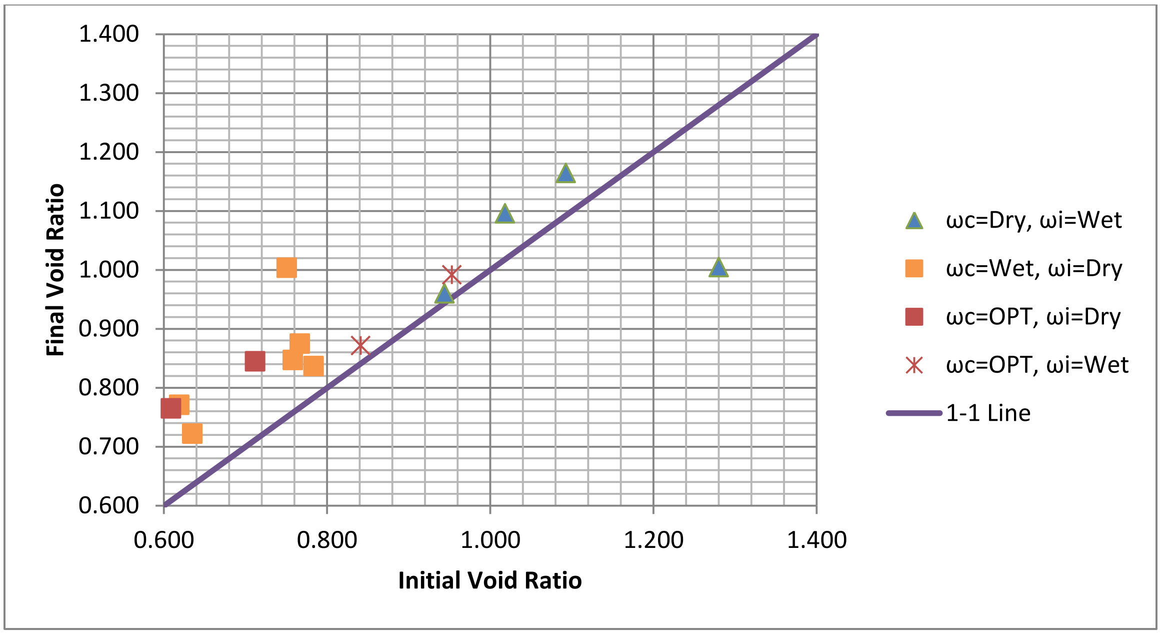

Figure 6.18: Initial vs. Final Void Ratio for Specimens Tested at Moisture Conditioned Moisture Contents

The nearly linear trend seen from those specimens tested at compaction conditions is not seen with much more variation in the range away from the 1 to 1 line. However, the same trend of flocculated specimens tending to start at higher initial void ratios is still observed as is the trend of dispersed specimens tending to have lower initial void ratios and ending at void ratios that are below those of the flocculated specimens. Thus, the fabric's role indicates that even with similar amount of swell, the void ratios between flocculated and dispersed specimens are very different.

After removing the influence of the initial moisture content, specimens with flocculated structures tended to swell less, with shorter time frame for primary swelling, and with less secondary swelling than those specimen's with a dispersed structure. Therefore, fabric's key role in swelling lies in the effect in the time to the end of primary swelling, the rate of secondary swelling, and a small influence in the amount of swelling. This research is important even though previous research has indicated that the natural shrink-swell cycles in the field may reduce the effect of initial fabric on the volumetric changes of in-situ soils (Allen and Gilbert 2006). In order to examine if the results of the fabric hold true for field specimens, the testing program needs to take a further step of examining how the in-situ fabric of a soil affects the swelling and a comparison to laboratory specimens that have been reconstituted.

6.5 Comparison between Results from ASTM D4546 Tests and Double Infiltration Centrifuge Tests

In order to compare the results between the ASTM D4546 test and the double infiltration centrifuge test, the results were separated for each condition based on the testing method. The swell versus initial moisture content between each condition and testing methodology is shown below in Figure 6.19 for those tested at the as-compacted moisture conditions and Figure 6.20 for those tested at moisture conditioned moisture conditions.

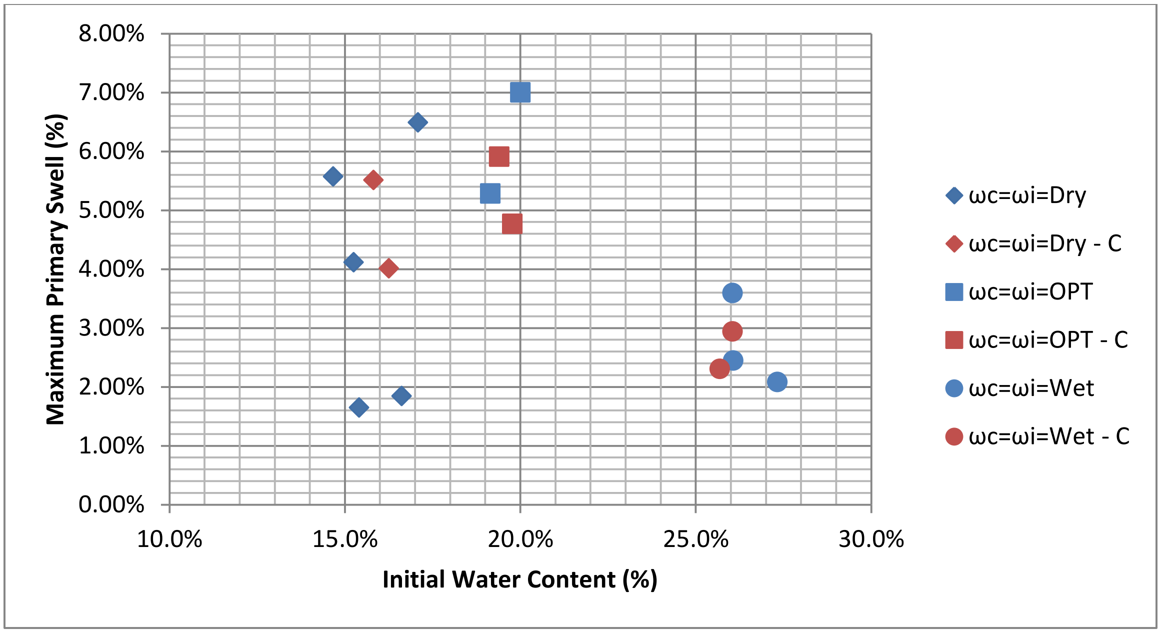

Figure 6.19: Swell Results between ASTM D4546 and Double Infiltration Centrifuge Test for As-Compacted Moisture Contents

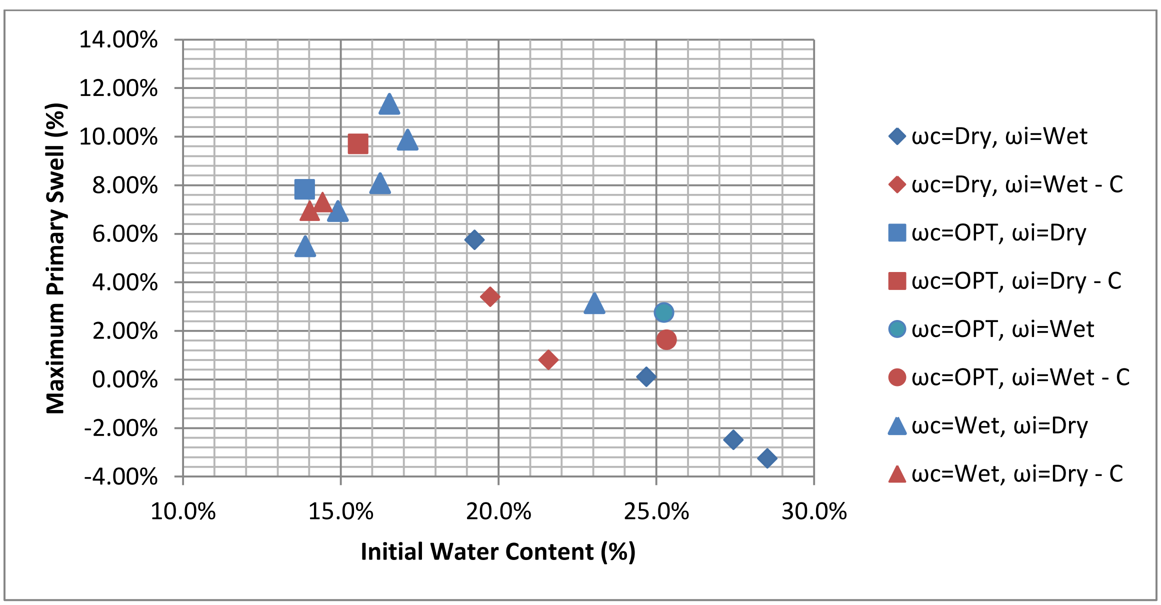

Figure 6.20: Swell Results between ASTM D4546 and Double Infiltration Centrifuge Test for Moisture Conditioned Moisture Contents

The results between tests cluster together based on their testing moisture content and fabric, regardless of the testing method. Therefore, the centrifuge method can be relied upon to produce results that are consistent with the ASTM D4546 tests, even when accounting for problematic moisture conditions like the dry to wet condition. Further, there tends to be less scatter between tests for the centrifuge method. As such, submerged centrifuge tests produce consistent results from those from the ASTM D4546 testing that are repeatable.

In order to verify the benefits of the test, the time to reach the end of primary swelling for each methodology and condition were examined in Figure 6.21 for those tested at the as-compacted moisture conditions and Figure 6.22 for those tested at moisture conditioned moisture conditions.

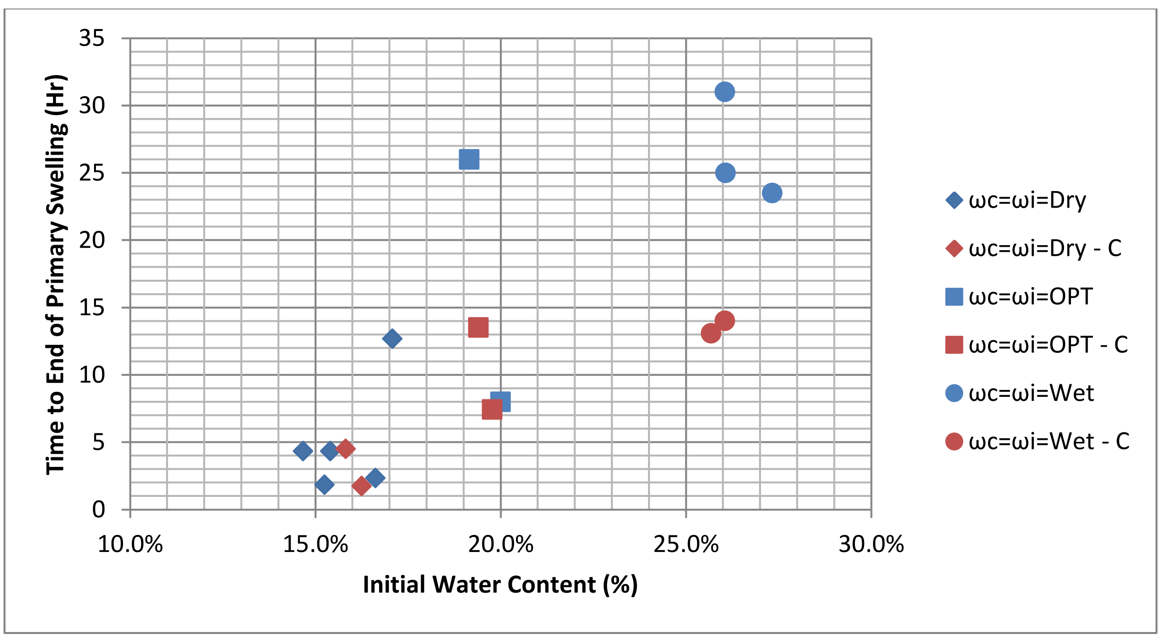

Figure 6.21: Time to End of Primary Swelling between ASTM D4546 and Double Infiltration Centrifuge Test for As-Compacted Moisture Contents

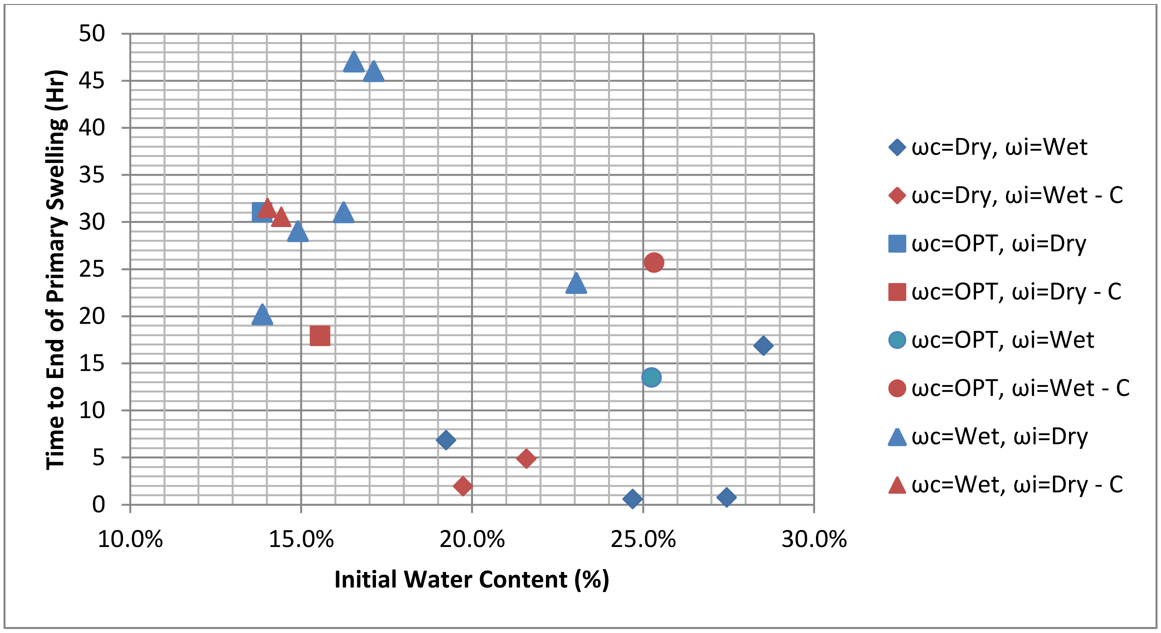

Figure 6.22: Time to End of Primary Swelling between ASTM D4546 and Double Infiltration Centrifuge Test for Moisture Conditioned Moisture Contents

There is a marked reduction in the time to reach the end of primary swelling for the centrifuge test for those tested at the initial conditions, especially for specimens compacted wet, stemming from an increase in the gravitational gradient. In the increased gravitational gradient, the flow of water is increased past the stage when the suction gradient drives the influx of moisture which is important for those specimens that begin with a relatively low suction value. Thus, voids that may have taken more time in a 1-g environment for the ASTM D4546 test will be reached more quickly. The decrease in time has more scatter for those with adjusted moisture content, but issues stemming from the effect of the dry density on the soil characteristics as well as the issues with the procedures on the adjustment of soil decrease the reliability of this scatter. Therefore, when considering test done on specimens that don't have density or volumetric strain issues and on specimens that may have an initially low suction value, one of the benefits of the centrifuge test is the decrease in the time frame of the primary swelling. This benefit will be important on testing soils that come from in-situ conditions that are initially wet as the timeframe for testing will not be as significant as tests done via the ASTM D4546 method.

The other benefit of the centrifuge testing again lies in the increased gravitational gradient that drives the flow of water towards the end and after primary swelling is completed. The rate of secondary swelling for each methodology and condition were examined in Figure 6.23 for those tested at the as-compacted moisture conditions and Figure 6.24 for those tested at moisture conditioned moisture conditions.

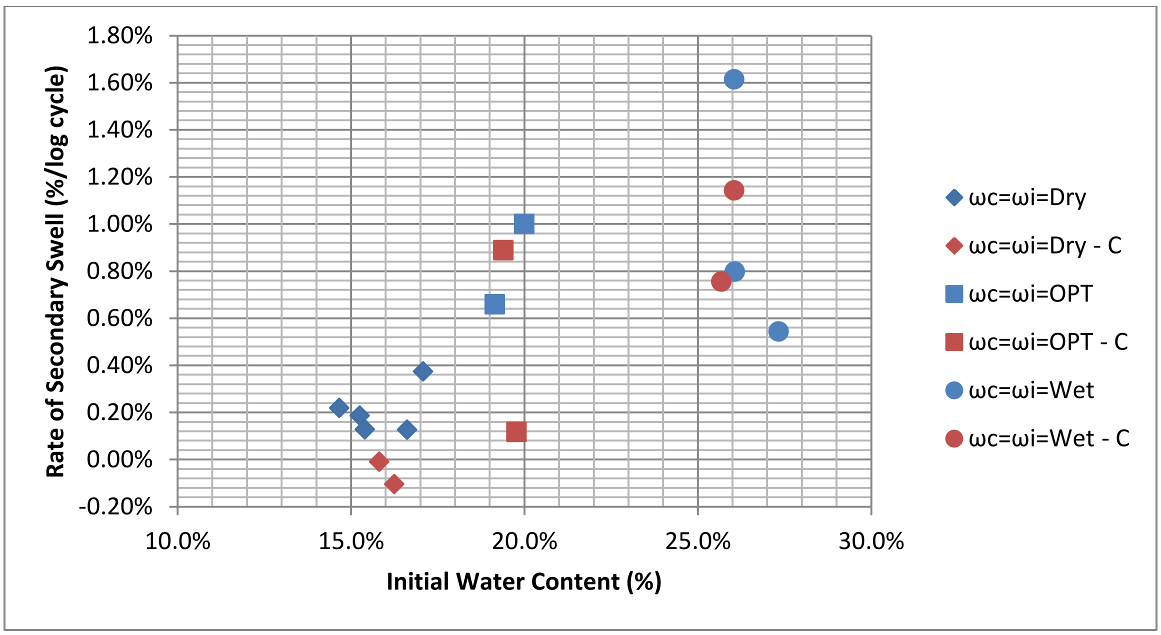

Figure 6.23: Time to End of Primary Swelling between ASTM D4546 and Double Infiltration Centrifuge Test for As-Compacted Moisture Contents

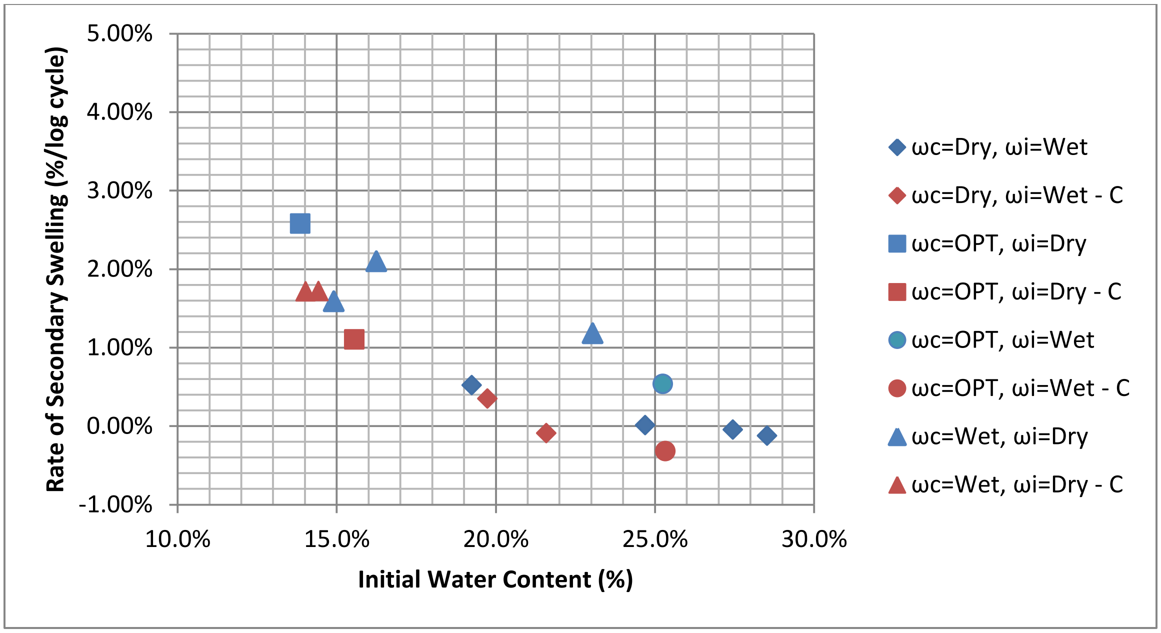

Figure 6.24: Time to End of Primary Swelling between ASTM D4546 and Double Infiltration Centrifuge Test for Moisture Conditioned Moisture Contents

The centrifuge tests tend to have a lower rate of secondary swelling than those imposed by the ASTM D4546, especially when the moisture conditions are adjusted from as-compacted conditions. With the increased gravitational gradient, the reduction in the amount of micro-voids that are not filled at the end of primary swelling will lead to the secondary swelling being reduced as well. Therefore, testing done in the double infiltration centrifuge environment will give results that have a reduction in secondary swelling that help to determine what is the reasoning and cause of this secondary swelling.

Overall, the new double infiltration centrifuge set-up will provide similar results for the swell at the end of primary swelling in a shorter time frame with less secondary swelling. Therefore, this method is highly recommended for implementation into the testing of in-situ specimens for the application of use in roadway design as well as for research purposes into the causes of secondary swelling.

6.6 Comparison between Results from Reconstituted and Trimmed Specimens

Figure 6.25 shows the results from the tests on trimmed specimens at OPT with the best fit line and tests from ASTM D4546 for the reconstituted specimens.

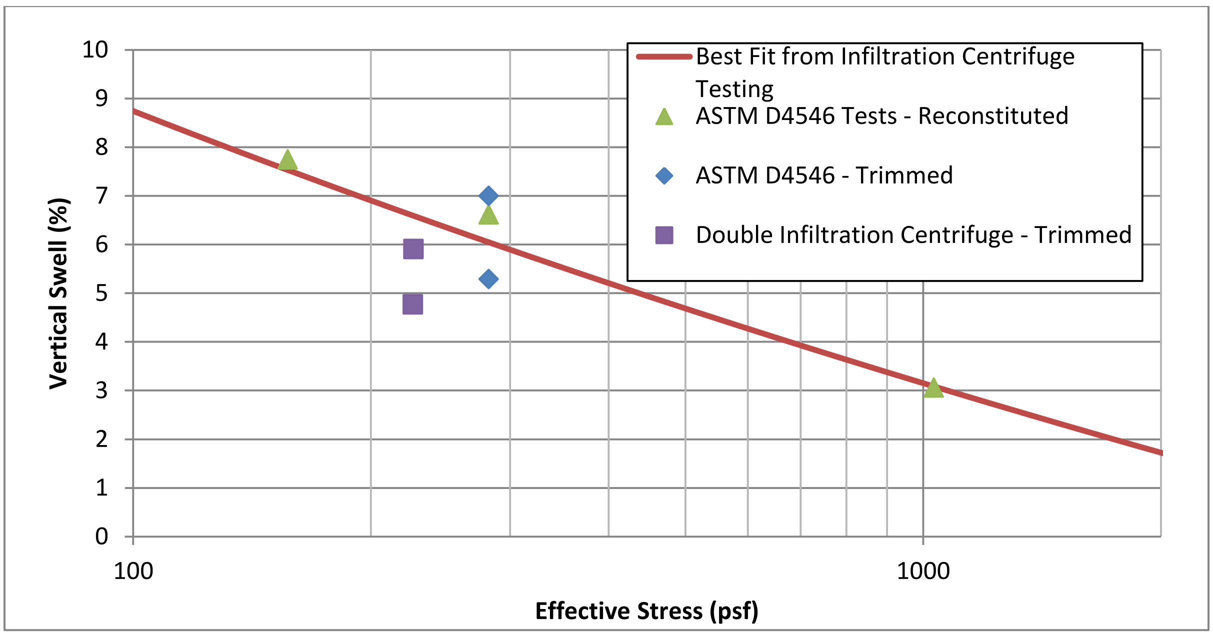

Figure 6.25: Comparison between Reconstituted and Trimmed Specimens

From the testing of reconstituted specimens at the same stress as those of the trimmed specimens, the primary swell of the soil should be approximately 6.5% which is similar to the results from the trimmed specimens. However, more variation between results exist for the trimmed specimens as the dry densities tested were not always at the same as the average dry density of the specimen as explained in Section 6.2.1. Therefore, the reconstituted specimens have a better control of their dry density due to the knowledge of the exact amount of soil added and control of the compaction which leads to more repeatable results at higher stresses. Despite this, the results indicate that samples that are reconstituted via kneading compaction give comparable results to those that are impact compacted within the Standard Proctor mold. Therefore, the previous single infiltration centrifuge methodology has been shown to be correct in the assumption that the targeted density should be based on the maximum dry density from a Standard Proctor test.

Chapter 7: Conclusions

The effect of fabric on the swelling of highly plastic clays was examined in this investigation. Specifically, the swelling of the Cook Mountain clay was evaluated using existing methodologies as well as a new centrifuge based method. The new centrifuge method was developed in this study in order to be able to test undisturbed specimens in an increased gravitational gradient based environment. Based on the test program results, several conclusions can be made about the effect of the initial fabric and density on the swelling of highly plastic clays.

- Flocculated soils were found to swell less than dispersed soils when tested using the same initial moisture content.
- Samples with a flocculated structure were found to swell more rapidly and to have less secondary swelling than those samples with a dispersed structure for tests at the same initial moisture content.
- Samples that were compacted dry of optimum and tested at the as-compacted moisture condition were found to have a lower than predicted swell due to issues with macro-voids and fissures. Thus, macro-voids in the soil's fabric are important in the soil's swelling potential, leading to a need for further research into how naturally formed voids, such as vugs or fissures, affect in-situ samples' swelling potential.
- Samples that have the same fabric and moisture content but are at a lower dry density will swell less than those at a higher dry density. Thus, as density increases, the amount of swelling will also increase.

Further, two conclusions can be made about the new testing procedure as well as the original compaction techniques for the single infiltration centrifuge method.

- The new double infiltration centrifuge set-up was found to produce comparable results to those from the ASTM D4546 tests. This method is found to be superior to both the ASTM D4546 test and single infiltration centrifuge test as it can produce results more rapidly and with less secondary swelling.
- Samples that are compacted within the proctor mold, i.e. trimmed samples compacted with impact compaction, were found to produce similar results to those that are compacted within the cutting ring or permeameter cup, i.e. reconstituted samples compacted with kneading compaction, at the same initial moisture content and dry density.

Overall, the fabric of soil was found to significantly affect the swelling characteristics. It is recommend that a study be done on samples taken from in-situ in order to further understand how the depositional environment and particle orientation from the field will affect vertical swelling properties compared to laboratory compacted specimens. Therefore, the author recommends that Shelby Tube samples of the Cook Mountain formation should be taken in order to examine how the undisturbed in-situ fabric affects the initial swelling of a soil deposit.

Appendix A: Results from Reconstituted Specimens

Note that results are presented in two groups, first the infiltration centrifuge tests and then the ASTM D4546 Free Swell tests, both ordered in terms of increasing magnitude of stress. A summary of the results is presented in Table A.1.

Table A.1: Summary of Results from Reconstituted Specimens

Date	Method	ω,i (%)	Swell (%)	σ' (psf)
11/7/2013	Centrifuge	20.5	13.30	28.1
3/11/2014	Centrifuge	20.1	11.84	31.6
3/11/2014	Centrifuge	20.1	10.65	33.9
3/10/2014	Centrifuge	20.1	9.79	75.8
3/10/2014	Centrifuge	20.1	11.43	81.7
11/22/2013	Centrifuge	19.5	8.82	83.3
11/22/2013	Centrifuge	19.5	8.42	83.9
11/12/2013	ASTM D4546	20.0	7.75	157
3/15/2014	ASTM D4546	19.6	6.61	282
3/12/2014	Centrifuge	20.1	4.96	550.2
11/25/2013	Centrifuge	21.3	3.33	641.4
3/15/2014	ASTM D4546	19.6	3.06	1032

CENTRIFUGE TEST		
	Date test conducted	11/7/2013
	Centrifuge used	1
	Cup Number	1
	Conducted by	Cameron

SOIL Information		
	Soil	CM
	Relative Compaction	100%
	Target Water Content	20%
	Water Content	OPT
	Specific Gravity	2.7

TESTING SETUP Information	Property	Target	Actual	Unit
	G-Level	5.00	8.56	gravity
	Initial ω	20.0%	20.5%	%
	Mass Soil added	49.40	49.39	g
	Dry Unit Weight	15.60	15.57	kN/m^3
	Relative Compaction	100%	100%	%
	Height of Sample	1.000	1.000	cm

TEST RESULTS Information	Property	Initial	Final	Unit
	Seating Height	-	0.000	cm
	Testing Height	0.998	1.131	cm
	Void Ratio, e	0.702	0.928	-
	ω	20.5%	39.2%	%
	Saturation	78.9%	100.0%	%
	Change in ω	-	18.7%	%
	Overburden Mass	-	14.92	g
	Height of water	-	2.00	cm
	Swell	-	13.3%	%

NOTES	

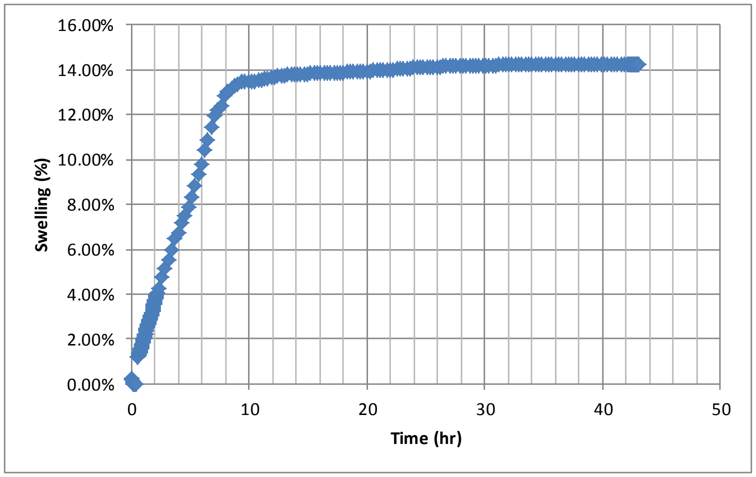

Slope of Primary Swelling	15.46%	%/log cycle
Slope of Secondary Swelling	0.96%	%/log cycle

Swell	13%
Time to Swell (hr)	8.78433
Stress (psf)	28.1

CENTRIFUGE TEST		
	Date test conducted	3/11/2014
	Centrifuge used	2
	Cup Number	1
	Conducted by	Chris

SOIL Information		
	Soil	CM
	Relative Compaction	100%
	Target Water Content	20%
	Water Content	OPT
	Specific Gravity	2.78

TESTING SETUP Information	Property	Target	Actual	Unit
	G-Level	10.00	11.44	gravity
	Initial ω	20.0%	20.1%	%
	Mass Soil added	48.83	48.81	g
	Dry Unit Weight	15.42	15.57	kN/m^3
	Relative Compaction	100%	101%	%
	Height of Sample	1.000	1.000	cm

TEST RESULTS Information	Property	Initial	Final	Unit
	Seating Height	-	0.000	cm
	Testing Height	0.989	1.106	cm
	Void Ratio, e	0.751	0.958	-
	ω	20.1%	35.4%	%
	Saturation	74.4%	100.0%	%
	Change in ω	-	15.3%	%
	Overburden Mass	-	14.70	g
	Height of water	-	3.00	cm
	Swell	-	11.8%	%

NOTES	

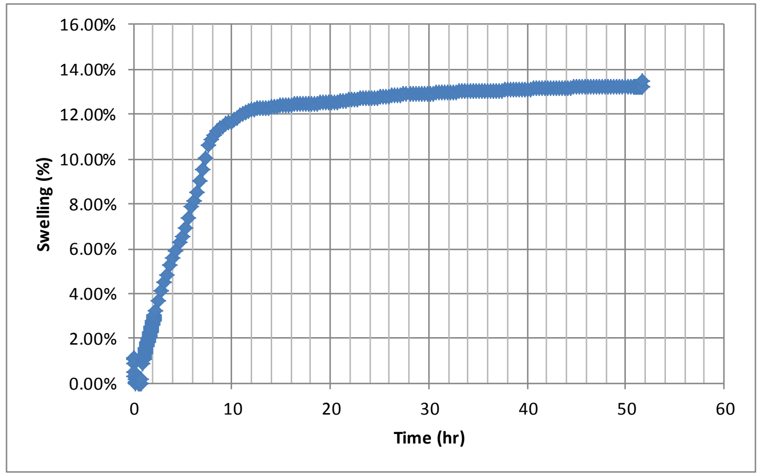

Swell	12%
Time to Swell (hr)	10.4787
Stress (psf)	31.6

Slope of Primary Swelling	19.48%	%/log cycle
Slope of Secondary Swelling	2.06%	%/log cycle

CENTRIFUGE TEST		
	Date test conducted	3/11/2014
	Centrifuge used	2
	Cup Number	3
	Conducted by	Chris

SOIL Information		
	Soil	CM
	Relative Compaction	100%
	Target Water Content	20%
	Water Content	OPT
	Specific Gravity	2.78

TESTING SETUP Information	Property	Target	Actual	Unit
	G-Level	10.00	11.44	gravity
	Initial ω	20.0%	20.1%	%
	Mass Soil added	48.83	48.89	g
	Dry Unit Weight	15.42	15.54	kN/m^3
	Relative Compaction	100%	101%	%
	Height of Sample	1.000	1.001	cm

TEST RESULTS Information	Property	Initial	Final	Unit
	Seating Height	-	0.001	cm
	Testing Height	0.993	1.099	cm
	Void Ratio, e	0.755	0.942	-
	ω	20.1%	36.1%	%
	Saturation	74.0%	100.0%	%
	Change in ω	-	16.0%	%
	Overburden Mass	-	14.45	g
	Height of water	-	3.00	cm
	Swell	-	10.6%	%

NOTES	

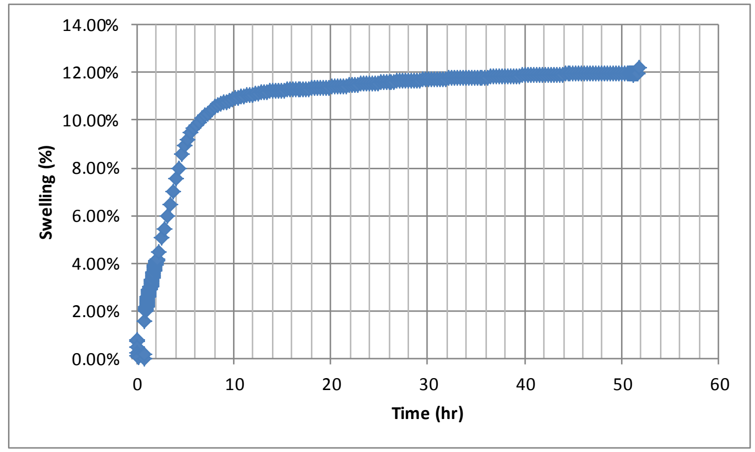

Swell	11%
Time to Swell (hr)	8.42869
Stress (psf)	33.9

Slope of Primary Swelling	12%	%/log cycle
Slope of Secondary Swelling	1%	%/log cycle

CENTRIFUGE TEST		
	Date test conducted	3/10/2014
	Centrifuge used	1
	Cup Number	4
	Conducted by	Chris

SOIL Information		
	Soil	CM
	Relative Compaction	100%
	Target Water Content	20%
	Water Content	OPT
	Specific Gravity	2.78

TESTING SETUP Information	Property	Target	Actual	Unit
	G-Level	25.00	28.11	gravity
	Initial ω	20.0%	20.1%	%
	Mass Soil added	48.83	48.91	g
	Dry Unit Weight	15.42	15.67	kN/m^3
	Relative Compaction	100%	102%	%
	Height of Sample	1.000	1.000	cm

TEST RESULTS Information	Property	Initial	Final	Unit
	Seating Height	-	-0.001	cm
	Testing Height	0.985	1.081	cm
	Void Ratio, e	0.740	0.910	-
	ω	20.1%	33.3%	%
	Saturation	75.5%	100.0%	%
	Change in ω	-	13.2%	%
	Overburden Mass	-	14.71	g
	Height of water	-	2.00	cm
	Swell	-	9.8%	%

NOTES	

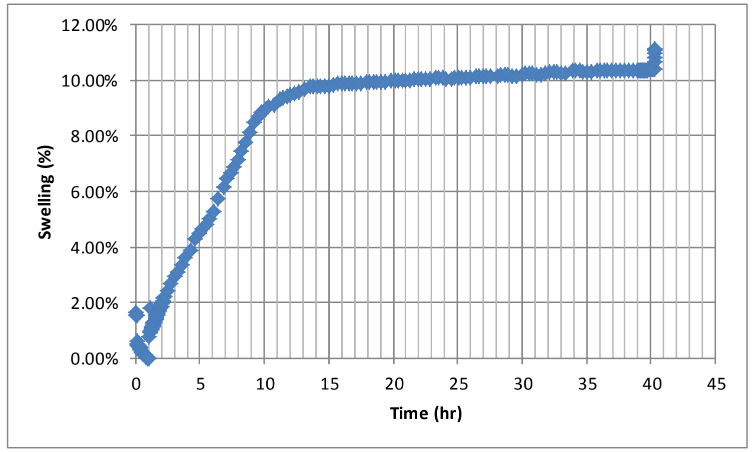

Swell	10%	
Time to Swell (hr)	14.3595	
Stress (psf)	75.8	

Slope of Primary Swelling	13%	%/log cycle
Slope of Secondary Swelling	2%	%/log cycle

CENTRIFUGE TEST

Date test conducted	3/10/2014
Centrifuge used	1
Cup Number	3
Conducted by	Chris

SOIL Information		
	Soil	CM
	Relative Compaction	100%
	Target Water Content	20%
	Water Content	OPT
	Specific Gravity	2.78

TESTING SETUP Information	Property	Target	Actual	Unit
	G-Level	25.00	28.11	gravity
	Initial ω	20.0%	20.1%	%
	Mass Soil added	48.83	48.88	g
	Dry Unit Weight	15.42	15.67	kN/m^3
	Relative Compaction	100%	102%	%
	Height of Sample	1.000	0.996	cm

TEST RESULTS Information	Property	Initial	Final	Unit
	Seating Height	-	-0.001	cm
	Testing Height	0.984	1.097	cm
	Void Ratio, e	0.740	0.939	-
	ω	20.1%	32.3%	%
	Saturation	75.5%	95.5%	%
	Change in ω	-	12.2%	%
	Overburden Mass	-	15.01	g
	Height of water	-	2.00	cm
	Swell	-	11.4%	%

NOTES	

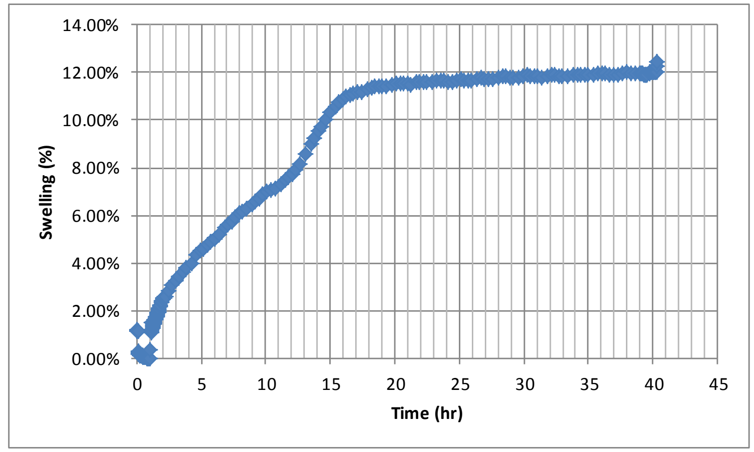

Swell	**11%**

Slope of Primary Swelling	7%	%/log cycle
Slope of Secondary Swelling	2%	%/log cycle

Time to Swell (hr)	**19.0222**
Stress (psf)	**81.7**

CENTRIFUGE TEST		
	Date test conducted	11/22/2013
	Centrifuge used	1
	Cup Number	4
	Conducted by	Cameron

SOIL Information	Soil	CM
	Relative Compaction	100%
	Target Water Content	20%
	Water Content	OPT
	Specific Gravity	2.7

TESTING SETUP Information	Property	Target	Actual	Unit
	G-Level	25.00	25.64	gravity
	Initial ω	20.0%	19.5%	%
	Mass Soil added	49.40	49.42	g
	Dry Unit Weight	15.60	15.88	kN/m^3
	Relative Compaction	100%	102%	%
	Height of Sample	1.000	0.996	cm

TEST RESULTS Information	Property	Initial	Final	Unit
	Seating Height	-	0.000	cm
	Testing Height	0.987	1.074	cm
	Void Ratio, e	0.668	0.815	-
	ω	19.5%	34.4%	%
	Saturation	78.8%	100.0%	%
	Change in ω	-	14.9%	%
	Overburden Mass	-	14.57	g
	Height of water	-	2.00	cm
	Swell	-	8.8%	%

NOTES	

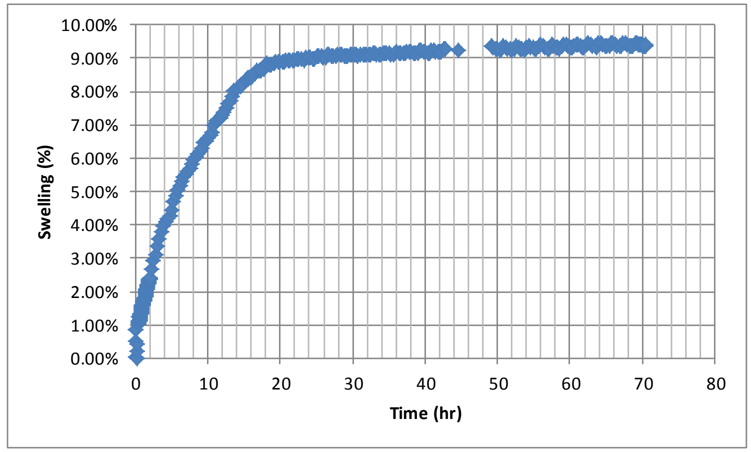

Slope of Primary Swelling	8%	%/log cycle
Slope of Secondary Swelling	1%	%/log cycle

Swell	9%
Time to Swell (hr)	18.5367
Stress (psf)	83.3

CENTRIFUGE TEST		
	Date test conducted	11/22/2013
	Centrifuge used	1
	Cup Number	3
	Conducted by	Cameron

SOIL Information		
	Soil	CM
	Relative Compaction	100%
	Target Water Content	20%
	Water Content	OPT
	Specific Gravity	2.7

TESTING SETUP Information	Property	Target	Actual	Unit
	G-Level	25.00	25.64	gravity
	Initial ω	20.0%	19.5%	%
	Mass Soil added	49.40	49.41	g
	Dry Unit Weight	15.60	15.79	kN/m^3
	Relative Compaction	100%	101%	%
	Height of Sample	1.000	1.001	cm

TEST RESULTS Information	Property	Initial	Final	Unit
	Seating Height	-	0.000	cm
	Testing Height	0.992	1.076	cm
	Void Ratio, e	0.677	0.818	-
	ω	19.5%	34.4%	%
	Saturation	77.8%	100.0%	%
	Change in ω	-	14.9%	%
	Overburden Mass	-	14.84	g
	Height of water	-	2.00	cm
	Swell	-	8.4%	%

NOTES	

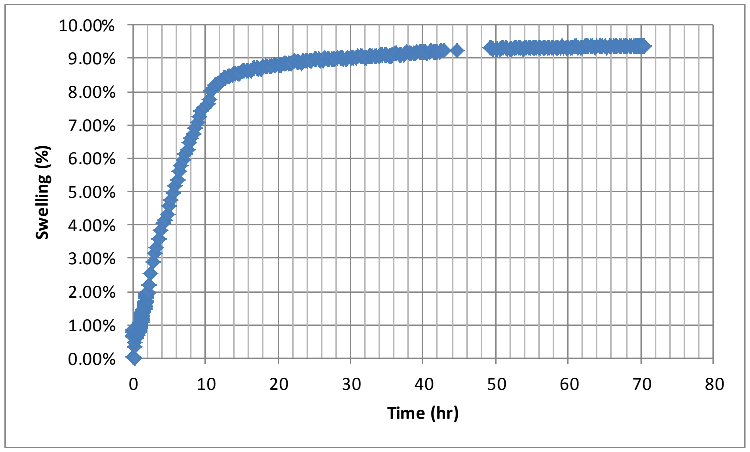

Slope of Primary Swelling	9%	%/log cycle
Slope of Secondary Swelling	1%	%/log cycle

Swell	8%
Time to Swell (hr)	12.8029
Stress (psf)	83.9

CENTRIFUGE TEST		
	Date test conducted	3/12/2014
	Centrifuge used	1
	Cup Number	2
	Conducted by	Chris

SOIL Information		
	Soil	CM
	Relative Compaction	100%
	Target Water Content	20%
	Water Content	OPT
	Specific Gravity	2.78

TESTING SETUP Information	Property	Target	Actual	Unit
	G-Level	200.00	192.46	gravity
	Initial ω	20.0%	20.1%	%
	Mass Soil added	48.83	48.84	g
	Dry Unit Weight	15.42	16.14	kN/m^3
	Relative Compaction	100%	105%	%
	Height of Sample	1.000	0.998	cm

TEST RESULTS Information	Property	Initial	Final	Unit
	Seating Height	-	0.001	cm
	Testing Height	0.955	1.002	cm
	Void Ratio, e	0.690	0.773	-
	ω	20.1%	29.1%	%
	Saturation	81.0%	100.0%	%
	Change in ω	-	9.0%	%
	Overburden Mass	-	14.79	g
	Height of water	-	3.00	cm
	Swell	-	5.0%	%

NOTES	

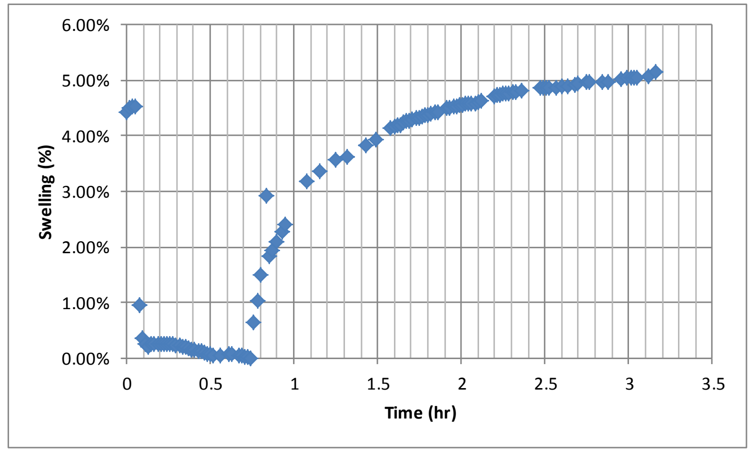

Swell	5%

Slope of Primary Swelling	3%	%/log cycle

Time to Swell (hr)	2.75028

Slope of Secondary Swelling	-	%/log cycle

Stress (psf)	550.2

CENTRIFUGE TEST		
	Date test conducted	11/25/2013
	Centrifuge used	1
	Cup Number	3
	Conducted by	Cameron

SOIL Information		
	Soil	CM
	Relative Compaction	100%
	Target Water Content	20%
	Water Content	OPT
	Specific Gravity	2.7

TESTING SETUP Information	Property	Target	Actual	Unit
	G-Level	200.00	197.83	gravity
	Initial ω	20.0%	21.3%	%
	Mass Soil added	49.40	49.42	g
	Dry Unit Weight	15.60	15.83	kN/m^3
	Relative Compaction	100%	101%	%
	Height of Sample	1.000	1.004	cm

TEST RESULTS Information	Property	Initial	Final	Unit
	Seating Height	-	-0.001	cm
	Testing Height	0.976	1.009	cm
	Void Ratio, e	0.674	0.729	-
	ω	21.3%	28.6%	%
	Saturation	85.2%	100.0%	%
	Change in ω	-	7.4%	%
	Overburden Mass	-	14.66	g
	Height of water	-	2.00	cm
	Swell	-	3.3%	%

NOTES	

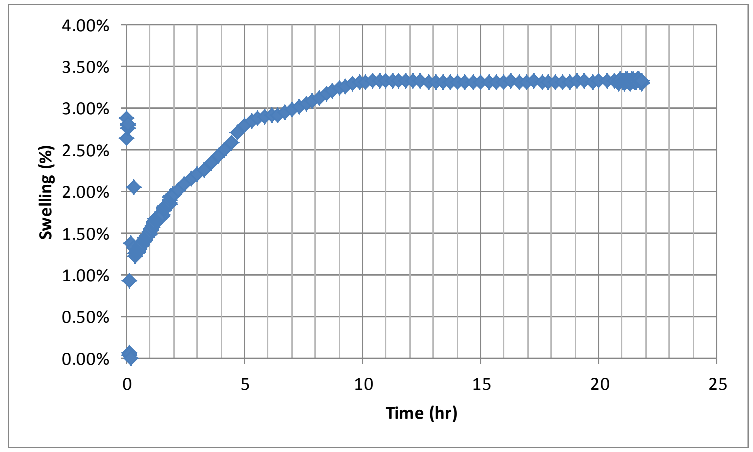

Swell	3%
Time to Swell (hr)	10.7015
Stress (psf)	641.4

Slope of Primary Swelling	2%	%/log cycle
Slope of Secondary Swelling	0%	%/log cycle

FREE SWELL TEST

Date test conducted	11/12/2013
Conducted by	Chris

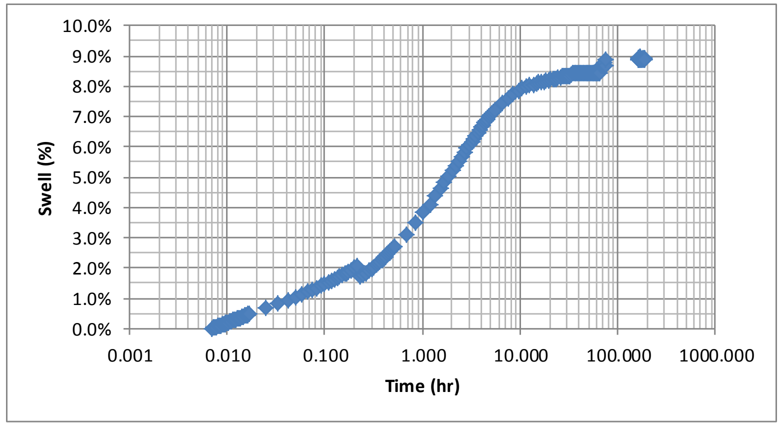

SOIL Information	**Soil**	CM
	Compacted or Reconstituted?	Reconstituted
	Specific Gravity	2.784

TESTING SETUP Information	**Property**	Target	Actual	Unit
	Mass Soil added	59.76	59.65	g
	Dry Density	1.573	1.572	g/cm^3
	Density	1.887	1.887	g/cm^3
	Height of Sample	1.000	0.998	cm

TEST RESULTS Information	**Property**	Initial	Final	Unit
	Seating Height	-	0.993	cm
	Testing Height	0.993	1.071	cm
	Void Ratio, e	0.768	0.896	-
	ω	20.0%	48.2%	%
	Saturation	72.4%	100.0%	%
	Change in ω	-	28.2%	%

Swell	**8%**

Slope of Primary Swelling	4%	%/log cycle
Slope of Secondary Swelling	1%	%/log cycle

Time to Swell (hr)	**9**
Stress (psf)	**157.0**

FREE SWELL TEST

Date test conducted	3/15/2014
Conducted by	Chris

SOIL Information		
	Soil	CM
	Compacted or Reconstituted?	Reconstituted
	Specific Gravity	2.784

TESTING SETUP Information	Property	Target	Actual	Unit
	Mass Soil added	59.76	59.72	g
	Dry Density	1.577	1.570	g/cm^3
	Density	1.887	1.878	g/cm^3
	Height of Sample	1.000	1.004	cm

TEST RESULTS Information	Property	Initial	Final	Unit
	Seating Height	-	0.997	cm
	Testing Height	0.989	1.054	cm
	Void Ratio, e	0.771	0.859	-
	ω	19.6%	34.9%	%
	Saturation	70.8%	100.0%	%
	Change in ω	-	15.2%	%

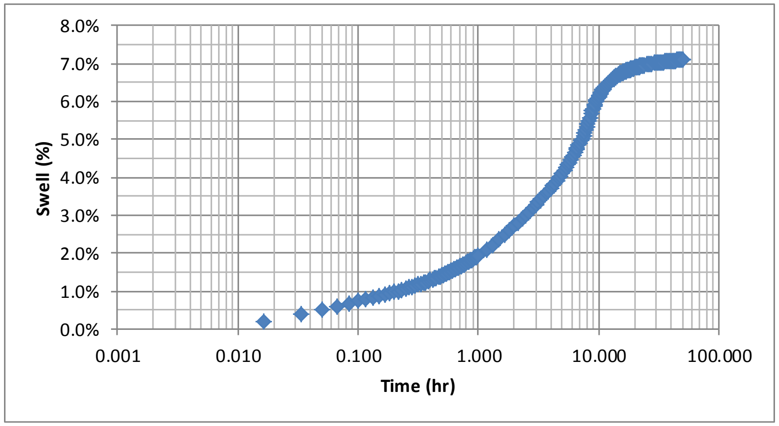

Swell	7%
Time to Swell (hr)	14
Stress (psf)	282.0

Slope of Primary Swelling	8%	%/log cycle
Slope of Secondary Swelling	1%	%/log cycle

FREE SWELL TEST	Date test conducted	3/15/2014
	Conducted by	Chris

SOIL Information	Soil	CM
	Compacted or Reconstituted?	Reconstituted
	Specific Gravity	2.784

TESTING SETUP Information	Property	Target	Actual	Unit
	Mass Soil added	59.76	59.73	g
	Dry Density	1.577	1.578	g/cm^3
	Density	1.887	1.888	g/cm^3
	Height of Sample	1.000	0.999	cm

TEST RESULTS Information	Property	Initial	Final	Unit
	Seating Height	-	0.993	cm
	Testing Height	0.967	1.017	cm
	Void Ratio, e	0.762	0.794	-
	ω	19.6%	32.1%	%
	Saturation	71.6%	100.0%	%
	Change in ω	-	12.5%	%

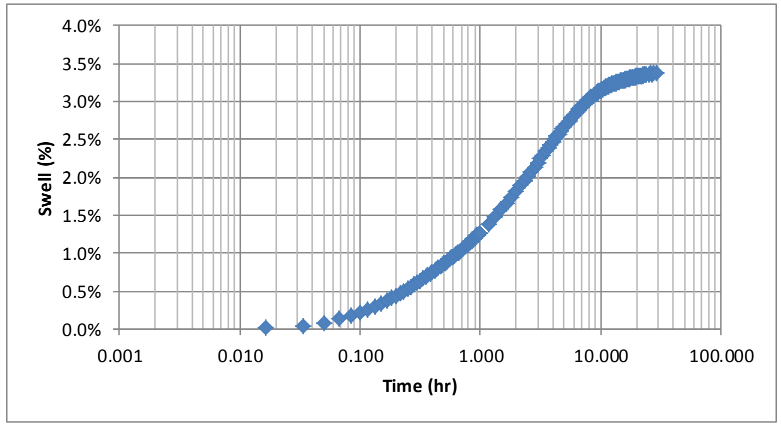

Swell	3%

Slope of Primary Swelling	2%	%/log cycle
Slope of Secondary Swelling	1%	%/log cycle

Time to Swell (hr)	8
Stress (psf)	1032.0

Appendix B: Results from Trimmed Specimens

Note that results are presented in two groups, first the ASTM D4546 Free Swell tests and then the new submerged centrifuge tests, both ordered chronologically.

FREE SWELL TEST

Date test conducted	3/14/2014
Conducted by	Chris

SOIL Information	**Soil**	CM
	Condition	OPT
	Specific Gravity	2.784

TESTING SETUP Information	**Property**	Target	Actual	Unit
	Mass Soil added	-	116.23	g
	Dry Density	-	1.488	g/cm^3
	Density	-	1.773	g/cm^3
	Height of Sample	2.000	2.070	cm

TEST RESULTS Information	**Property**	Initial	Final	Unit
	Seating Height	-	2.063	cm
	Testing Height	2.057	2.166	cm
	Void Ratio, e	0.868	0.954	-
	ω	19.1%	32.8%	%
	Saturation	61.3%	95.4%	%
	Change in ω	-	13.7%	%

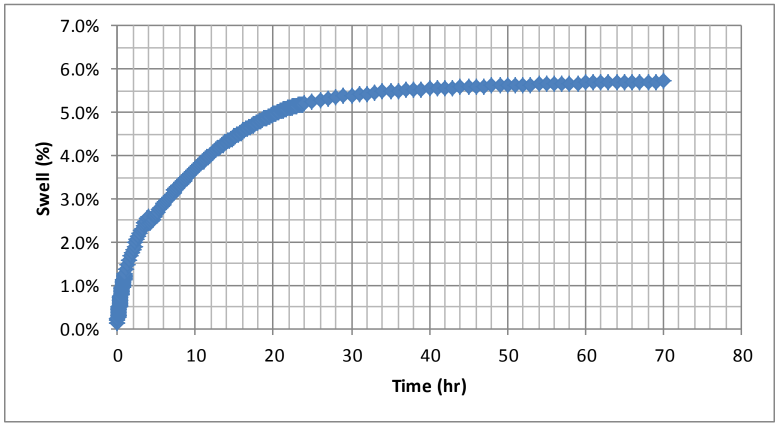

Swell	**5%**
Time to Swell (hr)	**26**
Stress (psf)	**282.0**

Slope of Primary Swelling	4.15% %/log cycle
Slope of Secondary Swelling	0.66% %/log cycle

FREE SWELL TEST

Date test conducted	3/16/2014
Conducted by	Chris

SOIL Information	Soil	CM
	Condition	Wet
	Specific Gravity	2.784

	Property	Target	Actual	Unit
TESTING SETUP Information	Mass Soil added	-	115.68	g
	Dry Density	-	1.471	g/cm^3
	Density	-	1.873	g/cm^3
	Height of Sample	2.000	1.950	cm

	Property	Initial	Final	Unit
TEST RESULTS Information	Seating Height	-	1.946	cm
	Testing Height	1.944	1.984	cm
	Void Ratio, e	0.889	0.923	-
	ω	27.3%	32.8%	%
	Saturation	85.4%	98.7%	%
	Change in ω	-	5.5%	%

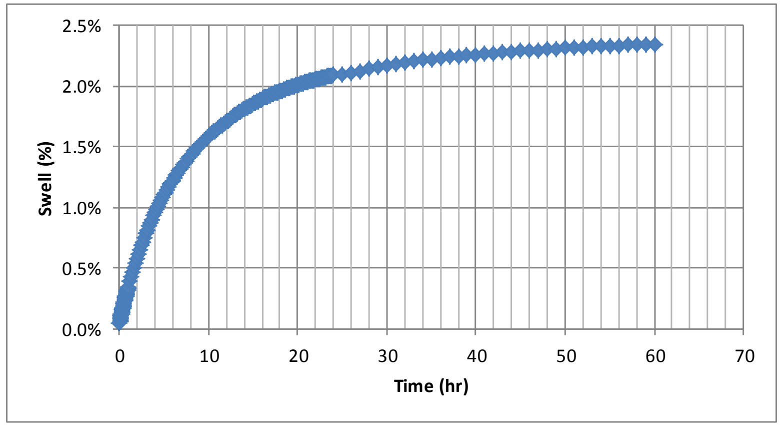

Swell	2%

Slope of Primary Swelling	1.49% %/log cycle

Time to Swell (hr)	23

Slope of Secondary Swelling	0.54% %/log cycle

Stress (psf)	282.0

FREE SWELL TEST

Date test conducted	3/17/2014
Conducted by	Chris

SOIL Information	Soil	CM
	Condition	Wet to Dry
	Specific Gravity	2.784

	Property	Target	Actual	Unit
TESTING SETUP Information	Mass Soil added	-	117.24	g
	Dry Density	-	1.559	g/cm^3
	Density	-	1.918	g/cm^3
	Height of Sample	2.000	1.930	cm

	Property	Initial	Final	Unit
TEST RESULTS Information	Seating Height	-	1.930	cm
	Testing Height	1.934	1.987	cm
	Void Ratio, e	0.784	0.836	-
	ω	23.0%	31.3%	%
	Saturation	81.8%	100.0%	%
	Change in ω	-	8.3%	%

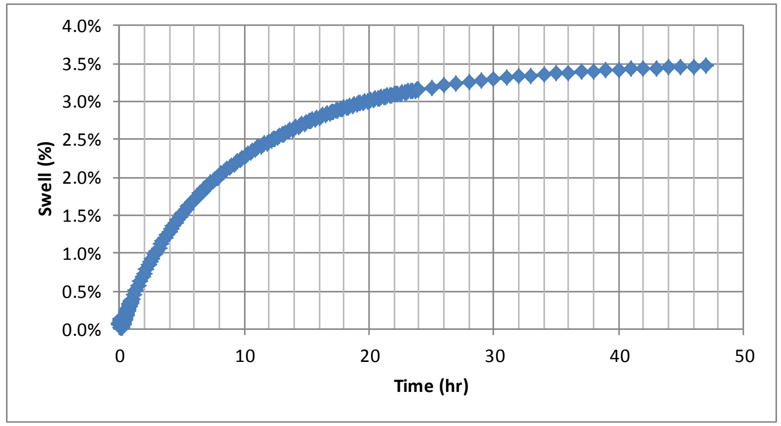

Slope of Primary Swelling	2.44%	%/log cycle
Slope of Secondary Swelling	1.18%	%/log cycle

Swell	3%
Time to Swell (hr)	24
Stress (psf)	282.0

FREE SWELL TEST

Date test conducted	3/19/2014
Conducted by	Chris

SOIL Information	Soil	CM
	Condition	Dry
	Specific Gravity	2.784

	Property	Target	Actual	Unit
TESTING SETUP Information	Mass Soil added	-	92.19	g
	Dry Density	-	1.240	g/cm^3
	Density	-	1.446	g/cm^3
	Height of Sample	2.000	2.014	cm

	Property	Initial	Final	Unit
TEST RESULTS Information	Seating Height	-	2.003	cm
	Testing Height	1.989	2.035	cm
	Void Ratio, e	1.243	1.267	-
	ω	16.6%	39.9%	%
	Saturation	37.2%	87.5%	%
	Change in ω	-	23.3%	%

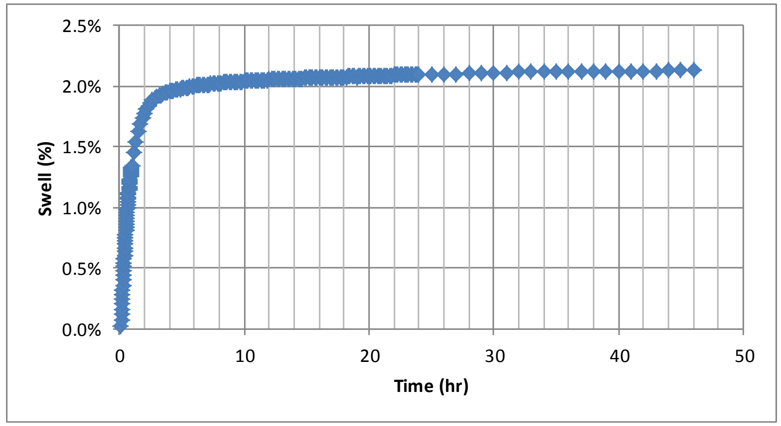

Swell	2%
Time to Swell (hr)	2
Stress (psf)	282.0

Slope of Primary Swelling	1.89%	%/log cycle
Slope of Secondary Swelling	0.13%	%/log cycle

FREE SWELL TEST		
	Date test conducted	3/19/2014
	Conducted by	Chris

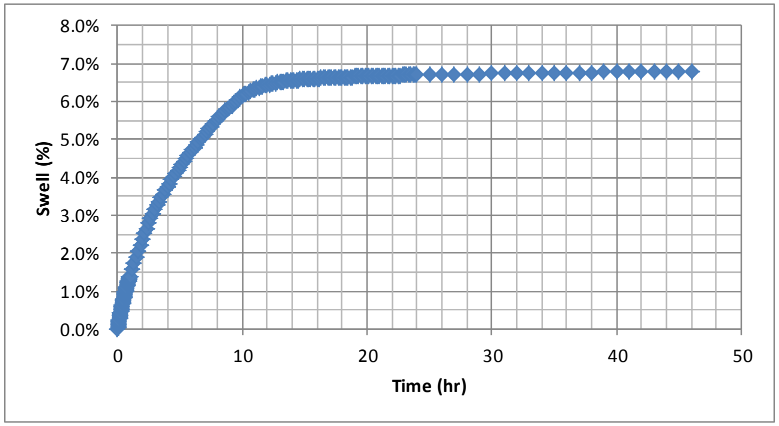

SOIL Information		
	Soil	CM
	Condition	Dry
	Specific Gravity	2.784

TESTING SETUP Information	Property	Target	Actual	Unit
	Mass Soil added	-	107.74	g
	Dry Density	-	1.449	g/cm^3
	Density	-	1.696	g/cm^3
	Height of Sample	2.000	2.006	cm

TEST RESULTS Information	Property	Initial	Final	Unit
	Seating Height	-	2.006	cm
	Testing Height	2.007	2.139	cm
	Void Ratio, e	0.919	1.046	-
	ω	17.1%	35.5%	%
	Saturation	51.7%	94.1%	%
	Change in ω	-	18.4%	%

Swell	6%	
Slope of Primary Swelling	5.85%	%/log cycle
Time to Swell (hr)	13	
Slope of Secondary Swelling	0.37%	%/log cycle
Stress (psf)	282.0	

FREE SWELL TEST

Date test conducted	3/20/2014
Conducted by	Chris

SOIL Information	**Soil**	CM
	Condition	Dry to Wet
	Specific Gravity	2.784

	Property	Target	Actual	Unit
TESTING SETUP Information	**Mass Soil added**	-	84.76	g
	Dry Density	-	1.027	g/cm^3
	Density	-	1.320	g/cm^3
	Height of Sample	2.000	2.027	cm

	Property	Initial	Final	Unit
TEST RESULTS Information	**Seating Height**	-	2.013	cm
	Testing Height	1.974	1.904	cm
	Void Ratio, e	1.706	1.542	-
	ω	28.5%	46.0%	%
	Saturation	46.5%	82.8%	%
	Change in ω	-	17.4%	%

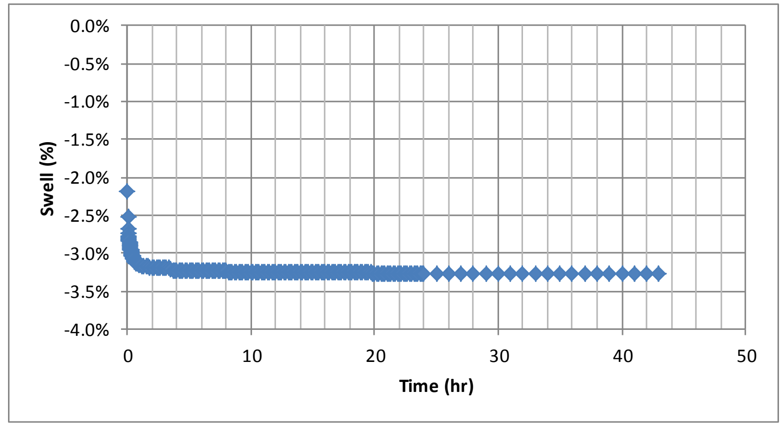

Swell	-3%
Time to Swell (hr)	17
Stress (psf)	282.0

Slope of Primary Swelling	-0.08%	%/log cycle
Slope of Secondary Swelling	-0.12%	%/log cycle

FREE SWELL TEST

Date test conducted	3/21/2014
Conducted by	Chris

SOIL Information	**Soil**	CM
	Condition	Wet
	Specific Gravity	2.784

	Property	Target	Actual	Unit
TESTING SETUP Information	**Mass Soil added**	-	112.83	g
	Dry Density	-	1.469	g/cm^3
	Density	-	1.851	g/cm^3
	Height of Sample	2.000	1.924	cm

	Property	Initial	Final	Unit
TEST RESULTS Information	**Seating Height**	-	1.922	cm
	Testing Height	1.918	1.964	cm
	Void Ratio, e	0.893	0.932	-
	ω	26.1%	32.4%	%
	Saturation	81.2%	96.4%	%
	Change in ω	-	6.3%	%

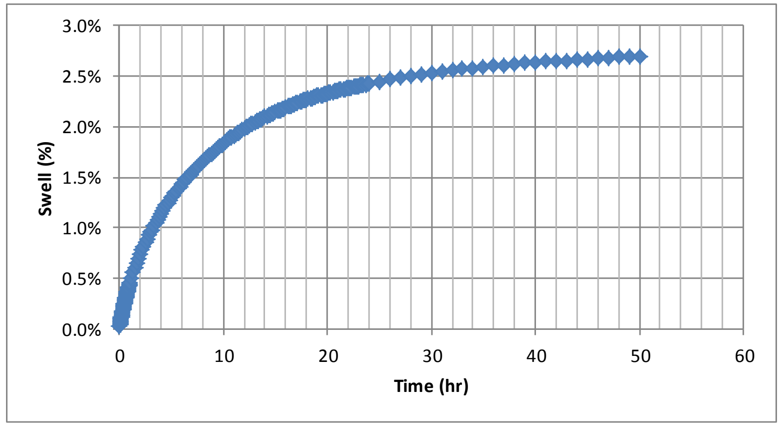

Swell	**2%**
Slope of Primary Swelling	1.74% %/log cycle
Time to Swell (hr)	**25**
Slope of Secondary Swelling	0.80% %/log cycle
Stress (psf)	**282.0**

FREE SWELL TEST	Date test conducted	3/22/2014
	Conducted by	Chris

SOIL Information	Soil	CM
	Condition	Wet to Dry
	Specific Gravity	2.784

TESTING SETUP Information	Property	Target	Actual	Unit
	Mass Soil added	-	105.93	g
	Dry Density	-	1.782	g/cm^3
	Density	-	1.846	g/cm^3
	Height of Sample	2.000	1.812	cm

TEST RESULTS Information	Property	Initial	Final	Unit
	Seating Height	-	1.787	cm
	Testing Height	1.776	2.073	cm
	Void Ratio, e	0.751	1.003	-
	ω	16.3%	31.2%	%
	Saturation	60.2%	86.4%	%
	Change in ω	-	15.0%	%

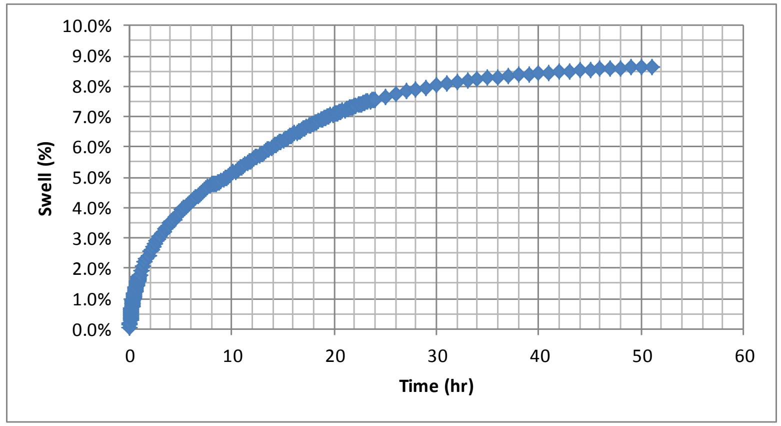

Swell	8%
Time to Swell (hr)	31
Stress (psf)	282.0

Slope of Primary Swelling	4.91% %/log cycle
Slope of Secondary Swelling	2.10% %/log cycle

FREE SWELL TEST	Date test conducted	3/22/2014
	Conducted by	Chris

SOIL Information	Soil	CM
	Condition	Wet to Dry
	Specific Gravity	2.784

TESTING SETUP Information	Property	Target	Actual	Unit
	Mass Soil added	-	104.40	g
	Dry Density	-	1.783	g/cm^3
	Density	-	1.808	g/cm^3
	Height of Sample	2.000	1.823	cm

TEST RESULTS Information	Property	Initial	Final	Unit
	Seating Height	-	1.814	cm
	Testing Height	1.808	1.935	cm
	Void Ratio, e	0.767	0.875	-
	ω	14.9%	31.7%	%
	Saturation	54.1%	100.0%	%
	Change in ω	-	16.8%	%

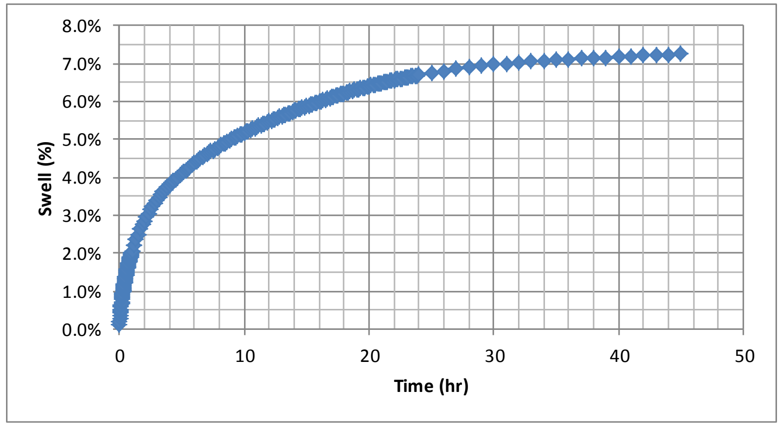

Swell	7%	
Slope of Primary Swelling	3.62%	%/log cycle
Time to Swell (hr)	29	
Slope of Secondary Swelling	1.59%	%/log cycle
Stress (psf)	282.0	

FREE SWELL TEST

Date test conducted	3/23/2014
Conducted by	Chris

SOIL Information	Soil	CM
	Condition	Dry
	Specific Gravity	2.784

	Property	Target	Actual	Unit
TESTING SETUP Information	Mass Soil added	-	100.54	g
	Dry Density	-	1.365	g/cm^3
	Density	-	1.565	g/cm^3
	Height of Sample	2.000	2.028	cm

	Property	Initial	Final	Unit
TEST RESULTS Information	Seating Height	-	2.023	cm
	Testing Height	2.018	2.131	cm
	Void Ratio, e	1.036	1.140	-
	ω	14.7%	38.8%	%
	Saturation	39.3%	94.6%	%
	Change in ω	-	24.1%	%

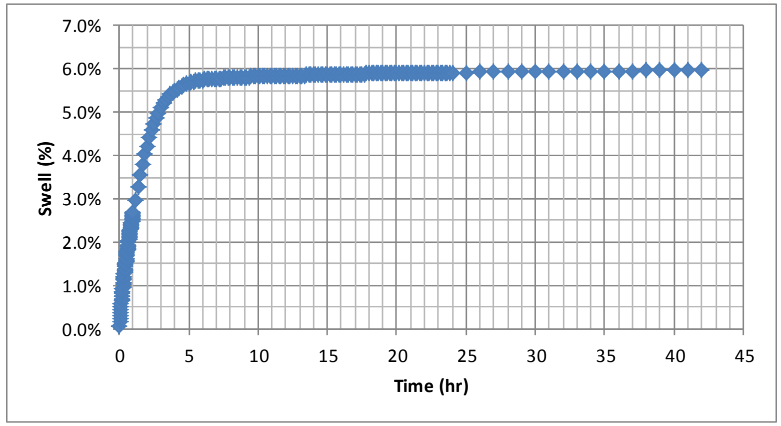

Swell	6%
Time to Swell (hr)	4
Stress (psf)	282.0

Slope of Primary Swelling	4.98%	%/log cycle
Slope of Secondary Swelling	0.22%	%/log cycle

FREE SWELL TEST

Date test conducted	3/24/2014
Conducted by	Chris

SOIL Information	Soil	CM
	Condition	Dry
	Specific Gravity	2.784

	Property	Target	Actual	Unit
TESTING SETUP Information	Mass Soil added	-	96.94	g
	Dry Density	-	1.256	g/cm^3
	Density	-	1.449	g/cm^3
	Height of Sample	2.000	2.112	cm

	Property	Initial	Final	Unit
TEST RESULTS Information	Seating Height	-	2.098	cm
	Testing Height	2.085	2.118	cm
	Void Ratio, e	1.214	1.220	-
	ω	15.4%	40.0%	%
	Saturation	35.3%	91.1%	%
	Change in ω	-	24.6%	%

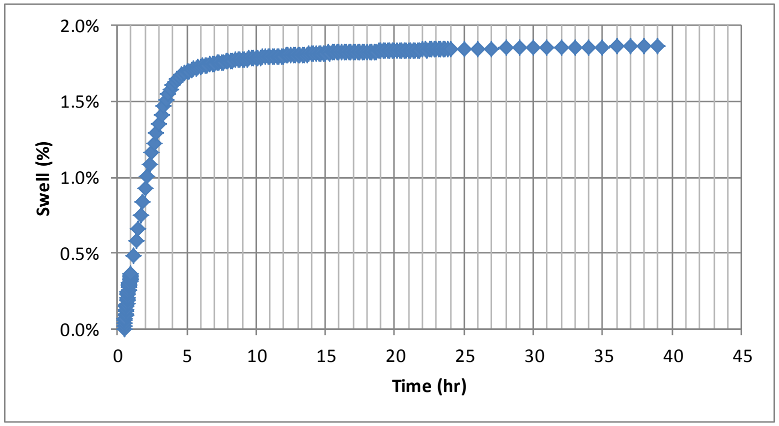

Swell	2%
Time to Swell (hr)	4
Stress (psf)	282.0

Slope of Primary Swelling	2.05%	%/log cycle
Slope of Secondary Swelling	0.13%	%/log cycle

FREE SWELL TEST	Date test conducted	3/24/2014
	Conducted by	Chris

SOIL Information	Soil	CM
	Condition	Dry to Wet
	Specific Gravity	2.784

TESTING SETUP Information	Property	Target	Actual	Unit
	Mass Soil added	-	102.18	g
	Dry Density	-	1.377	g/cm^3
	Density	-	1.642	g/cm^3
	Height of Sample	2.000	1.964	cm

TEST RESULTS Information	Property	Initial	Final	Unit
	Seating Height	-	1.946	cm
	Testing Height	1.932	2.040	cm
	Void Ratio, e	1.018	1.096	-
	ω	19.2%	37.2%	%
	Saturation	52.5%	94.2%	%
	Change in ω	-	17.9%	%

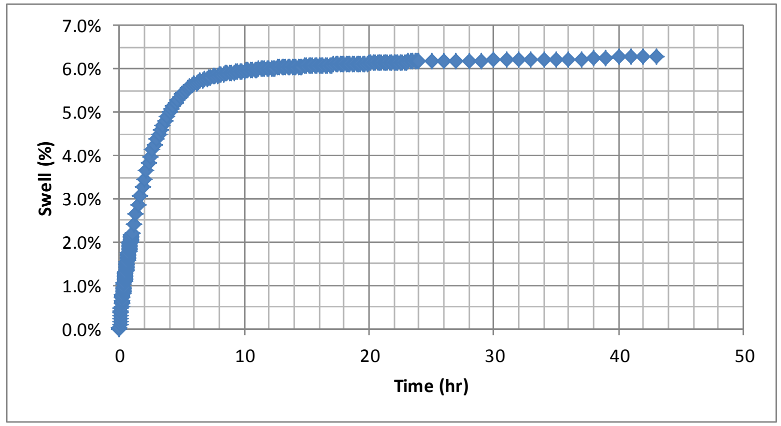

Swell	6%

Slope of Primary Swelling	5.10%	%/log cycle
Slope of Secondary Swelling	0.52%	%/log cycle

Time to Swell (hr)	7
Stress (psf)	282.0

FREE SWELL TEST

Date test conducted	3/25/2014
Conducted by	Chris

SOIL Information	Soil	CM
	Condition	OPT
	Specific Gravity	2.784

	Property	Target	Actual	Unit
TESTING SETUP Information	Mass Soil added	-	108.14	g
	Dry Density	-	1.461	g/cm^3
	Density	-	1.753	g/cm^3
	Height of Sample	2.000	1.948	cm

	Property	Initial	Final	Unit
TEST RESULTS Information	Seating Height	-	1.942	cm
	Testing Height	1.936	2.074	cm
	Void Ratio, e	0.903	1.026	-
	ω	20.0%	34.8%	%
	Saturation	61.6%	94.0%	%
	Change in ω	-	14.8%	%

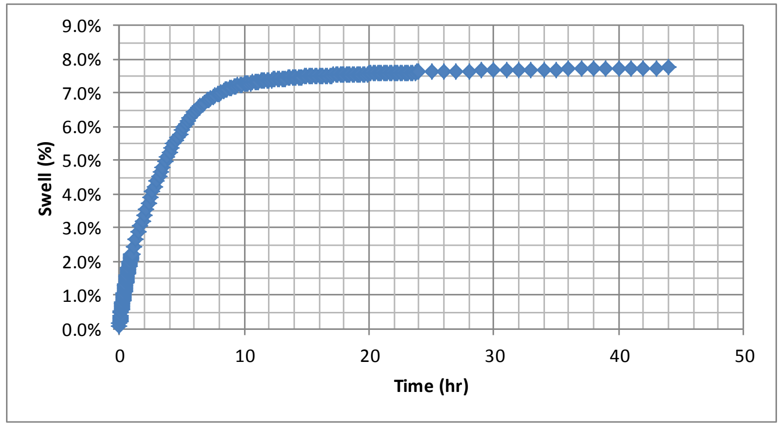

Swell	7%

Slope of Primary Swelling	6.60% %/log cycle

Time to Swell (hr)	8

Slope of Secondary Swelling	0.60% %/log cycle

Stress (psf)	282.0

FREE SWELL TEST

Date test conducted	3/26/2014
Conducted by	Chris

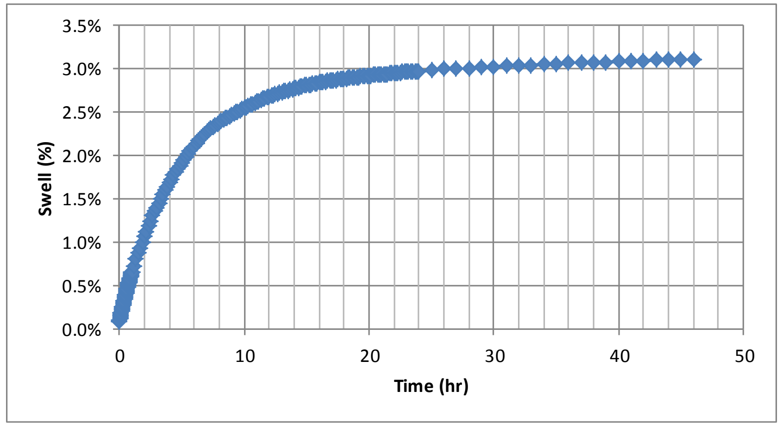

SOIL Information		
	Soil	CM
	Condition	OPT to Wet
	Specific Gravity	2.784

TESTING SETUP Information	Property	Target	Actual	Unit
	Mass Soil added	-	112.36	g
	Dry Density	-	1.423	g/cm^3
	Density	-	1.783	g/cm^3
	Height of Sample	2.000	1.990	cm

TEST RESULTS Information	Property	Initial	Final	Unit
	Seating Height	-	1.983	cm
	Testing Height	1.975	2.029	cm
	Void Ratio, e	0.953	0.991	-
	ω	25.2%	34.4%	%
	Saturation	73.6%	96.3%	%
	Change in ω	-	9.2%	%

Slope of Primary Swelling	2.27%	%/log cycle
Slope of Secondary Swelling	0.54%	%/log cycle

Swell	3%
Time to Swell (hr)	14
Stress (psf)	282.0

FREE SWELL TEST	Date test conducted	3/26/2014
	Conducted by	Chris

SOIL Information	Soil	CM
	Condition	OPT to Dry
	Specific Gravity	2.784

TESTING SETUP Information	Property	Target	Actual	Unit
	Mass Soil added	-	110.34	g
	Dry Density	-	1.751	g/cm^3
	Density	-	1.849	g/cm^3
	Height of Sample	2.000	1.884	cm

TEST RESULTS Information	Property	Initial	Final	Unit
	Seating Height	-	1.877	cm
	Testing Height	1.880	2.031	cm
	Void Ratio, e	0.712	0.845	-
	ω	13.9%	31.5%	%
	Saturation	54.1%	100.0%	%
	Change in ω	-	17.6%	%

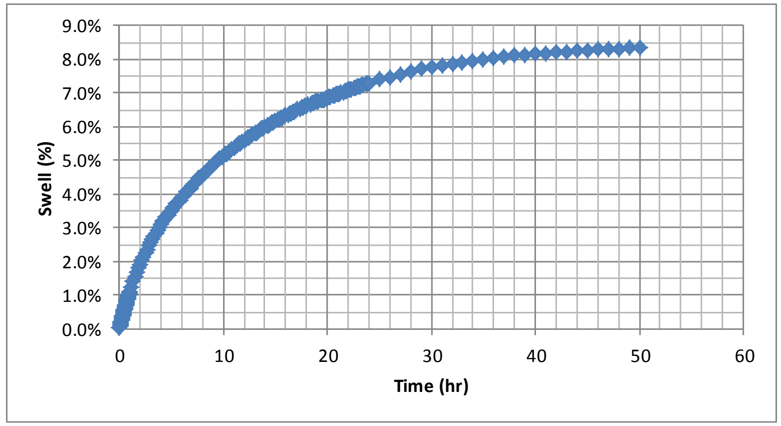

Swell	8%

Slope of Primary Swelling	5.88%	%/log cycle
Slope of Secondary Swelling	2.58%	%/log cycle

Time to Swell (hr)	31
Stress (psf)	282.0

FREE SWELL TEST

Date test conducted	3/28/2014
Conducted by	Chris

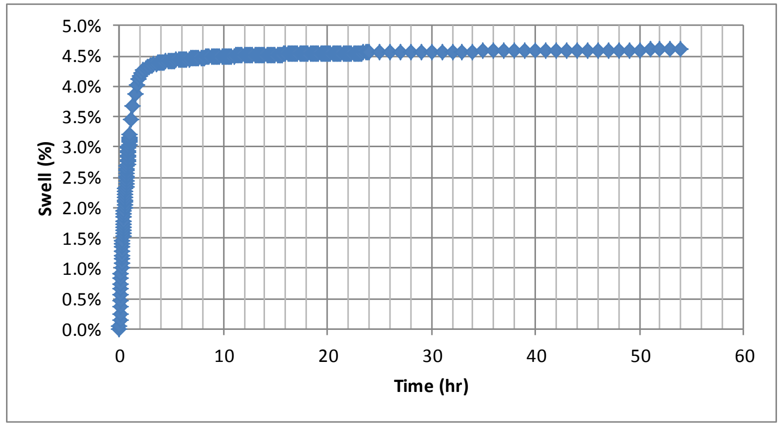

SOIL Information	**Soil**	CM
	Condition	Dry
	Specific Gravity	2.784

	Property	Target	Actual	Unit
TESTING SETUP Information	**Mass Soil added**	-	99.83	g
	Dry Density	-	1.338	g/cm^3
	Density	-	1.542	g/cm^3
	Height of Sample	2.000	2.044	cm

	Property	Initial	Final	Unit
TEST RESULTS Information	**Seating Height**	-	2.029	cm
	Testing Height	2.023	2.106	cm
	Void Ratio, e	1.078	1.141	-
	ω	15.3%	40.3%	%
	Saturation	39.3%	98.2%	%
	Change in ω	-	25.1%	%

Swell	**4%**	
Slope of Primary Swelling	4.12%	%/log cycle
Time to Swell (hr)	**2**	
Slope of Secondary Swelling	0.19%	%/log cycle
Stress (psf)	**282.0**	

FREE SWELL TEST	Date test conducted	3/28/2014
	Conducted by	Chris

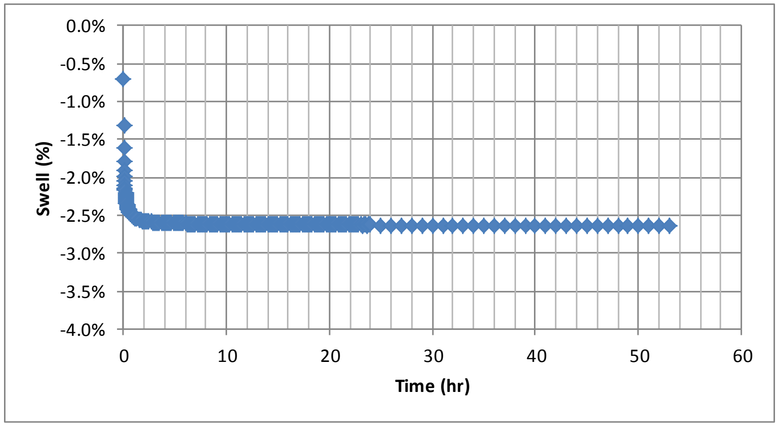

SOIL Information		
	Soil	CM
	Condition	Dry to Wet
	Specific Gravity	2.784

TESTING SETUP Information	Property	Target	Actual	Unit
	Mass Soil added	-	73.17	g
	Dry Density	-	0.954	g/cm^3
	Density	-	1.216	g/cm^3
	Height of Sample	2.000	1.900	cm

TEST RESULTS Information	Property	Initial	Final	Unit
	Seating Height	-	1.870	cm
	Testing Height	1.773	1.728	cm
	Void Ratio, e	1.914	1.650	-
	ω	27.5%	48.5%	%
	Saturation	39.9%	81.6%	%
	Change in ω	-	21.0%	%

Swell	-2%	
Slope of Primary Swelling	-0.35%	%/log cycle
Time to Swell (hr)	1	
Slope of Secondary Swelling	-0.05%	%/log cycle
Stress (psf)	282.0	

FREE SWELL TEST

Date test conducted	3/28/2014
Conducted by	Chris

SOIL Information	**Soil**	CM
	Condition	Dry to Wet
	Specific Gravity	2.784

	Property	Target	Actual	Unit
TESTING SETUP Information	**Mass Soil added**	-	97.81	g
	Dry Density	-	1.219	g/cm^3
	Density	-	1.520	g/cm^3
	Height of Sample	2.000	2.031	cm

	Property	Initial	Final	Unit
TEST RESULTS Information	**Seating Height**	-	2.019	cm
	Testing Height	2.005	1.786	cm
	Void Ratio, e	1.280	1.005	-
	ω	24.7%	41.0%	%
	Saturation	53.6%	100.0%	%
	Change in ω	-	16.3%	%

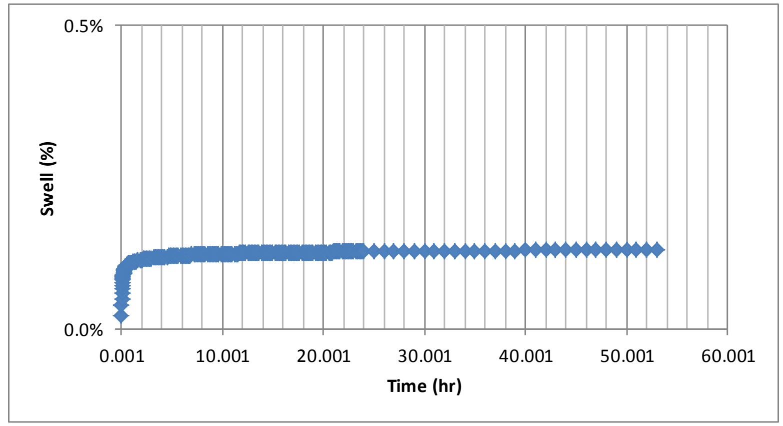

Swell	**0%**
Time to Swell (hr)	**1**
Stress (psf)	**282.0**

Slope of Primary Swelling	0.06% %/log cycle
Slope of Secondary Swelling	0.01% %/log cycle

FREE SWELL TEST

Date test conducted	3/31/2014
Conducted by	Chris

SOIL Information		
	Soil	CM
	Condition	Wet
	Specific Gravity	2.784

TESTING SETUP Information	Property	Target	Actual	Unit
	Mass Soil added	-	115.02	g
	Dry Density	-	1.513	g/cm^3
	Density	-	1.907	g/cm^3
	Height of Sample	2.000	1.904	cm

TEST RESULTS Information	Property	Initial	Final	Unit
	Seating Height	-	1.893	cm
	Testing Height	1.873	1.941	cm
	Void Ratio, e	0.838	0.873	-
	ω	26.0%	31.2%	%
	Saturation	86.5%	99.2%	%
	Change in ω	-	5.2%	%

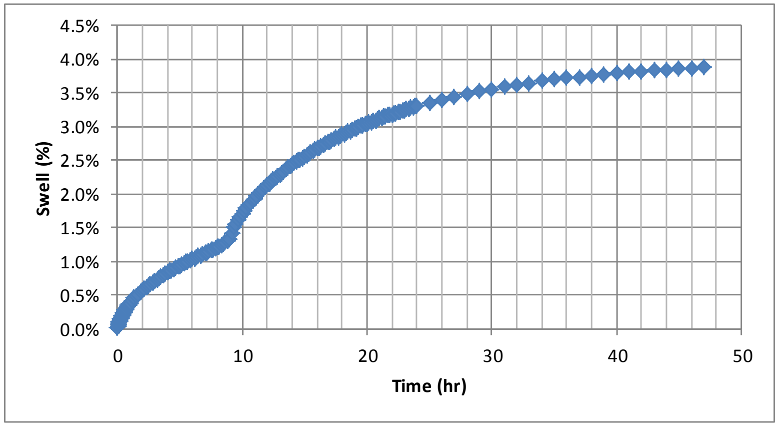

Swell	4%

Slope of Primary Swelling	4.14%	%/log cycle
Slope of Secondary Swelling	1.61%	%/log cycle

Time to Swell (hr)	31
Stress (psf)	282.0

FREE SWELL TEST

Date test conducted	4/1/2014
Conducted by	Chris

SOIL Information

Soil	CM
Condition	Wet to Dry
Specific Gravity	2.784

TESTING SETUP Information

Property	Target	Actual	Unit
Mass Soil added	-	131.90	g
Dry Density	-	1.700	g/cm^3
Density	-	1.982	g/cm^3
Height of Sample	2.000	2.102	cm

TEST RESULTS Information

Property	Initial	Final	Unit
Seating Height	-	2.091	cm
Testing Height	2.083	2.214	cm
Void Ratio, e	0.635	0.722	-
ω	16.6%	28.5%	%
Saturation	72.5%	100.0%	%
Change in ω	-	12.0%	%

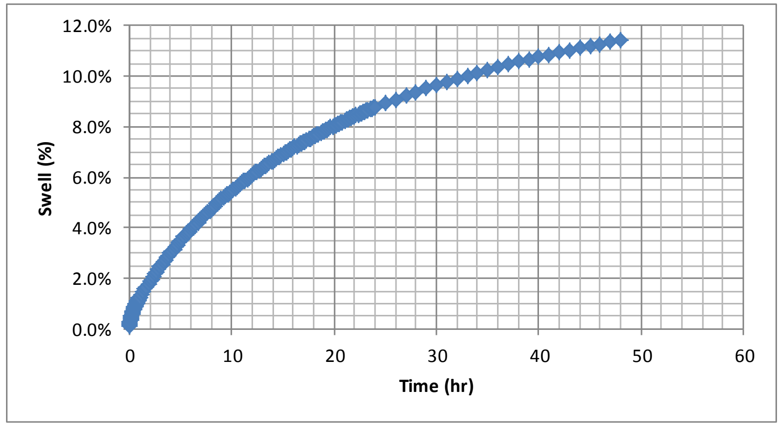

Swell	11%
Time to Swell (hr)	47
Stress (psf)	282.0

Slope of Primary Swelling	8.32%	%/log cycle
Slope of Secondary Swelling	-	%/log cycle

FREE SWELL TEST

Date test conducted	4/1/2014
Conducted by	Chris

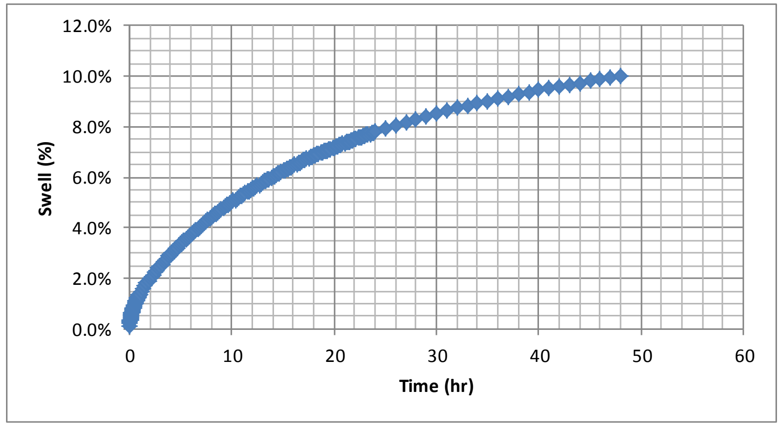

SOIL Information	**Soil**	CM
	Condition	Wet to Dry
	Specific Gravity	2.784

TESTING SETUP Information	**Property**	Target	Actual	Unit
	Mass Soil added	-	129.95	g
	Dry Density	-	1.717	g/cm^3
	Density	-	2.011	g/cm^3
	Height of Sample	2.000	2.040	cm

TEST RESULTS Information	**Property**	Initial	Final	Unit
	Seating Height	-	2.034	cm
	Testing Height	2.029	2.231	cm
	Void Ratio, e	0.619	0.771	-
	ω	17.1%	28.4%	%
	Saturation	76.9%	100.0%	%
	Change in ω	-	11.2%	%

Swell	**10%**
Time to Swell (hr)	**46**
Stress (psf)	**282.0**

Slope of Primary Swelling	6.14% %/log cycle
Slope of Secondary Swelling	- %/log cycle

FREE SWELL TEST

Date test conducted	4/2/2014
Conducted by	Chris

SOIL Information	**Soil**	CM
	Condition	Wet to Dry
	Specific Gravity	2.784

TESTING SETUP Information	**Property**	Target	Actual	Unit
	Mass Soil added	-	106.03	g
	Dry Density	-	1.807	g/cm^3
	Density	-	1.801	g/cm^3
	Height of Sample	2.000	1.859	cm

TEST RESULTS Information	**Property**	Initial	Final	Unit
	Seating Height	-	1.845	cm
	Testing Height	1.839	1.953	cm
	Void Ratio, e	0.758	0.846	-
	ω	13.9%	31.4%	%
	Saturation	50.9%	100.0%	%
	Change in ω	-	17.5%	%

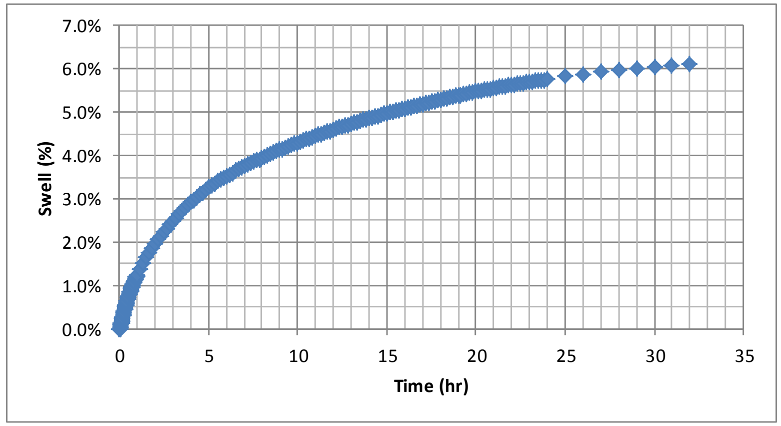

Swell	**6%**

Slope of Primary Swelling	3.61% %/log cycle
Slope of Secondary Swelling	- %/log cycle

Time to Swell (hr)	**31**
Stress (psf)	**282.0**

SUBMERGED CENTRIFUGE TEST

Date test conducted	3/26/2014
Centrifuge used	1
Cup Number	1
Conducted by	Chris

	Property	Information	Unit
SOIL Information	**Soil**	CM-Dry	
	Boring	-	
	Depth	-	ft
	Specific Gravity	2.78	
	Mass of Soil	66.86	g
	Dry Unit Weight	1484%	kN/m^3
	Height of Sample	2.049	cm

	Property	Initial	Final	Unit
TEST Results	**G-Level**	-	32.39	gravity
	Seating Height	-	-0.002	cm
	Testing Height	2.032	2.144	cm
	Void Ratio, e	0.840	0.941	-
	ω	15.8%	37.6%	%
	Saturation	52.4%	100.0%	%
	Change in ω	-	21.7%	%
	Overburden Mass	-	73.56	g
	Height of water	1.60	1.83	cm
	Swell	-	5.5%	%
	Max. Swell	-	6.5%	%
	Volume	38.15	40.25	cm^3
	Change in Volume	-	2.10	cm^3
	Mass of Water Lost	-	1.06	g

NOTES	

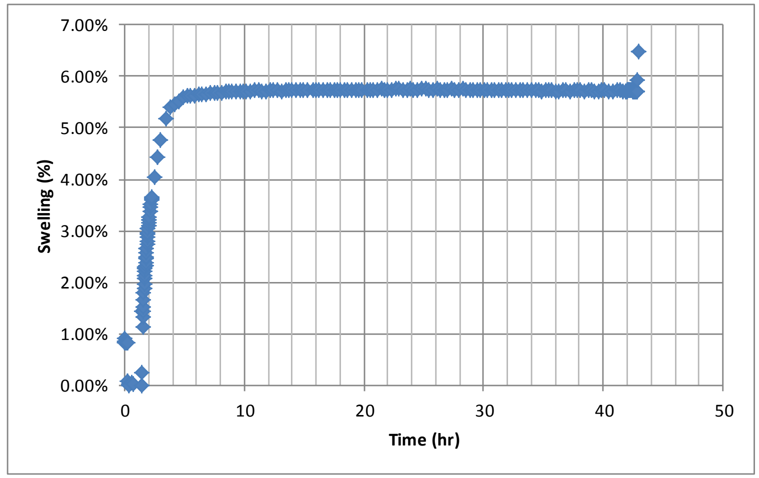

Swell	**5.5%**

Slope of Primary Swelling	13.06%	%/log cycle

Time to Swell (hr)	**4.49**

Slope of Secondary Swelling	-0.01%	%/log cycle

Stress (psf)	**257.8**

SUBMERGED CENTRIFUGE TEST

Date test conducted	3/26/2014
Centrifuge used	1
Cup Number	2
Conducted by	Chris

SOIL Information

Property	Information	Unit
Soil	CM-Dry	
Boring	-	
Depth	-	ft
Specific Gravity	2.78	
Mass of Soil	59.37	g
Dry Unit Weight	1378%	kN/m^3
Height of Sample	1.951	cm

TEST Results

Property	Initial	Final	Unit
G-Level	-	32.39	gravity
Seating Height	-	-0.002	cm
Testing Height	1.936	2.013	cm
Void Ratio, e	0.981	1.061	-
ω	16.3%	42.1%	%
Saturation	46.1%	100.0%	%
Change in ω	-	25.9%	%
Overburden Mass	-	73.06	g
Height of water	1.60	2.92	cm
Swell	-	4.0%	%
Max. Swell	-	4.8%	%
Volume	36.34	37.80	cm^3
Change in Volume		1.46	cm^3
Mass of Water Lost	-	2.22	g

NOTES	

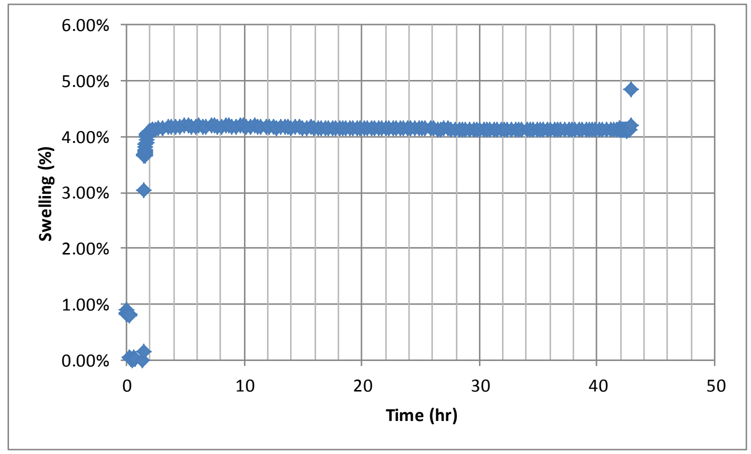

Swell	**4.0%**

Slope of Primary Swelling	6.33%	%/log cycle

Time to Swell (hr)	**1.73**

Slope of Secondary Swelling	-0.10%	%/log cycle

Stress (psf)	**250.3**

SUBMERGED CENTRIFUGE TEST

Date test conducted	3/26/2014
Centrifuge used	1
Cup Number	3
Conducted by	Chris

SOIL Information	Property	Information	Unit
	Soil	CM-Wet	
	Boring	-	
	Depth	-	ft
	Specific Gravity	2.78	
	Mass of Soil	65.43	g
	Dry Unit Weight	1582%	kN/m^3
	Height of Sample	1.731	cm

TEST Results	Property	Initial	Final	Unit
	G-Level	-	32.39	gravity
	Seating Height	-	-0.003	cm
	Testing Height	1.719	1.770	cm
	Void Ratio, e	0.726	0.777	-
	ω	25.7%	34.4%	%
	Saturation	98.4%	100.0%	%
	Change in ω	-	8.7%	%
	Overburden Mass	-	73.29	g
	Height of water	1.60	2.72	cm
	Swell	-	2.9%	%
	Max. Swell	-	3.6%	%
	Volume	32.28	33.23	cm^3
	Change in Volume	-	0.95	cm^3
	Mass of Water Lost	-	1.51	g

NOTES	

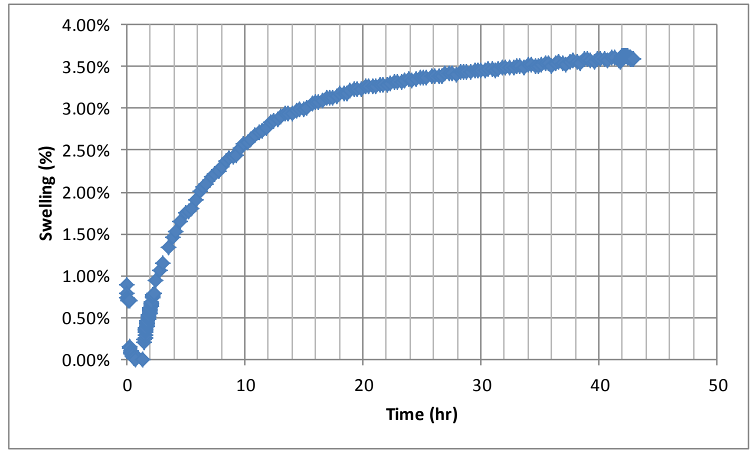

Swell	**2.9%**

Slope of Primary Swelling	2.82%	%/log cycle

Time to Swell (hr)	**14.01**

Slope of Secondary Swelling	1.14%	%/log cycle

Stress (psf)	**256.1**

SUBMERGED CENTRIFUGE TEST		
	Date test conducted	3/26/2014
	Centrifuge used	1
	Cup Number	4
	Conducted by	Chris

	Property	Information	Unit
SOIL Information	Soil	CM-Wet	
	Boring	-	
	Depth	-	ft
	Specific Gravity	2.78	
	Mass of Soil	70.17	g
	Dry Unit Weight	1619%	kN/m^3
	Height of Sample	1.819	cm

	Property	Initial	Final	Unit
TEST Results	G-Level	-	32.39	gravity
	Seating Height	-	-0.001	cm
	Testing Height	1.798	1.839	cm
	Void Ratio, e	0.687	0.726	-
	ω	26.0%	33.0%	%
	Saturation	105.2%	100.0%	%
	Change in ω	-	7.0%	%
	Overburden Mass	-	73.28	g
	Height of water	1.60	2.16	cm
	Swell	-	2.3%	%
	Max. Swell	-	2.8%	%
	Volume	33.76	34.54	cm^3
	Change in Volume		0.78	cm^3
	Mass of Water Lost	-	1.43	g

NOTES	

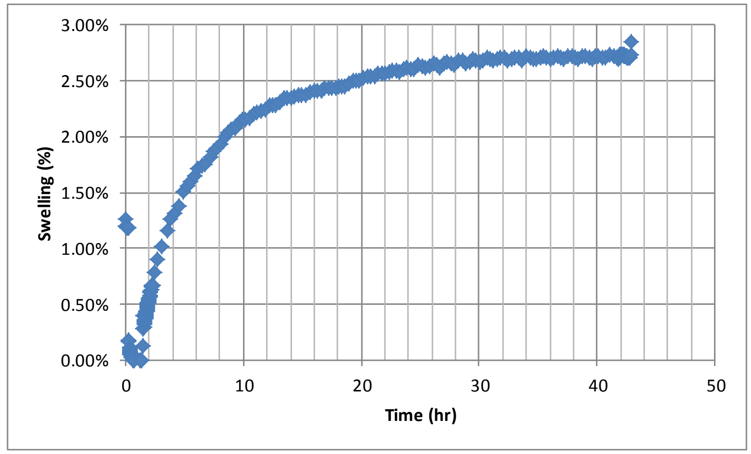

Swell	2.3%

Slope of Primary Swelling	2.26%	%/log cycle

Time to Swell (hr)	13.08

Slope of Secondary Swelling	0.76%	%/log cycle

Stress (psf)	259.2

SUBMERGED CENTRIFUGE TEST

Date test conducted	3/30/2014
Centrifuge used	1
Cup Number	1
Conducted by	Chris

	Property	Information	Unit
SOIL Information	**Soil**	CM-WOPT to Dry	
	Boring	-	
	Depth	-	ft
	Specific Gravity	2.78	
	Mass of Soil	67.16	g
	Dry Unit Weight	1805%	kN/m^3
	Height of Sample	1.793	cm

	Property	Initial	Final	Unit
TEST Results	**G-Level**	-	40.85	gravity
	Seating Height	-	0.000	cm
	Testing Height	1.781	1.904	cm
	Void Ratio, e	0.513	0.690	-
	ω	14.0%	29.9%	%
	Saturation	76.1%	100.0%	%
	Change in ω	-	15.9%	%
	Overburden Mass	-	73.52	g
	Height of water	1.60	1.55	cm
	Swell	-	7.0%	%
	Max. Swell	-	7.6%	%
	Volume	32.01	35.76	cm^3
	Change in Volume	-	3.74	cm^3
	Mass of Water Lost	-	2.52	g

NOTES	

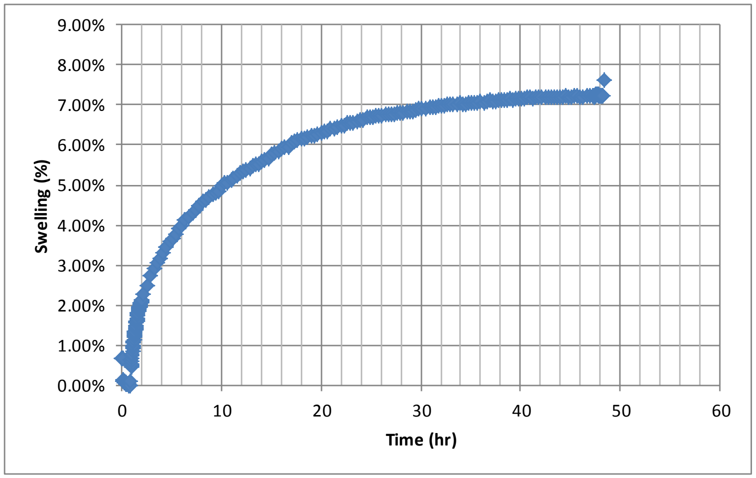

Swell	**6.95%**

Slope of Primary Swelling	4.49%	%/log cycle
Slope of Secondary Swelling	1.72%	%/log cycle

Time to Swell (hr)	**31.48**
Stress (psf)	**359.6**

SUBMERGED CENTRIFUGE TEST

Date test conducted	3/30/2014
Centrifuge used	1
Cup Number	2
Conducted by	Chris

SOIL Information

Property	Information	Unit
Soil	CM-WOPT to Dry	
Boring	-	
Depth	-	ft
Specific Gravity	2.78	
Mass of Soil	66.63	g
Dry Unit Weight	1789%	kN/m^3
Height of Sample	1.791	cm

TEST Results

Property	Initial	Final	Unit
G-Level	-	40.85	gravity
Seating Height	-	0.000	cm
Testing Height	1.780	1.910	cm
Void Ratio, e	0.526	0.715	-
ω	14.4%	30.3%	%
Saturation	76.3%	100.0%	%
Change in ω	-	15.9%	%
Overburden Mass	-	73.23	g
Height of water	1.60	1.62	cm
Swell	-	7.3%	%
Max. Swell	-	7.9%	%
Volume	31.92	35.87	cm^3
Change in Volume		3.94	cm^3
Mass of Water Lost	-	2.32	g

NOTES	

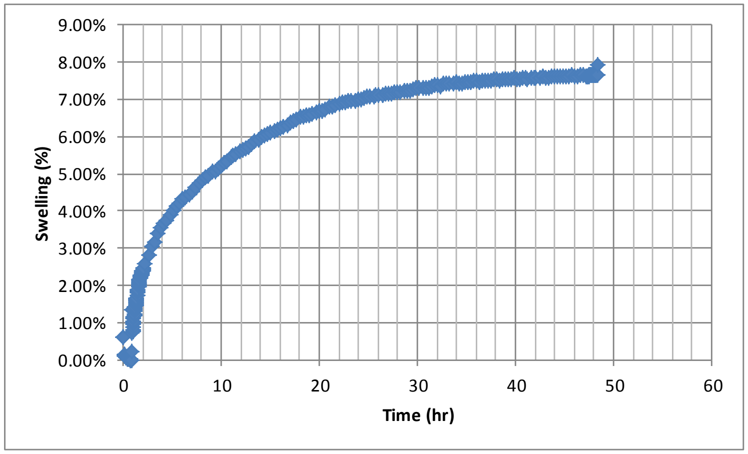

Swell	**7.31%**	
Slope of Primary Swelling	4.61%	%/log cycle
Time to Swell (hr)	**30.54**	
Slope of Secondary Swelling	1.72%	%/log cycle
Stress (psf)	**358.1**	

SUBMERGED CENTRIFUGE TEST

Date test conducted	3/30/2014
Centrifuge used	1
Cup Number	3
Conducted by	Chris

	Property	Information	Unit
SOIL Information	**Soil**	CM-DOPT to Wet	
	Boring	-	
	Depth	-	ft
	Specific Gravity	2.78	
	Mass of Soil	53.73	g
	Dry Unit Weight	1405%	kN/m^3
	Height of Sample	1.726	cm

	Property	Initial	Final	Unit
TEST Results	**G-Level**	-	40.85	gravity
	Seating Height	-	-0.002	cm
	Testing Height	1.643	1.657	cm
	Void Ratio, e	0.944	0.960	-
	ω	21.6%	39.3%	%
	Saturation	63.7%	100.0%	%
	Change in ω	-	17.7%	%
	Overburden Mass	-	73.59	g
	Height of water	1.60	1.69	cm
	Swell	-	0.8%	%
	Max. Swell	-	4.4%	%
	Volume	30.86	31.11	cm^3
	Change in Volume	-	0.25	cm^3
	Mass of Water Lost	-	1.90	g

NOTES	

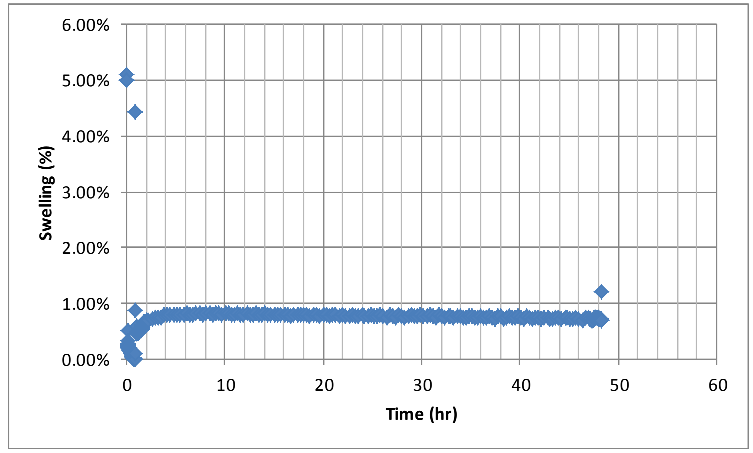

Slope of Primary Swelling	0.34%	%/log cycle
Slope of Secondary Swelling	-0.09%	%/log cycle

Swell	**0.80%**
Time to Swell (hr)	**4.87**
Stress (psf)	**352.6**

SUBMERGED CENTRIFUGE TEST		
	Date test conducted	3/30/2014
	Centrifuge used	1
	Cup Number	4
	Conducted by	Chris

	Property	Information	Unit
SOIL Information	Soil	CM-DOPT to Wet	
	Boring	-	
	Depth	-	ft
	Specific Gravity	2.78	
	Mass of Soil	51.14	g
	Dry Unit Weight	1305%	kN/m^3
	Height of Sample	1.727	cm

	Property	Initial	Final	Unit
TEST Results	G-Level	-	40.85	gravity
	Seating Height	-	0.001	cm
	Testing Height	1.710	1.768	cm
	Void Ratio, e	1.093	1.164	-
	ω	19.7%	35.7%	%
	Saturation	50.3%	85.4%	%
	Change in ω	-	16.0%	%
	Overburden Mass	-	73.37	g
	Height of water	1.61	1.79	cm
	Swell	-	3.4%	%
	Max. Swell	-	4.3%	%
	Volume	32.11	33.20	cm^3
	Change in Volume		1.09	cm^3
	Mass of Water Lost	-	2.24	g

NOTES	

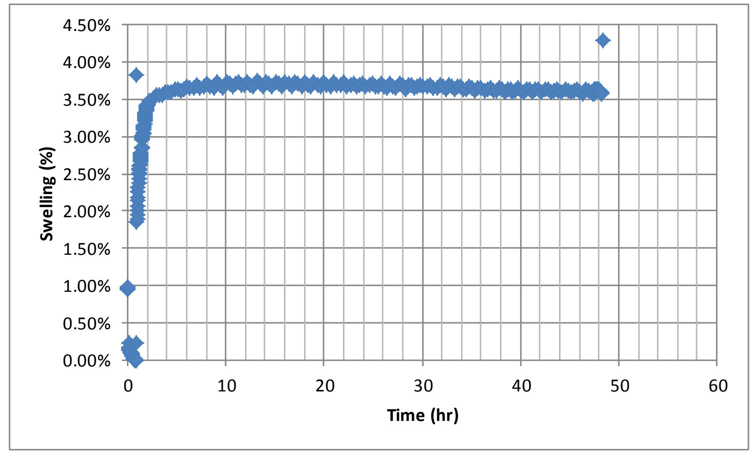

Swell	3.40%

Slope of Primary Swelling	4.67%	%/log cycle
Slope of Secondary Swelling	0.35%	%/log cycle

Time to Swell (hr)	1.93
Stress (psf)	350.9

SUBMERGED CENTRIFUGE TEST

Date test conducted	4/2/2014
Centrifuge used	1
Cup Number	1
Conducted by	Chris

	Property	Information	Unit
SOIL Information	**Soil**	CM - Opt	
	Boring	-	
	Depth	-	ft
	Specific Gravity	2.78	
	Mass of Soil	70.90	g
	Dry Unit Weight	1591%	kN/m^3
	Height of Sample	1.966	cm

	Property	Initial	Final	Unit
TEST Results	**G-Level**	-	28.16	gravity
	Seating Height	-	-0.002	cm
	Testing Height	1.950	2.065	cm
	Void Ratio, e	0.717	0.818	-
	ω	19.4%	33.5%	%
	Saturation	75.4%	100.0%	%
	Change in ω	-	14.1%	%
	Overburden Mass	-	73.55	g
	Height of water	1.62	1.69	cm
	Swell	-	5.9%	%
	Max. Swell	-	6.4%	%
	Volume	36.62	38.78	cm^3
	Change in Volume	-	2.16	cm^3
	Mass of Water Lost	-	1.09	g

NOTES	

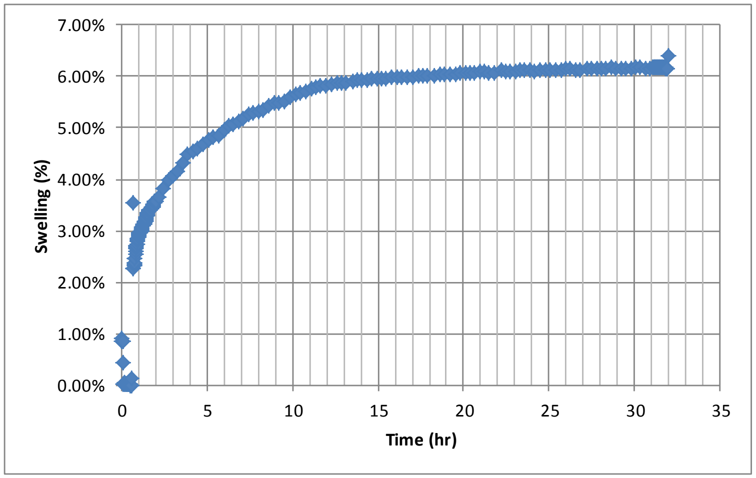

Swell	**5.91%**

Slope of Primary Swelling	2.89%	%/log cycle
Slope of Secondary Swelling	0.89%	%/log cycle

Time to Swell (hr)	**13.50**
Stress (psf)	**226.5**

SUBMERGED CENTRIFUGE TEST

Date test conducted	4/2/2014
Centrifuge used	1
Cup Number	2
Conducted by	Chris

	Property	Information	Unit
SOIL Information	**Soil**	CM - Opt	
	Boring	-	
	Depth	-	ft
	Specific Gravity	2.78	
	Mass of Soil	65.77	g
	Dry Unit Weight	1578%	kN/m^3
	Height of Sample	1.824	cm

	Property	Initial	Final	Unit
TEST Results	**G-Level**	-	28.16	gravity
	Seating Height	-	-0.002	cm
	Testing Height	1.819	1.905	cm
	Void Ratio, e	0.731	0.814	-
	ω	19.8%	33.0%	%
	Saturation	75.3%	100.0%	%
	Change in ω	-	13.3%	%
	Overburden Mass	-	73.60	g
	Height of water	1.62	1.79	cm
	Swell	-	4.8%	%
	Max. Swell	-	5.1%	%
	Volume	34.15	35.77	cm^3
	Change in Volume		1.63	cm^3
	Mass of Water Lost	-	1.04	g

NOTES	

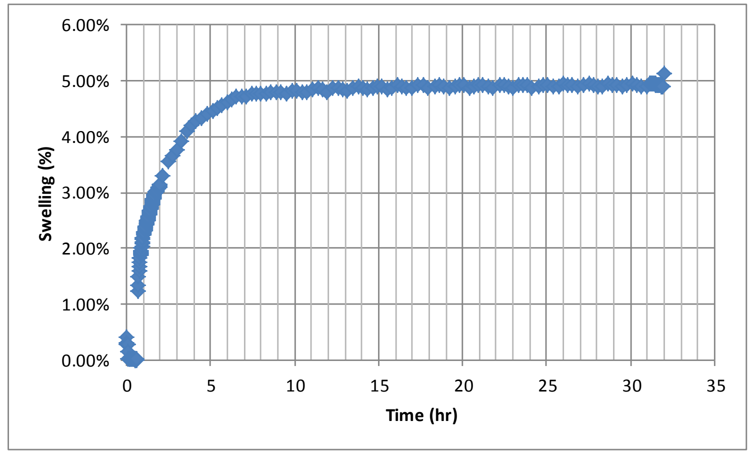

Swell	**4.77%**

Slope of Primary Swelling	3.40%	%/log cycle

Time to Swell (hr)	**7.43**

Slope of Secondary Swelling	0.12%	%/log cycle

Stress (psf)	**226.0**

SUBMERGED CENTRIFUGE TEST

Date test conducted	4/2/2014
Centrifuge used	1
Cup Number	3
Conducted by	Chris

	Property	Information	Unit
SOIL Information	**Soil**	CM - Opt to Dry	
	Boring	-	
	Depth	-	ft
	Specific Gravity	2.78	
	Mass of Soil	65.89	g
	Dry Unit Weight	1698%	kN/m^3
	Height of Sample	1.758	cm

	Property	Initial	Final	Unit
TEST Results	**G-Level**	-	28.16	gravity
	Seating Height	-	-0.001	cm
	Testing Height	1.755	1.925	cm
	Void Ratio, e	0.609	0.765	-
	ω	15.6%	32.1%	%
	Saturation	71.2%	100.0%	%
	Change in ω	-	16.5%	%
	Overburden Mass	-	73.44	g
	Height of water	1.62	1.70	cm
	Swell	-	9.7%	%
	Max. Swell	-	10.4%	%
	Volume	32.95	36.14	cm^3
	Change in Volume	-	3.19	cm^3
	Mass of Water Lost	-	1.45	g

NOTES	

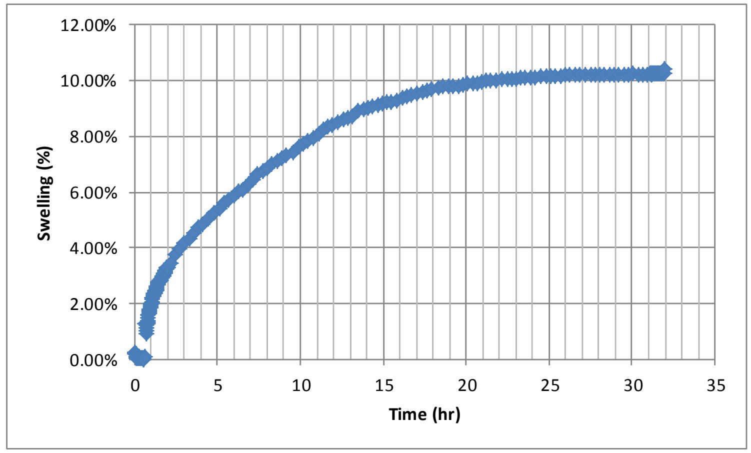

Swell	**9.70%**

Slope of Primary Swelling	7.75%	%/log cycle

Time to Swell (hr)	**17.91**

Slope of Secondary Swelling	1.10%	%/log cycle

Stress (psf)	**226.8**

SUBMERGED CENTRIFUGE TEST

Date test conducted	4/2/2014
Centrifuge used	1
Cup Number	4
Conducted by	Chris

	Property	Information	Unit
SOIL Information	Soil	CM - Opt to Wet	
	Boring	-	
	Depth	-	ft
	Specific Gravity	2.78	
	Mass of Soil	66.60	g
	Dry Unit Weight	1483%	kN/m^3
	Height of Sample	1.939	cm

	Property	Initial	Final	Unit
TEST Results	G-Level	-	28.16	gravity
	Seating Height	-	-0.006	cm
	Testing Height	1.872	1.902	cm
	Void Ratio, e	0.841	0.871	-
	ω	25.3%	35.0%	%
	Saturation	83.8%	100.0%	%
	Change in ω	-	9.7%	%
	Overburden Mass	-	73.30	g
	Height of water	1.62	1.86	cm
	Swell	-	1.6%	%
	Max. Swell	-	2.0%	%
	Volume	35.15	35.72	cm^3
	Change in Volume		0.57	cm^3
	Mass of Water Lost	-	1.10	g

NOTES	

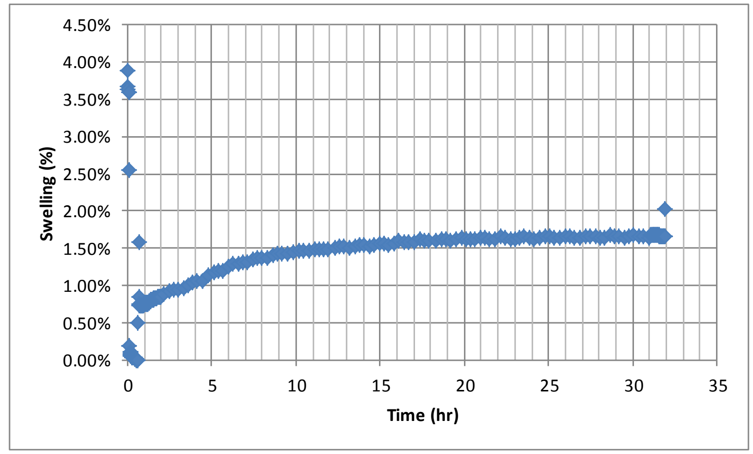

Swell	1.63%	
Slope of Primary Swelling	0.63%	%/log cycle
Time to Swell (hr)	25.70	
Slope of Secondary Swelling	-0.32%	%/log cycle
Stress (psf)	224.0	

References

Allen, J. and Gilbert, R. (2006). Accelerated Swell-Shrink Test for Predicting Vertical Movement in Expansive Soils. *Unsaturated Soils*, 2006.

ASTM D422-63. *Standard Test Method for Particle-Size Analysis of Soils*. American Society of Testing Materials.

ASTM D2216. *Standard Test Method for Laboratory Determination of Water (Moisture) Content of Soil and Rock by Mass*. American Society of Testing Materials.

ASTM D2435. *Standard Test Method for One-Dimensional Consolidation Properites of Soils Using Incremental Loading*. American Society of Testing Materials.

ASTM D4318. *Standard Test Method for Liquid Limit, Plastic Limit, and Plasticity Indecies of Soils*. American Society of Testing Materials.

ASTM D4546. *Standard Test Methods for One-Dimensional Swell or Collapse of Cohesive Soils*. American Society of Testing Materials.

ASTM D854-02. *Standard Test Method for Specific Gravity of Soil Solids by Water Pycnometer*. American Society of Testing Materials.

Attom, M., Abu-Zreig, M., and Obaidat, M. (2001). Changes in Clay Swelling and Shear Strength Properties with Different Sample Preparation Techniques. *Geotechnical Testing Journal*, Vol. 23, p. 157-163.

Barnes, V.E. 1981. Geologic Atlas of Texas, Austin Sheet, digitized from Barnes 1981 map: Texas Water Development Board, scale 1:250,000.

Beal, A. O. 1964. Stratigraphy of the Taylor Formation (Upper Cretaceous), East-Central Texas. Baylor Geological Studies Bulletin No. 6, Baylor University.

Chen, F.H. 1988. Foundations on Expansive Soils. Amsterdam: Elsevier.

Covar, A. and Lytton, R. (2001). Estimating Soil Swelling Behavior using Soil Classification Properities. *Expansive Clay Soils and Vegetive Influences on Shallow Foundations, ASCE Geotechnical Publications*. 44.

Dif, A. and Bluemel, W. (1991). Expansive Soils under Cyclic Drying and Wetting. *Geotechnical Testing Journal.* Vol. 14. 96-102.

Ewing, T.E. (1994). The Cook Mountain problem: stratigraphic reality and semantic confusion. *Gulf Coast Association of Geological Societies Transactions*, Vol. 44, p. 225–232.

Ferber, V., Auriol, J.C., Cui, Y.J., and Magnan, J.P. (2009). On the Swelling Potential of Compacted High Plasticity Clays. *Engineering Geology.* Vol. 104. 200-210.

Fityus, S. and Buzzi, O. The Place of Expansive Clays in the Framework of Unsaturated Soil Mechanics. *Applied Clay Science.* Vol. 43. 150-155.

Frydman, S. and Weisberg, E. (1991). A Study of Centrifuge Modeling of Swelling Clay. In *Centrifuge 91*. 113-120.

Gadre, A.D. and Chandrasekaran, V.S. (1994). Swelling of Black Cotton Soil using Centrifuge Modeling. *Journal of Geotechnical Engineering.* Vol. 120, p. 914-919.

Hackley, P.C., 2012, Geologic assessment of undiscovered conventional oil and gas resources—Middle Eocene Claiborne Group, United States part of the Gulf of Mexico Basin: U.S. Geological Survey Open–File Report 2012 – 1144.

Krohn, J., & Slosson, J. (1980). Assessment of expansive soils in the United States. *Fourth International Conference on Expansive Soils*, (pp. 596-608). Denver.

Kuhn, J. (2010). Characterization of the Swelling Potential of Expansive Clays using Centrifuge Technology. The University of Texas at Austin.

Lambe, T.W. (1958). The Structure of Compacted Clay.*Journal of thr Soil Mechanics and Foundation Division*, ASCE. Vol. 84, p. 1654-1 to 1654-35.

Lin, B. and Cerato, A. (2013). Hysteretic Soil Water Characteristics and Cyclic Swell-Shrink Paths of Compacted Expansive Soils. *Bulletin of Engineering Geology, the Environment.* Vol. 72. 61-70.

Lytton, R., Aubeny, C., and Bulut, R. Design Procedures for Pavements on Expansive Soils: Volume 1. Technical Report 0-4518-1, Texas Transporatation Institute, 2006.

McDowell, C. (1959). The Reation of Laboratory Testing to Design for Pavements and Structures on Expansive Soils. *Quarterly of the Colorado School of Mines.* Vol. 54. 129-153.

Nayak, N. and Christenesen, R. (1974). Swelling Characteristics of Compacted Expansive Soils. *Clays and Clay Minerals*. Vol. 19. 251-261.

Nelson, J. and Miller, D. 1992. Expansive Soils: Problems and Practice in Foundation and Pavement Engineering. New York: John Wiley & Sons, Inc.

Olive, W., Chleborad, A., Frahme, C., Schlocker, Julius, Schneider, R., et al. (1998). *U.S. Geological Survey Swelling Clays Map of Counterminous U.S. Soil Map of Texas and Oklahoma.* Retrieved March 9th, 2014 from SureVoid: http://www.surevoid.com/soil_maps/tx.php.

Olson, R. E. (2009). Expansive clay course notes.

Plaisted, M. D. (2009). Centrifuge Testing of an Expansive Clay. The University of Texas at Austin.

Rao, A., Phanikumar, B., and Sharma, R. (2004). Prediction of Swelling Characteristics of Remoulded and Compacted Expansive Soils using Free Swell Index. *Quarterly Journal of Engineering Geology and Hydrogeology.* Vol. 37. 217-226.

Tex-124-E. *Determing Potential Vertical Rise.* Texas Department of Transportation.

Vijayavergiya, V. and Ghazzaly, O. (1973). Prediction of Swelling Potential for Natural Clays. In *Proceedings of the 3rd International Conference on Expansive Soils.* Haifa, Israel. Vol. 1. 227-236.

Walker, T. (2012). Quantification using Centrifuge of Variables Governing the Swelling of Clays. The University of Texas at Austin.

Zemenu, G., Martine, A., and Roger, C. (2009). Analysis of the Behaviour of a Natural Expansive Soil under Cyclic Drying and Wetting. *Bulletin of Engineering Geology, the Environment.* Vol. 68. 421-436.

Zornberg, J.G., Armstrong, C.P., Plaisted, M.D., and Walker, T.M. (2013). Swelling of Highly Plastic Clays under Centrifuge Loading. Center for Transportation Research (CTR), Product Report No. 5-6048-01-P2, Austin, Texas, May, 8 p.

Zornberg, J.G. (2012). Properties of Compacted Clay in Geoenvironmental Engineering course notes.

Vita

Christian Philip Armstrong was born in El Paso, Texas in January 1990 to his parents, Dale and Ofelia Armstrong. He attended Carroll Senior High School in Southlake, Texas where he was a member of the 2006 State Championship football team. In 2008, he began his studies at the University of Texas at Austin which were completed in December 2011 with a Bachelor's of Science in Civil Engineering with Honors. In August 2012, he began his studies at the University of Texas at Austin for graduate school.

Permanent address: 1044 Winding Creek W Dr, Grapevine, TX 76051

This thesis was typed by Christian Armstrong (christian.armstrong@utexas.edu)

S.D.G.